



HAL
open science

Cellular events and regulations during leaf margin morphogenesis in *Arabidopsis thaliana*

Léo Serra

► **To cite this version:**

Léo Serra. Cellular events and regulations during leaf margin morphogenesis in *Arabidopsis thaliana*. Vegetal Biology. Université Paris Saclay (COMUE), 2019. English. NNT : 2019SACLS102 . tel-02724721

HAL Id: tel-02724721

<https://theses.hal.science/tel-02724721>

Submitted on 2 Jun 2020

HAL is a multi-disciplinary open access archive for the deposit and dissemination of scientific research documents, whether they are published or not. The documents may come from teaching and research institutions in France or abroad, or from public or private research centers.

L'archive ouverte pluridisciplinaire **HAL**, est destinée au dépôt et à la diffusion de documents scientifiques de niveau recherche, publiés ou non, émanant des établissements d'enseignement et de recherche français ou étrangers, des laboratoires publics ou privés.

“Les plantes semblent avoir été semées avec profusion sur la terre, comme les étoiles dans le Ciel, pour inviter l’Homme, par l’attrait du plaisir et de la curiosité, à l’étude de la nature ” (J.J. Rousseau, VII.prom. quoted by Linée in *Philosophia Botanica* 1751)

“From first to last, the plant is nothing but leaf” Goethe

"Ohne Wuchsstoff, kein Wachstum" (without auxin, no growth) Went 1928

REMERCIEMENTS:

Comme je ne sais plus qui disait : « la route est droite, mais la pente est raide », la pente est raide certes, mais la route est pas franchement droite non plus. Mais ce n'est pas grave il y a plein de choses à faire sur cette route : on peut observer les petites **feuilles** pousser sur le bord du chemin, respirer l'air à plein poumon et se dégager les **sinus**, il faut toutefois regarder où on met les pieds pour ne pas trébucher et se casser les **dents**. La route nous mène sans cesse vers de nouveaux horizons où nous pouvons découvrir des paysages inconnus. En chemin on croise plein de monde, et du coup la pente est moins raide...

Tout ça pour dire merci à tous, ce petit bout de chemin à vos côtés était fort sympathique.

Merci aux Jean du sous-sol pour la bonne ambiance : Jean-Denis, Jean-Christophe, Jean-Luc, Jean-Philippe, Jean-Yannick, Jean-Julien Jean-Sebastien, Jean-Lionel, Jean-Marine et Jean-Marianne.

Merci aussi aux informaticiens du bout du couloir pour les nombreuses discussions que j'ai eues avec eux, allant de la philosophie de la feuille aux statistiques pour les nuls en passant par l'hétérogénéité multi-intégrative du bruit et la variabilité sur de multiples échelles.

Merci à tous les membres de l'équipe FTA présents et passés pour la bonne ambiance et les mots fléchés.

Merci bien sûr aussi aux membres de mon comité de thèse : Christophe, Pradeep et Frédéric, vos conseils m'ont été d'une grande utilité.

Je viens de passer 3 ans dans un sous-sol à cliquer sur des cellules et quand je voulais me changer les idées j'allais m'enfermer dans l'obscurité de la salle des microscopes. J'en profite pour remercier tous les acolytes de la microscopie.

Merci Catherine, pour ta confiance et la grande liberté que tu m'as laissé dans la gestion de ce projet, merci aussi de ne t'être jamais formalisée pour mes méthodes de travail non-conventionnelles (dans le style feuilles volantes et rédaction sur les chapeaux de roues).

Je n'oublie pas la famille et les amis, sans vous je n'en serais sûrement pas là. Merci au Giffois, nos soirées hebdomadaires m'ont aidé à tenir ma réalité pendant ces trois années. Merci aussi au groupe de Boisemont, nos discussions ont grandement contribué à maintenir éveillée ma curiosité pour tous les aspects de cette chose étrange qui nous entoure : le monde.

Merci Sov, pour la nourriture, le soutien et puis tout le reste, sans toi le chemin serait moins drôle.

Et finalement merci à vous, membres du jury, d'avoir accepté d'évaluer mon travail.

SOMMAIRE

Chapter I: An introduction to plant morphogenesis from cells to shape through differential growth.....	7
Morphogenesis: shapes, cells and growth	7
Plant morphogenesis: a complex multiscale process	9
Cell cycle and cell division events:	9
Cell expansion	12
A specific view on plant morphogenesis: Heterogeneity.....	16
Differential growth shapes the above ground plant body plan.	25
Meristem boundaries and primordia.....	25
Role of CUCs in shaping the plant body plan.....	31
Leaf (margin): a model to study differential growth	35
Structural organization of leaves and associated cell types.....	35
Main growth axis and control of leaf size	37
New growth axis at the leaf margin	39
Main objective of the project.....	45
Chapter II: CUC3 mediates differential growth at the leaf margin by reducing cell growth.....	49
Chapter III: Auxin responses and mapping of TIR1/AFB during leaf serration	73
Core auxin signaling pathway: from perception to transcriptional outputs.....	73
Structural organization of auxin signaling components:.....	75
TIR/AFBs-AUX/IAAs interaction: affinity and specificity.....	77
AUX/IAAs inhibitory action on auxin transcriptional output	78
ARFs oligomerization and organization of AuxREs drive the diversity of auxin responses.....	79
Other levels of ARF regulations.....	80
Auxin signaling components involved in leaf serration.....	85
Results:.....	87
Pattern of auxin responses during leaf serration:.....	87
Pattern of TIR1, AFB2 and AFB3 during leaf serration:	91
Leaf phenotype of <i>tir1/afb</i> mutants:	91
Discussion:	94
Material and methods:	96
Chapter IV: General discussion and perspectives	99
Growth control: multicellular levels and cell wall properties	99
From mechanosensing to transcriptional activation of CUC3	102
Differential auxin distribution and differential growth.....	104
Toward an integrative understanding of morphogenesis: interplay between developmental biology and computational science.	105
References:	107

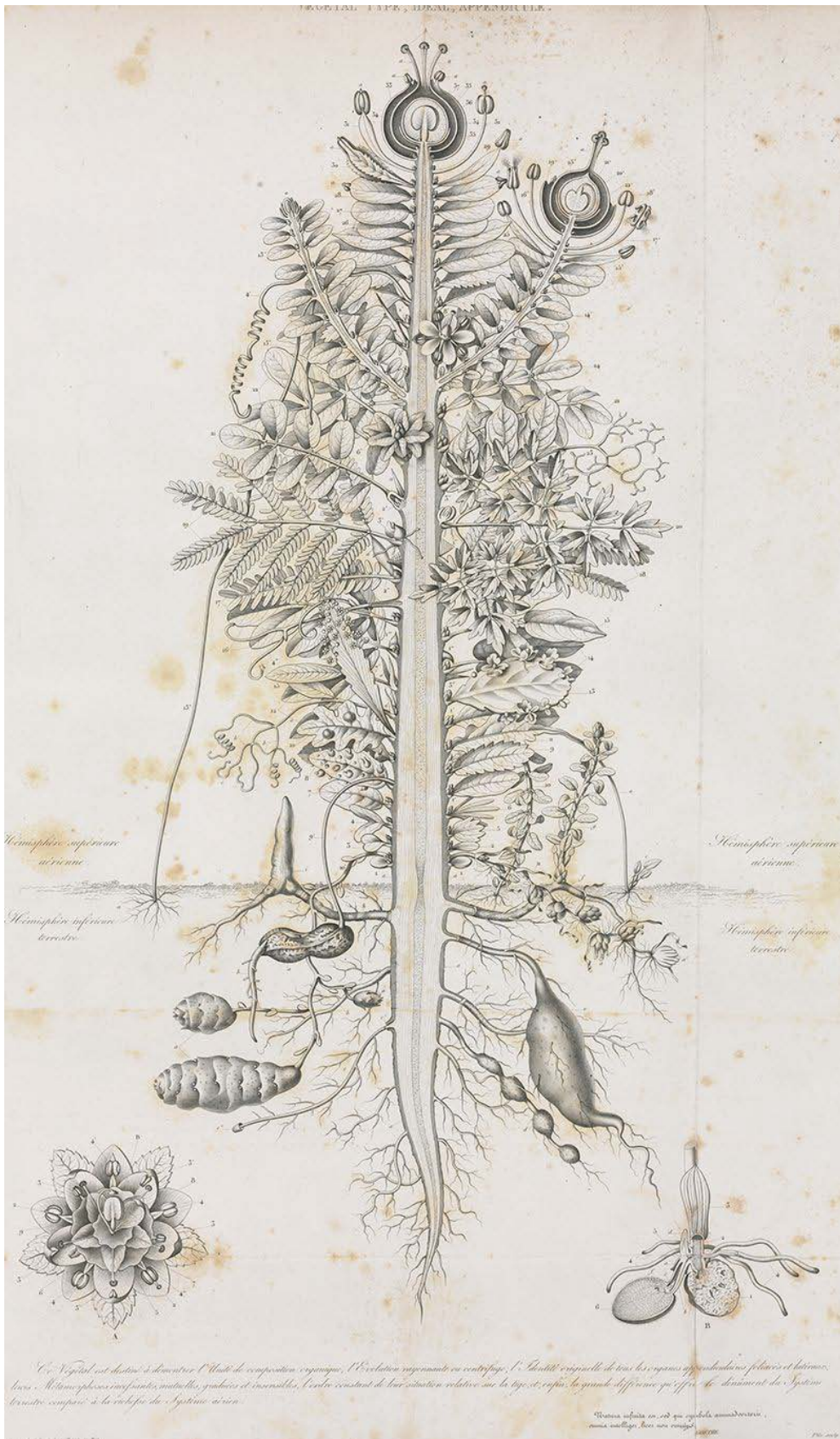


Figure 0: The Archetype plant. Drawn by Pierre Jean Turpin under request of Johann Wolfgang von Goethe.

Chapter I: An introduction to plant morphogenesis from cells to shape through differential growth.

Morphogenesis: shapes, cells and growth

Since its origins, life has continuously produced a plethora of organisms which have colonized almost every part of earth. One of the most striking features of this diversity is the huge variety of shapes found in nature (for an illustration of shape diversity in plants see Figure 0); cataloguing this diversity of species and describing their shapes have occupied scientists from classical time to nowadays. While most of these works consisted in describing morphological differences between organs and species, the work of Johann Wolfgang von Goethe aimed to investigate the underlying homologies behind the apparent diversity of plant organs. For instance, he postulated that leaves are archetypic organs from which all the aerial part of plant derives (Goethe, 1790) and thus opened the field of comparative morphology. Before Goethe's founding works, the invention of microscopes by Robert Hook (1665) and the latter improvements by Antoni Van Leewenhoeck (1676) in the XVII century made the discovery of cells possible. This discovery has led to the formalization of the cell theory by Matthias Schleiden (1838) and Theodor Schwann (1839) in the XIX century, the theory benefits from improvements by Robert Remak (1852) and Rudolf Virchow (1858) later in the same century. Cell theory can be resumed as follow: all organisms are made of cell(s), life functions of organisms occur within cells and all cells arise from division of existing cells. The cell theory considers multicellularity as the result of cell aggregation, cell being the individual organism at which level all the fundamental processes of life take place while the multicellular body only consists in a "republic of cells" (reviewed in(Ribatti, 2018)). Very early after its genesis the cell theory encountered criticisms by the supporters of the organismal theory. These criticisms arise mainly from botanists and plant morphologists, indeed some particularity of plant cell and plant tissue organization make plant architecture less

suitable than animal ones to be explained by the cell theory. For instance Wilhelm Hofmeister (1867) argued that plants subdivide themselves into cells by new wall insertion rather than being constituted of cells. From growth and morphogenesis perspectives, he considered changes in cell shape and size more as a marker of global growth than a causal process. In plants the debate between supporters of the cell theory and those of the organismal theory is still open and some recent results can be interpreted in favor of the organismal theory. First, plant cells are surrounded by a cell wall, constraining growth of individual cells. Single cell growth- if not directed by global growth of organs- has to be coordinated between cells. Secondly, a same size and shape of an organ could be obtained with distinct number of cells, as it was observed in the comparison between *Arabidopsis* sepals of distinct genetic backgrounds. For instance lines with distinct levels of LOSS OF GIANT CELLS FROM ORGANS (a gene involved in promotion of endoreplication) exhibit sepals with similar shape but with higher or lower number of epidermal giant cells (LGOoe and *lgo* lines) (Schwarz and Roeder, 2016). Lastly, recent studies using 4D imaging of growing plant organs have revealed the existence of stereotypic growth pattern at tissue/organ scales despite apparent heterogeneity in shape, size and growth of individual cells (Hervieux et al., 2016; Hong et al., 2016). Some issue related to this debate are addressed and discussed among others in the review presented later in this introduction but I would like to mention here that co-authors and I believe that while some signals controlling plant morphogenesis are integrated from the cell level to the tissue and organ levels, others are integrated from the organ and tissue levels to the cell level suggesting that cell and organismal theories are not necessary exclusive one to the other. Another important contribution to the field of morphogenesis has been made by D'Arcy Wentworth Thompson in his books "On growth and form" published in 1917. Thompson's major idea was that shape of any particular organism is the result of the "law of growth"; organ could therefore be seen as a "diagram of force" (the ones that have underlined the shape arising). He also stood for a formalization of the "law of growth" in the language of mathematics. It is only recently that an integrative understanding of growth and morphogenesis over multiple scales has been possible thank to progresses in molecular genetics, modeling, live imaging and quantitative measurements (Thompson, 1917) (Hamant, 2017).

From the work of scientists of previous centuries it is now clear that shape arises from growth and growth occurs at distinct levels including the cellular level, we will now go back to the basics of cellular events associated with growth in plants.

Plant morphogenesis: a complex multiscale process

Plant morphogenesis is sustained by a vast array of actors and processes occurring at multiple scales including the cell level. Here, I will present the mechanisms associated with cell cycle progression, cell division events and cell expansion.

Cell cycle and cell division events:

All plant cells originate from the division of a mother cell into two daughter cells. From birth to division, cells go through the four phases of the cell cycle. The two main phases of the cell cycle are the replication of DNA (S phase) and the mitosis associated with cytokinesis (M phase). These two phases are separated by Gap phases (G1 and G2). The progression through different phases of the cycle (G1/S, G2/M) involves a set of distinct CYCLIN-DEPENDENT KINASES (CDKs) and CYCLINS acting in complexes to phosphorylate substrates. These proteins have rapid turnover thus distinct complexes are transiently present at specific points of the cell cycle allowing specific phase dependent modulation of the expression of cell cycle progression genes. In association with the cell cycle and DNA replication, increase in cell volume is required, potentially in order to keep a reasonable cell volume after division. This type of cell growth is sometimes referred to as cytoplasmic growth, but unfortunately most cell cycle studies have been conducted without taking growth into account. This is a serious issue because as Fleming A.J. pointed out, cell division without growth will only produce a large number of smaller cells whose total volume will be quite identical to the volume of the initial mother cell (Figure 1). However it is known that cytoplasmic growth involves neosynthesis of cytoplasmic and cell wall components (Perrot-Rechenmann, 2010). Neosynthesis of proteins is a high energy-consuming process and therefore a tight coordination between cytoplasmic growth and metabolism is needed. Indeed TARGET OF RAPAMYCINE

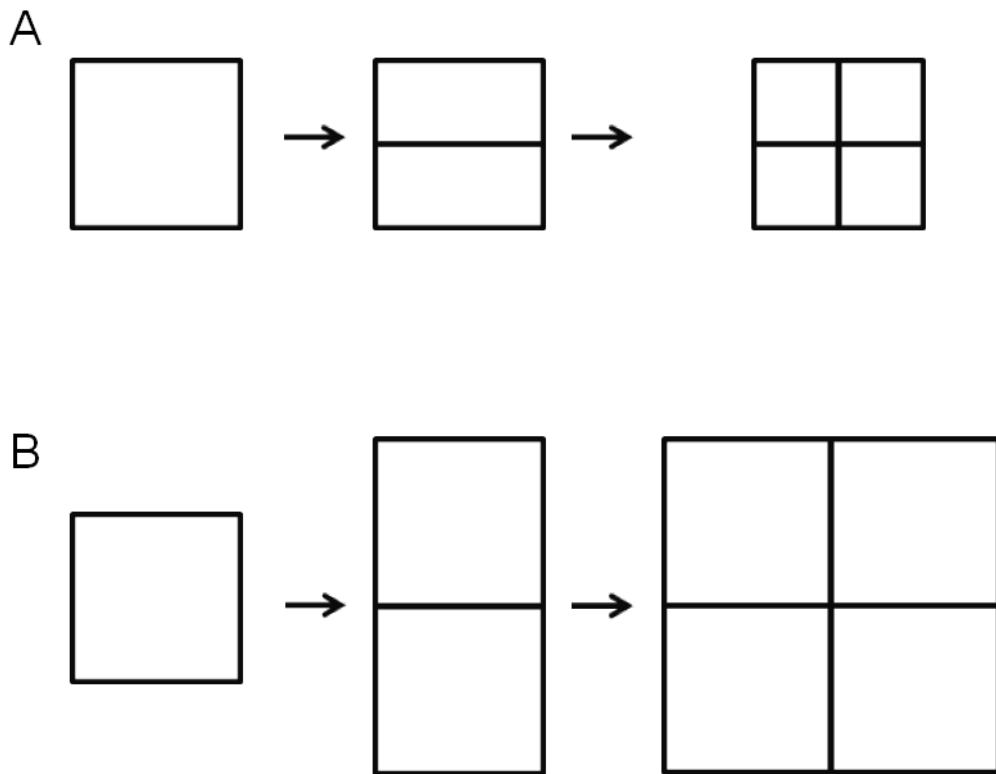


Figure 1: Cell division and growth can be separable. In theory, cell division could occur without growth (**A**), this would be associated with an overall decrease in mean cell size over generations. Most of the time cell division is associated with growth (**B**) which allows the clone/organ/organism to grow and keep a mean cell size constant over generations. In plants both situations occur and control of growth in cycling cells is important for the overall control of clone/organ/organism growth. Adapted from Fleming A.J 2005

(TOR) serine/threonine kinase has been reported to control various cellular processes such as ribosome synthesis, translation initiation and autophagy (Kalve et al., 2014). It has recently been shown that cell size at division, cell cycle G1 and G2 length and growth rate are linked in order to maintain the relative homogeneity in cell size in the central zone of the shoot apical meristem (Willis et al., 2016; Jones et al., 2017).

Beside the separation of sister chromatids between sister cells, mitosis is associated with the formation of new plasma membrane and cell wall during the process of cytokinesis. Neo-formed plasma membrane and cell wall are together called the cell plate. The cell plate is formed by the fusion of vesicles, transported from the golgi and trans-golgi network by the phragmoplast, a fibrillary structure mainly made of microtubules (Samuels et al., 1995; Segui-Simarro et al., 2004). These vesicles both carry the plasma membrane material and some proteins involved in cell wall component synthesis like cellulose synthases for instance (Miar et al., 2014). The phragmoplast moves centrifugally and the cell plate is formed according to the same direction and finally reaches the edges of the mother cell. This contact site is defined by the position of a ring-shaped array of cortical microtubules: the Preprophase Band (PPB). The PPB is initiated at the end of the G2 phase and becomes completely recognizable in prophase (Yabuuchi et al., 2015). Proper formation of the PPB is required to ensure the robustness of the orientation of the cell division plane since mutation in TRMs (key components of PPB formation) increases greatly the variability in orientation of cell division plane (Schaefer et al., 2017). Proper orientation of division plane during cytokinesis is important for plant development since it is a way to control both the topology and geometry of cells and tissues (Jackson et al., 2019). It has originally been postulated by Léo Errera (1886) that cell behaves like soap bubble and that position of division plane tends to minimize the area of the new interface between sister cells. Errera's rules also known as "the shortest path" rule have undergone some improvements since its first formulation. It has been shown that cells not always divide according to the shortest path but rather along one of the shortest path following probabilistic rules (Besson and Dumais, 2011). More recently it has been shown that in tissues under tension, the orientation of division plane aligns according to the maximal direction of tensile stress (Louveaux et al., 2016). In the specific context of morphogenesis, proliferation

has at least two important interconnected roles: i) subdividing the tissue/organ into functional units allowing the spatial organization of domains with distinct fate and growth properties; and ii) participating in the setup of differential growth by modulating spatial or temporal cytoplasmic growth. Another emerging concept is that orientation of cell division plane could affect the topology of the tissue, thus affecting the distribution and transport of signaling molecules (hormones, peptides) across tissues (Jackson et al., 2019).

Cell expansion

Plant cell can exit the cell cycle to enter into endoreplication where replication still occurs but is not followed anymore by mitosis and cytokinesis. This leads to an increase in DNA ploidy and is associated with cell size increase. Cell expansion results from a change in the balance between turgor pressure and the resistance to this pressure by the cell wall. Although it has been proposed that increase in turgor pressure could participate in cell expansion (Marty, 1999), this is still questionable since it has been shown that solutes and water fluxes through plasmodesmata could efficiently buffer pressure differences between adjacent cells (Rutschow et al., 2011). Whether or not turgor pressure is controlled to modulate cell expansion is still a matter of debate, however the pressure containment by the cell wall has to be released in order to allow growth, and this is done through cell wall remodeling. Cell wall is a complex network of cellulose microfibrils (glucose polymer), pectins (combination of homogalacturonan and rhamnogalacturonan polymers), and hemicelluloses (xyloglucans and arabinoxylans). One of the first known events in cell wall loosening is a softening of the pectin matrix; this is done by removing methyl groups from the homogalacturonan chains. Methyl-esterification status is regulated in part by the complex activity of PECTIN METHYL ESTERASE (PMEs) and PECTIN METHYL ESTERASE INHIBITOR (PMEIs) enzymes. A simplified view is that PMEs remove methyls while PMEIs inhibit the action of PMEs leading to softening and stiffening of the cell wall, respectively (Cosgrove, 2005; Hofte and Voxeur, 2017; Majda and Robert, 2018). Another group of apoplastic proteins, the EXPANSINs (EXPs) are efficient to disrupt hydrogen bonds between hemicelluloses and cellulose microfibrils at acidic pH (pH between 4.5 and 6) thus facilitating cell wall matrix

deformation (Cosgrove, 2016)(figure 2). PME and PME1 activities are also known to be pH sensitive and since their activity causes changes in apoplastic pH, their impact on cell wall stiffness is not as straightforward as previously thought. A role for cell wall acidification in cell expansion is known from decades; indeed, experiments in the past century have shown that expansion is associated with cell wall acidification and that blocking proton extrusion inhibits cell wall extensibility (Cleland, 1973). Auxin has long been connected to anisotropic cell expansion, according to the so called “acid growth theory”. The modern view of the acid growth theory is that auxin induces cell wall acidification through H⁺ extrusion by activation of the plasma membrane proton pump ATPase (AHAs). The activation of the H⁺ ATPase results from phosphorylation of a threonine residue and binding of a 14.3.3 protein. SMALL AUXIN UP RNA (SAURs) proteins also mediate H⁺ATPase regulation by inhibiting PP2C-D phosphatases thus providing conditions for H⁺ATPase activation. These two interconnected events lead to cell wall loosening by expansins. Wall loosening proteins cause cellulose microfibrils moving apart and increase wall porosity, new cell wall material reaches the cell surface via vesicular trafficking before being inserted into the cell wall. In shoots, auxin-dependent expansion was recently shown to rely on the so-called canonical auxin signaling (Fendrych et al., 2016). Canonical auxin signaling will be described in details at the beginning of chapter 3 but the following lines will give a very brief overview. Indole-3-acetic acid (IAA) is sensed by a co-receptor made of one of the members of the TRANSPORT INHIBITOR RESPONSE 1 and AUXIN F-BOX 1 to 5 (TIR/AFBs) F-box subfamily and a member of the AUXIN/INDOLE-ACETIC ACID (Aux/IAAs) transcriptional repressor family. Their interaction is mediated by IAA and leads to the poly-ubiquitination of Aux/IAA by the ubiquitin ligase E3 SCF^{TIR/AFBs} and subsequent addressing and protein degradation by the 26 S proteasome (reviewed in (Parcy et al., 2016; Weijers and Wagner, 2016; Han and Hwang, 2018)). Aux/IAA degradation allows the activation of auxin transcriptional responses by activators of the AUXIN RESPONSE FACTOR family (ARF Activators). Interestingly, an auxin concentration required to trigger cell expansion in shoots inhibits cell expansion in roots. This discrepancy is partially explained by a higher sensitivity to auxin in roots than in shoots. In fact auxin responses have long been known to be dose dependent with an auxin maximum promoting an optimal response. Between roots and shoots, a longstanding

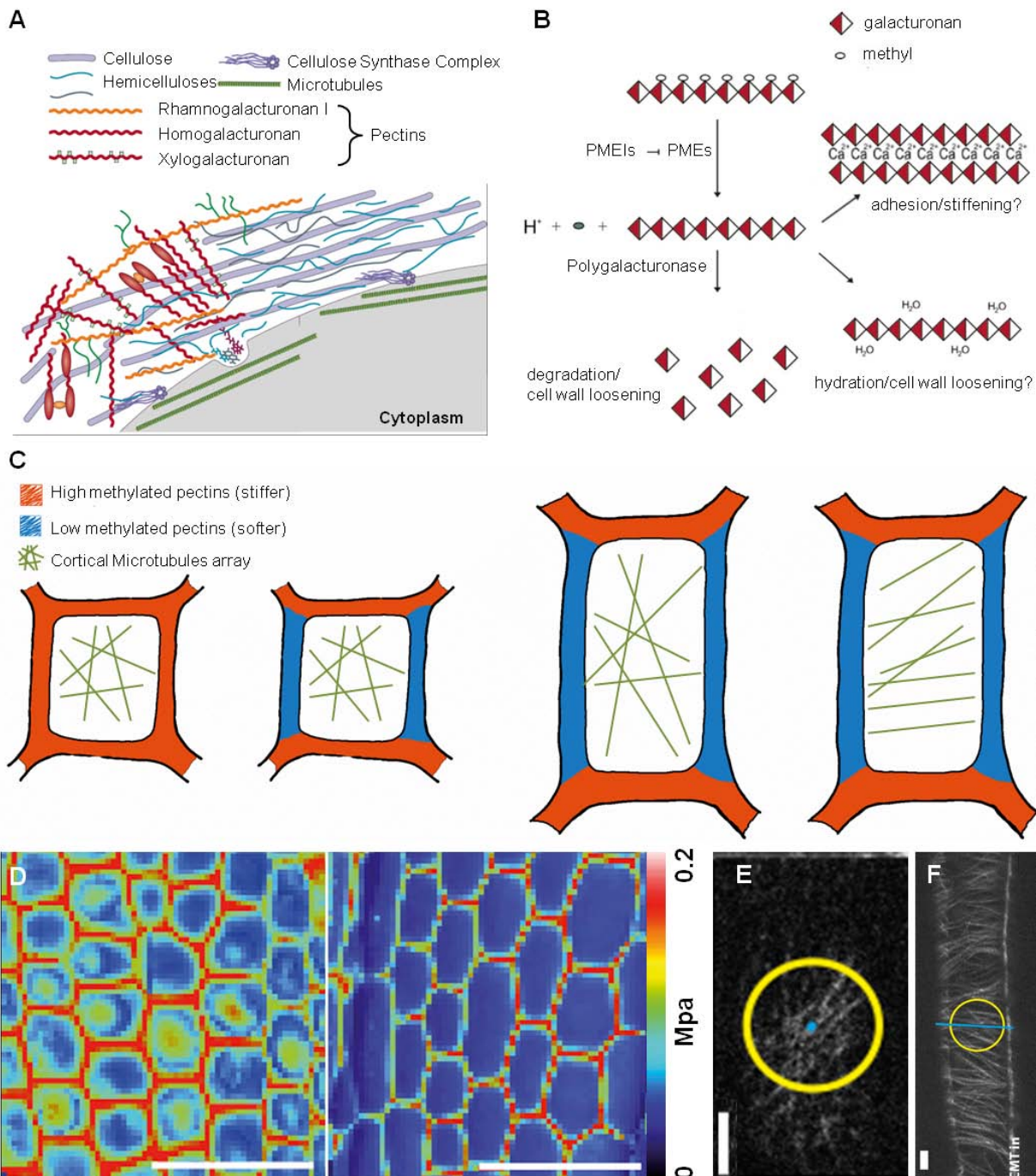


Figure 2: Changes in cell wall properties drive anisotropic cell expansion. Cell wall is a complex matrix of pectins hemicelluloses and cellulose, the orientation of cellulose microfibrils is highly correlated with the main direction of cortical microtubule (CMT) arrays possibly due to interaction between cellulose synthase complexes and CMT (A). Physical properties of homogalacturonan (HG) the main pectin, can be partially changed by its methyl-esterification status (B), HG are demethylated by PMEs, PME activity is inhibited by PMEs. Demethylated HG could be degraded by polygalacturonase, leading to cell wall loosening. Alternatively they could be hydrated potentially leading to softening of the cell wall. Some Ca^{2+} mediated bound can be formed between demethylated HG leading to stiffening of the cell wall. One current view (C) on anisotropic cell growth is that the cell wall is homogeneously stiff due to HG methylation, then HG demethylation softens the longitudinal wall leading to mechanical anisotropy. This mechanical cell wall anisotropy coupled with internal turgor pressure of the cell is the basis for anisotropic growth.

hypothesis is that the optimal concentration triggering a response (i.e. cell growth) is shifted between the two organs (Went, 1937).

Cell expansion is most often anisotropic like in hypocotyl epidermis where it has been shown that both cellulose microfibrils and cortical microtubules are oriented transversely to the main direction of growth. The underlying mechanisms of this coordination could result from a tight connection between microtubules and CELLULOSE SYNTHASE (CESAs) complexes responsible for cellulose microfibrils synthesis. This transversal reorientation of cellulose microfibrils and microtubules has been thought to be the first event in the switch between isotropic to anisotropic growth, but it has also been shown that pectin de-methylesterification of longitudinal walls of hypocotyl cells precedes the shift from isotropy to anisotropy (and the reorientation of cortical microtubules) (Peaucelle et al., 2015). The transverse reorientation of microtubules would prevent radial cell expansion (Figure 2). The regulation of cell wall properties appears to be essential for the control of cell expansion and one might postulate that it is also essential for cytoplasmic growth.

After anisotropic growth has started, the CMT array shifts from isotropic organization to a preferential transverse orientation, this will prevent radial cell expansion. AFM based transverse cell wall stiffness map before and during cell elongation show the softening of longitudinal cell walls **(D)**. Microtubules in the inner cell face of epidermal hypocotyl cells have no main orientation at the beginning of cell expansion **(E)**. CMT array shifts to a preferential transverse direction only after anisotropic growth has started **(F)**. Scale bar in **(D)**: 50 μm . PME: PECTIN METHYL ESTERASE, PME I: PME INHIBITORS. **(A)** is adapted from Cosgrove 2005, **(B)** is adapted from Wolf and Greiner 2012 and **(D to F)** are from Peaucelle et al 2015.

A specific view on plant morphogenesis: Heterogeneity

Having described the main processes and actors involved in plant morphogenesis we can move forward to an integrative view of morphogenesis with an emphasis on an emerging concept in the field: the role of heterogeneity. As first author of this review I took part in every aspects of the work including the choice of the topics, literature survey, writing, conceptualization and realization of the figure.



Heterogeneity and its multiscale integration in plant morphogenesis

Léo Serra, Nicolas Arnaud, Faïçal Selka,
Catherine Rechenmann, Philippe Andrey and Patrick Laufs

Heterogeneity is observed at all levels in living organisms, but its role during the development of an individual is not well understood. Heterogeneity has either to be limited to ensure robust development or can be an actor of the biological processes leading to reproducible development. Here we review the sources of heterogeneity in plants, stress the interplay between noise in elementary processes and regulated biological mechanisms, and highlight how heterogeneity is integrated at multiple scales during plant morphogenesis.

Address

Institut Jean-Pierre Bourgin, INRA, AgroParisTech, CNRS, Université Paris-Saclay, 78000 Versailles, France

Corresponding author: Laufs, Patrick (patrick.laufs@inra.fr)

Current Opinion in Plant Biology 2018, **46**:18–24

This review comes from a themed issue on **Cell biology**

Edited by **Ram Dixit** and **Elizabeth Haswell**

<https://doi.org/10.1016/j.pbi.2018.07.001>

1369-5266/© 2018 Elsevier Ltd. All rights reserved.

Introduction

Heterogeneity^γ (γ=see definition in glossary in [Box 1](#)) is an inherent feature of all living organisms. It is observed at all organization levels and contributes to the function of higher-level structures: diverse molecules interact to form specialized sub-cellular structures that together build cells which, in multicellular organisms, can acquire different identities and form complex organs. Recently, another type of heterogeneity within specific structures, which could at first sight appear homogeneous, has gained attention. For instance, at the organ level, seemingly identical lateral root primordia can be formed by heterogeneous contributions of founder cells [1^{*}]; at the tissue level, *Arabidopsis* leaf epidermal pavement cells are heterogeneous in size and shape [2]; and at the cellular level cortical microtubules (CMT) and cellulose synthase trajectories vary between the different sides of epidermal cells of etiolated hypocotyls [3,4].

With the expansion of quantitative approaches, the number of processes that now appear as involving heterogeneity is rapidly increasing. This raises two major questions: how is heterogeneity generated, and what are its biological consequences? In this review, we discuss some recent insights gained from reports of heterogeneity at different scales and its integration^γ between different functional levels within a plant.

Subcellular processes are sources of heterogeneity

Gene expression is by nature a highly stochastic^γ process [5]. At the whole plant level, gene expression shows noise^γ levels that are under genetic control, but the origin (intrinsic^γ or extrinsic noise^γ) could not be identified [6]. At the individual cell level, gene expression fluctuates over time in leaf cells, mostly as a consequence of extrinsic noise [7^{*}] ([Figure 1](#)), as reported for prokaryotes and other eukaryotes [[7^{*}]]. At the system level, additional levels of noise may arise from the gene regulatory network (GRN) topology. For instance, the noise in the expression of a gene coding for a transcription factor affects the expression of its downstream targets and when TFs target TF genes, noise propagates within the GRN [9]. One way to reduce this propagation relies on redundant regulations by multiple TFs that provide robustness to the transcriptional output of a gene [10,11].

Noise in gene expression can be used to generate heterogeneity in plants. For instance, a link between noise and plasticity in gene expression has been observed in *Arabidopsis* [12]. Noisiness of gene expression is used to drive differentiation during sepal development [13^{**}]. Expression of the ATML1 TF in epidermal sepal cells shows a high level of noise. When ATML1 level exceeds a threshold in receptive cells in the G2 phase, it triggers endoreduplication and hence giant cell formation. This generates a loose pattern within the epidermis where the average proportion of giant cells, but not their position, is determined. This resembles the formation of retinal mosaics in *Drosophila* [14] or the selection of odorant receptors in mammals [15]. Relying on noise in gene expression to control cell fate when a precise pattern is not absolutely required may be more cost efficient than complex deterministic networks.

Stochasticity can also drive heterogeneity in other cellular components such as the cell wall. At the molecular level,

Box 1 Glossary

Heterogeneity is a property of a system that refers to its composite nature or to the variability of the elements that compose this system.

Integration refers to the processes/mechanisms whereby the individual characteristics and behaviors of cells are summed, leading to global growth at the tissue or organ scale.

Noise refers to the random variations in a biological process. For instance, gene expression level can fluctuate over time in a single cell (*intrinsic noise*), or vary between genetically identical cells growing in a homogenous environment (*extrinsic noise*). Noise can be measured by the coefficient of variation, the dimensionless ratio of the standard deviation over the mean.

Intrinsic noise is directly related to the stochasticity of the molecular interactions driving a biological process and occurs without variations in the number of molecules. It differentially affects biological processes of the same kind within a given cell.

Extrinsic noise results from variations in the amount or activity of molecules that drive a biological process. Such variations can be observed between individual cells and affect similarly all the biological processes of the same kind occurring in a cell.

Robustness is an inherent property of a system that provides invariable output in response to input variations or heterogeneity.

Stochasticity refers to a random biological process that cannot be accurately predicted as it is governed by probabilistic laws. Stochasticity is observed in chemical reactions involving multiple partners present at low numbers leading to infrequent interactions.

while overall occurrence of the different monomers in lignin polymers is genetically and developmentally controlled, their precise polymerization pattern in the cell wall appears stochastic, leading to a high diversity of structures [16,17]. At a larger scale, cell walls are also heterogeneous, as a result of biologically regulated processes. In the epidermis of dark-grown *Arabidopsis* hypocotyls, specific loosening of the longitudinal anticlinal cell walls triggers anisotropic cell expansion. It is only in the latter step that CMT arrays and associated cellulose deposition switch to a preferentially transverse orientation to consolidate anisotropic growth [18]. The formation of lobes in *Arabidopsis* leaf epidermal pavement cells involves heterogeneity not only along but also across the cell wall [19**]. In both cases, spatial heterogeneity in the mechanical properties of the cell wall was attributed to heterogeneous distribution of pectins with different chemical properties, which suggests that pectins offer a more versatile way of tuning cell wall mechanical properties than other components such as cellulose microfibrils. These examples illustrate how chemical heterogeneity leads to mechanical heterogeneity, which in turn drives growth anisotropy.

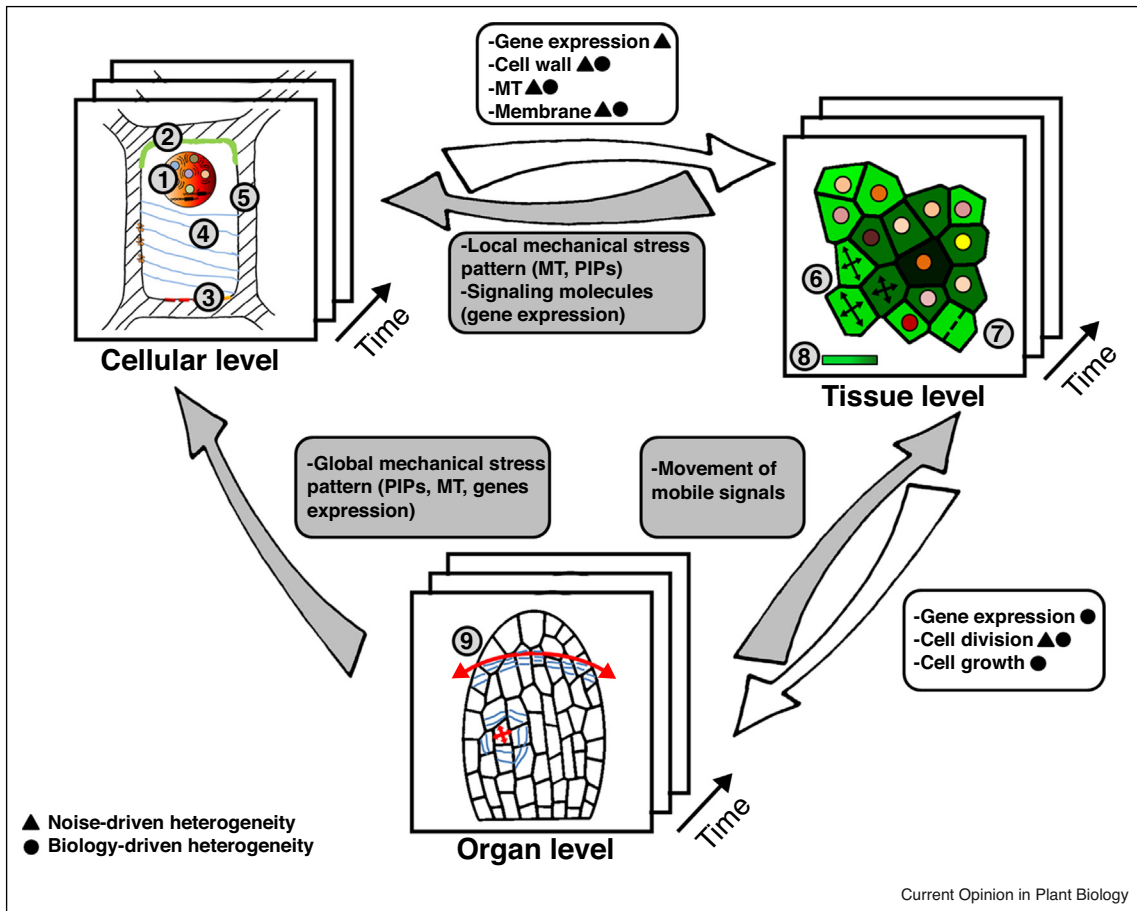
Heterogeneity is also observed in the cell membrane system at multiple scales. Within the plasma membrane, the importance of polar distribution of proteins for patterning processes and physiology has been well demonstrated [20,21]. At the scale of the entire membrane system, rare phospholipids, the phosphatidylinositol-phosphates

(PIPs), are heterogeneously distributed, with the amount of phosphatidylinositol 4-phosphate (PI4P) increasing from the Golgi apparatus to the endosomal compartments to reach a maximum at the plasma membrane [22–24]. The local accumulation of this anionic lipid in the inner layer of the plasma membrane provides negative membrane surface charges, which establish a specific electrostatic identity and direct the plasma membrane localization of proteins such as PINOID or BRI1 KINASE INHIBITOR1 involved in hormone signaling [23,25**]. In animal cells, interaction between cationic residues of membrane protein and PIPs promotes the formation of nanodomains within the membrane [26,27], a mechanism also occurring in plants as the localization of the REMORIN proteins into nanodomains requires PI4P [28**]. This example illustrates the interaction between stochastic physical mechanisms and regulation by biological processes in the generation of heterogeneity at the cellular level.

Cell growth and division are heterogeneous processes

Heterogeneity in cellular patterns progressively appears during the formation of most organs: for instance, in both the developing embryo or in the lateral root primordium, growth and division patterns are initially stereotypical but become later more variable while preserving a stereotypical organ shape and size [1*,29,30]. This suggests that fundamental cellular processes such as division and growth generate heterogeneity in the cellular patterns during development. In the shoot apical meristem (SAM), in which cell size is rather uniform, cell division timing and cell growth are coordinated at the individual cell level by a size-dependent accumulation of cyclin-dependent kinase activity that controls cell cycle progression [31,32**]. Cell division can be described according to a complex rule intermediate between critical size and critical size increment models [33**]. In addition, precision in the orientation of the division plane is controlled by a particular CMT structure, the preprophase band [34**]. Despite these regulatory systems, cell size just after division is variable due to unequal division [32**]. Cell division is an important source of heterogeneity, not only because daughter cells can have unequal sizes but also because of the unequal partitioning of molecules that may increase noise in biological processes such as gene expression [35]. Following an asymmetrical division, the smallest daughter cell grows at a faster rate than the largest one, thus partially compensating for the original difference in size [33**]. A similar observation was made at a larger scale in the sepal, in which smaller epidermal cell lineages grow faster to catch up with larger cell lineages resulting in a homogenization of cell size [36*]. However, at later stages, differences in clone sizes are further amplified by growth. This indicates that mechanisms that integrate cell growth and cell division are acting at the multicellular or organ levels and that they are subjected to developmental regulations. However,

Figure 1



Heterogeneity and its integration over multiple scales in plant morphogenesis. Heterogeneity is found at all levels of the organism, from the cellular to the organ level. At each level, the heterogeneity can be spatial and/or temporal. At the cellular level, gene expression fluctuates over time or can vary from cell-to-cell (1); plasma membrane proteins are polarly distributed (2); distinct phosphatidylinositol-phosphates (PIPs) are found in the membrane system (3) and microtubules (MT) orientation (4) and cell wall composition and structure (5) are variable. At the tissue level, neighboring cells have distinct growth rates and directions (6); cell division is unequal (7) and the concentration of mobile signals varies between cells (8). At the organ level, main directions of mechanical stress vary within the organ (9). This heterogeneity originates either from noise (triangles) or from biologically regulated process (discs). Heterogeneity at a low level impacts the functioning of the higher level (white arrows): for instance, noise-driven heterogeneity between different cells can impact tissue formation. Conversely, the higher level feeds back on the heterogeneity at the lower level (grey arrows): for instance local mechanical stress pattern generated at the tissue level by growth heterogeneity feeds back at the cellular level by impacting MT dynamics.

heterogeneity in cellular processes can paradoxically contribute to robustness^y in development. Indeed, in developing sepals, the variability in cell growth is spatio-temporally smoothed out and this variability is required for the production of organs with reproducible size and shape [37^{**}].

Mechanical stress as a contributor to cell integration

At any scale, heterogeneous growth generates heterogeneous mechanical stresses. At a small scale, in the SAM, mechanical stress can feedback on growth by enhancing heterogeneity between neighboring cells [38]. In developing sepals, mechanical stress generated by the fast growing trichomes leads to a mechanical shielding by

the neighboring cells, thus buffering growth heterogeneity and reinforcing organ shape robustness [39^{*}]. At the organ scale, mechanical stress provides a shape sensing mechanism contributing to the growth arrest at the sepal tip [40]. In addition to feeding back on cell growth, maximal tensile stress affects the orientation of division planes [41] or cell polarity [42], thus pointing to a possible coordination of different cellular processes by mechanical signals and to the existence of multiple morphogenetic loops operating in parallel.

In many of these processes, the dynamic reorientation of CMT upon stress is the main mechanism associated with the multiscale integration of mechanical signals into morphogenesis, although microtubule-independent

stress responses have also been reported [42]. However, how mechanical stresses are translated into CMT dynamics is still unknown. Mechanical stress has been proposed to contribute to the accumulation of PIP in the boundary around organ primordia in the shoot apical meristem, which in turn may impact CMT and signaling, thus possibly forming a multiscale feedback between the organ, tissue and cellular levels [43^{*}]. Mechanical stress could feed into morphogenesis by other pathways. Cell walls and plasma membrane may constitute both sensors and the source of signals. For instance, wall associated kinases and mechanosensitive ion channels are involved in the mechanotransduction pathway [44]. One emerging actor of the mechanotransduction pathway acting at the PM is DEFECTIVE KERNEL 1 (DEK1), a transmembrane protein exhibiting similarity to animal calpains, a class of Ca²⁺-dependent cysteine proteases. The transmembrane domain of DEK1 is required for mechanosensitive Ca²⁺ influx, which in turn promotes the autocatalytic cleavage of DEK1, releasing the C-terminal cytosolic calpain-like domain [45^{**}]. Because this domain is sufficient to complement embryo lethality of *dek1* mutants [46], it suggests that it may act as an integrator of mechanical signals, responding to Ca²⁺. Mechanical stresses have also other effects on the PM, inducing dynamic reorientation of polarly distributed PM associated proteins, like for instance PIN-FORMED1 [47] which may involve Ca²⁺ modulation of the PINOID kinase [48–50]. Finally, mechanical signals contribute also to robust gene expression patterns [51]. In summary, mechanical stress emerges as a signal patterning and coordinating growth at multiple scales.

Communication between cells organizes heterogeneity

Cell-to-cell communication is essential for multicellular organisms and can have opposite effects on cellular heterogeneity. Developmentally regulated symplastic cell-to-cell movement of informative molecules such as proteins, hormones or small RNAs through plasmodesmata contributes to the establishment and maintenance of heterogeneous cell identities or growth patterns [52–54]. One characteristic of such movement is that it can generate gradients of molecules that contribute to heterogeneity at the organ level. For instance, in the SAM, movement of the WUSCHEL protein out of the organizing centre provides cues for the spatial separation between domains of distinct cell fates [55,56^{*}]. Movement of small RNAs produced from the epidermis on either side of the developing leaf establishes clear-cut expression patterns of their targets and hence position a robust developmental boundary in the leaf [57,58,59^{*}]. Based on modeling, it was suggested that diffusing signals emanating from the SAM epidermis could provide the link between SAM geometry and stem cell niche homeostasis [60]. Although these examples illustrate how cell-to-cell communication reinforce heterogeneity,

intercellular movement of proteins can also coordinate growth between different cell layers in the leaf [61]. Because the topology of the mobile signal sources within the organ shapes the gradients, cell-to-cell communication may constitute a feedback loop between organ and tissue heterogeneity. Thus, short range mobile signals contribute to organize the heterogeneity at the organ/tissue scale by enabling the formation of distinct domains or by reducing heterogeneity.

Conclusion and perspectives

During the last years, research on heterogeneity in plants has widely expanded. However, while heterogeneity at the cellular level (mainly cell growth and cell division in relation with the associated mechanical stress) is starting to be characterised, heterogeneity at lower scales is far less studied. In particular, the level and roles of heterogeneity in gene expression as a result of noise in gene transcription and translation are still poorly characterised compared to what is known in other systems [8,62,63].

An emerging conclusion from these studies is that heterogeneity is not only a biologically-generated process but can be a biological readout of noise in elementary reactions. Understanding how the biological context in turn affects the level of noise and what are the constraints it imposes on the translation of noise into a biological response are challenges for the future. These studies also underline the importance of the integration across different scales, with multiple mechanisms allowing either to exploit or on the contrary to buffer heterogeneity from one scale to the other. In this respect it is important to stress that such integration does not only occur from small to large scales but also conversely from organ to the tissue or cell level. Such an integrative view requires a systemic vision of heterogeneity in order to understand its contribution to morphogenesis.

By allowing the objective assessment of noise and cellular heterogeneity together with the prediction of mechanical stresses and growth patterns, image analysis and computational modeling have been instrumental in many studies reported here. The recent advent of deep learning in image enhancement, restoration, segmentation and classification tasks [64] will strengthen and widen the importance of digital image analysis in quantitative cell biology. However, dealing with heterogeneity also introduces new image analysis problems, in particular when it comes to identify principles of organization from noisy spatial image data. Methods based on image normalization and spatial statistics are emerging to address such problems [65,66]. Similarly, it can be anticipated that stochastic modeling approaches will be promoted in the coming years, as deterministic models have shown their limits when addressing noise and heterogeneity in various processes such as cell division [67] or phyllotaxis [68]. An additional challenge for the future will be to shift towards

multiscale models integrating the various dimensions of noise and heterogeneity to better decipher the processes involved in the building of robust organ shapes.

Funding sources

This work was supported by the Agence Nationale de la Recherche grant Serration (ANR-2014-OE11-0018) and by the 'Institut de Modélisation des Systèmes Vivants' of Idex Paris-Saclay (ANR-11-IDEX-0003-02). The IJPB benefits from the support of the LabEx Saclay Plant Sciences-SPS (ANR-10-LABX-0040-SPS).

References and recommended reading

Papers of particular interest, published within the period of review, have been highlighted as

- of special interest
- of outstanding interest

1. von Wangenheim D, Fangerau J, Schmitz A, Smith RS, Leitte H, Stelzer EH, Maizel A: **Rules and self-organizing properties of post-embryonic plant organ cell division patterns.** *Curr Biol* 2016, **26**:439-449.

The authors use light sheet microscopy observations and modelling to analyse the patterns of cell division during lateral root formation in *Arabidopsis*. They show in particular that the initial asymmetric division has long-term effects on division patterns.

2. Asl LK, Dhondt S, Boudolf V, Beemster GT, Beeckman T, Inze D, Govaerts W, De Veylder L: **Model-based analysis of Arabidopsis leaf epidermal cells reveals distinct division and expansion patterns for pavement and guard cells.** *Plant Physiol* 2011, **156**:2172-2183.
3. Crowell EF, Timpano H, Desprez T, Franssen-Verheijen T, Emons AM, Hofte H, Vernhettes S: **Differential regulation of cellulose orientation at the inner and outer face of epidermal cells in the Arabidopsis hypocotyl.** *Plant Cell* 2011, **23**:2592-2605.
4. Chan J, Eder M, Crowell EF, Hampson J, Calder G, Lloyd C: **Microtubules and CESA tracks at the inner epidermal wall align independently of those on the outer wall of light-grown Arabidopsis hypocotyls.** *J Cell Sci* 2011, **124**:1088-1094.
5. Elowitz MB, Levine AJ, Siggia ED, Swain PS: **Stochastic gene expression in a single cell.** *Science* 2002, **297**:1183-1186.
6. Jimenez-Gomez JM, Corwin JA, Joseph B, Maloof JN, Kliebenstein DJ: **Genomic analysis of QTLs and genes altering natural variation in stochastic noise.** *PLoS Genet* 2011, **7**: e1002295.
7. Araujo IS, Pietsch JM, Keizer EM, Greese B, Balkunde R, Fleck C, Hulskamp M: **Stochastic gene expression in Arabidopsis thaliana.** *Nat Commun* 2017, **8**:2132.

Similarly to what was widely done in unicellular organisms, the authors use a dual reporter system to study extrinsic and intrinsic noise in marker gene expression. They show that stochastic gene expression mostly results from extrinsic noise.

8. Raser JM, O'Shea EK: **Noise in gene expression: origins, consequences, and control.** *Science* 2005, **309**:2010-2013.
9. Pedraza JM, van Oudenaarden A: **Noise propagation in gene networks.** *Science* 2005, **307**:1965-1969.
10. Pruneda-Paz JL, Breton G, Nagel DH, Kang SE, Bonaldi K, Doherty CJ, Ravelo S, Gallii M, Ecker JR, Kay SA: **A genome-scale resource for the functional characterization of Arabidopsis transcription factors.** *Cell Rep* 2014, **8**:622-632.
11. Van den Broeck L, Dubois M, Vermeersch M, Storme V, Matsui M, Inze D: **From network to phenotype: the dynamic wiring of an Arabidopsis transcriptional network induced by osmotic stress.** *Mol Syst Biol* 2017, **13**:961.

12. Hirao K, Nagano AJ, Awazu A: **Noise-plasticity correlations of gene expression in the multicellular organism Arabidopsis thaliana.** *J Theor Biol* 2015, **387**:13-22.

13. Meyer HM, Teles J, Formosa-Jordan P, Refahi Y, San-Bento R, Ingram G, Jonsson H, Locke JC, Roeder AH: **Fluctuations of the transcription factor ATML1 generate the pattern of giant cells in the Arabidopsis sepal.** *Elife* 2017, **6**:e19131.

This paper shows that levels of ATML1 fluctuate in sepal epidermal cells and that its level during a specific phase of the cell cycle (G2) determines the fate of the cell. If ATML1 level is above a certain threshold at G2 the cell enters endoreduplication and becomes a giant cell. This exemplifies how noise in gene expression can trigger differentiation and create cellular patterns.

14. Wernet MF, Mazzoni EO, Celik A, Duncan DM, Duncan I, Desplan C: **Stochastic spineless expression creates the retinal mosaic for colour vision.** *Nature* 2006, **440**:174-180.

15. Chess A, Simon I, Cedar H, Axel R: **Allelic inactivation regulates olfactory receptor gene expression.** *Cell* 1994, **78**:823-834.

16. Mottiar Y, Vanholme R, Boerjan W, Ralph J, Mansfield SD: **Designer lignins: harnessing the plasticity of lignification.** *Curr Opin Biotechnol* 2016, **37**:190-200.

17. Zhao Q: **Lignification: flexibility, biosynthesis and regulation.** *Trends Plant Sci* 2016, **21**:713-721.

18. Peaucelle A, Wightman R, Hofte H: **The control of growth symmetry breaking in the Arabidopsis hypocotyl.** *Curr Biol* 2015, **25**:1746-1752.

19. Majda M, Gronos P, Sintorn IM, Vain T, Milani P, Krupinski P, Zagorska-Marek B, Viotti C, Jonsson H, Mellerowicz EJ et al.: **Mechanochemical polarization of contiguous cell walls shapes plant pavement cells.** *Dev Cell* 2017, **43**:290-304 e294.

The authors used atomic force microscopy to reveal mechanical heterogeneities across and along anticlinal walls of leaf epidermis pavement cells and show that it contributes to formation of the lobes of these cells.

20. Naramoto S: **Polar transport in plants mediated by membrane transporters: focus on mechanisms of polar auxin transport.** *Curr Opin Plant Biol* 2017, **40**:8-14.

21. Nakamura M, Grebe M: **Outer, inner and planar polarity in the Arabidopsis root.** *Curr Opin Plant Biol* 2018, **41**:46-53.

22. Kost B, Lemichez E, Spielhofer P, Hong Y, Tolia K, Carpenter C, Chua NH: **Rac homologues and compartmentalized phosphatidylinositol 4,5-bisphosphate act in a common pathway to regulate polar pollen tube growth.** *J Cell Biol* 1999, **145**:317-330.

23. Simon ML, Platre MP, Assil S, van Wijk R, Chen WY, Chory J, Dreux M, Munnik T, Jaillais Y: **A multi-colour/multi-affinity marker set to visualize phosphoinositide dynamics in Arabidopsis.** *Plant J* 2014, **77**:322-337.

24. Hirano T, Stecker K, Munnik T, Xu H, Sato MH: **Visualization of phosphatidylinositol 3,5-bisphosphate dynamics by a tandem ML1N-based fluorescent protein probe in Arabidopsis.** *Plant Cell Physiol* 2017, **58**:1185-1195.

25. Simon ML, Platre MP, Marques-Bueno MM, Armengot L, Stanislas T, Bayle V, Caillaud MC, Jaillais Y: **A PtdIns(4)P-driven electrostatic field controls cell membrane identity and signalling in plants.** *Nat Plants* 2016, **2**:16089.

Building on a set of PIP markers they previously developed [23], the authors show here that PI4P accumulation at the plasma membrane establishes a specific electrostatic field, which in turn controls the PM localization and function of several proteins.

26. Gc JB, Gerstman BS, Stahelin RV, Chapagain PP: **The Ebola virus protein VP40 hexamer enhances the clustering of PI(4,5)P2 lipids in the plasma membrane.** *Phys Chem Chem Phys* 2016, **18**:28409-28417.

27. Remorino A, De Beco S, Cayrac F, Di Federico F, Cornilleau G, Gautreau A, Parrini MC, Masson JB, Dahan M, Coppey M: **Gradients of Rac1 nanoclusters support spatial patterns of Rac1 signaling.** *Cell Rep* 2017, **21**:1922-1935.

28. Gronnier J, Crowet JM, Habenstein B, Nasir MN, Bayle V, Hosy E, Platre MP, Gouguet P, Raffaele S, Martinez D et al.: **Structural**

basis for plant plasma membrane protein dynamics and organization into functional nanodomains. *Elife* 2017, **6**.

Using an impressive broad palette of biophysical methods, super-resolution microscopy and physiology, the authors show that the interaction of the REMORIN protein with PM lipids leads to a conformational change of the protein which stabilizes it into the inner-leaflet of the PM and contributes to its localization in nanodomains.

29. Malamy JE, Benfey PN: **Organization and cell differentiation in lateral roots of *Arabidopsis thaliana*.** *Development* 1997, **124**:33-44.

30. Yoshida S, Barbier de Reuille P, Lane B, Bassel GW, Prusinkiewicz P, Smith RS, Weijers D: **Genetic control of plant development by overriding a geometric division rule.** *Dev Cell* 2014, **29**:75-87.

31. Serrano-Mislata A, Schiessl K, Sablowski R: **Active control of cell size generates spatial detail during plant organogenesis.** *Curr Biol* 2015, **25**:2991-2996.

32. Jones AR, Forero-Vargas M, Withers SP, Smith RS, Traas J, Dewitte W, Murray JAH: **Cell-size dependent progression of the cell cycle creates homeostasis and flexibility of plant cell size.** *Nat Commun* 2017, **8**:15060.

In this paper, the authors investigate the cell size control and show that a size-dependent regulation of CDKs allows cell autonomous coordination of cell size and cell division.

33. Willis L, Refahi Y, Wightman R, Landrein B, Teles J, Huang KC, Meyerowitz EM, Jonsson H: **Cell size and growth regulation in the *Arabidopsis thaliana* apical stem cell niche.** *Proc Natl Acad Sci U S A* 2016, **113**:E8238-E8246.

This study carefully examines several possible rules directing cell size and cell division regulation in the *Arabidopsis* meristem.

34. Schaefer E, Belcram K, Uyttewaal M, Duroc Y, Goussot M, Legland D, Laruelle E, de Tazua-Moreau ML, Pastuglia M, Bouchez D: **The preprophase band of microtubules controls the robustness of division orientation in plants.** *Science* 2017, **356**:186-189.

This paper revisits the role of the PPB during cell division and shows that it is not a causal determinant of the cell division plane but that it adds on independently-defined spatial cues to provide precision in the division plane orientation.

35. Soltani M, Vargas-Garcia CA, Antunes D, Singh A: **Intercellular variability in protein levels from stochastic expression and noisy cell cycle processes.** *PLoS Comput Biol* 2016, **12**: e1004972.

36. Tsugawa S, Hervieux N, Kierzkowski D, Routier-Kierzkowska AL, Sapala A, Hamant O, Smith RS, Roeder AHK, Boudaoud A, Li CB: **Clones of cells switch from reduction to enhancement of size variability in *Arabidopsis* sepals.** *Development* 2017, **144**:4398-4405.

In this study, the authors show that clones in the epidermis of sepals exhibit distinct types of growth depending on the age of the clone and the size of the initial mother cell.

37. Hong L, Dumond M, Tsugawa S, Sapala A, Routier-Kierzkowska AL, Zhou Y, Chen C, Kiss A, Zhu M, Hamant O *et al.*: **Variable cell growth yields reproducible organ development through spatiotemporal averaging.** *Dev Cell* 2016, **38**:15-32.

The authors found that sepals average variations in cellular growth over space and time to achieve constant morphology. They also show that reactive oxygen species interfere with this process by promoting organ maturation.

38. Uyttewaal M, Burian A, Alim K, Landrein B, Borowska-Wykret D, Dedieu A, Peaucelle A, Ludynia M, Traas J, Boudaoud A *et al.*: **Mechanical stress acts via katanin to amplify differences in growth rate between adjacent cells in *Arabidopsis*.** *Cell* 2012, **149**:439-451.

39. Hervieux N, Tsugawa S, Fruleux A, Dumond M, Routier-Kierzkowska AL, Komatsuzaki T, Boudaoud A, Larkin JC, Smith RS, Li CB *et al.*: **Mechanical shielding of rapidly growing cells buffers growth heterogeneity and contributes to organ shape reproducibility.** *Curr Biol* 2017, **27**:3468-3479 e3464.

This paper reveals the mechanical conflict resulting from higher growth rate of trichomes in the sepal epidermis and shows how their mechanical isolation buffers growth heterogeneity to ensure robustness in organ shape.

40. Hervieux N, Dumond M, Sapala A, Routier-Kierzkowska AL, Kierzkowski D, Roeder AH, Smith RS, Boudaoud A, Hamant O: **A mechanical feedback restricts sepal growth and shape in *Arabidopsis*.** *Curr Biol* 2016, **26**:1019-1028.

41. Louveaux M, Julien JD, Mirabet V, Boudaoud A, Hamant O: **Cell division plane orientation based on tensile stress in *Arabidopsis thaliana*.** *Proc Natl Acad Sci U S A* 2016, **113**:E4294-4303.

42. Bringmann M, Bergmann DC: **Tissue-wide mechanical forces influence the polarity of stomatal stem cells in *Arabidopsis*.** *Curr Biol* 2017, **27**:877-883.

43. Stanislas T, Platre MP, Liu M, Rambaud-Lavigne LES, Jaillais Y, Hamant O: **A phosphoinositide map at the shoot apical meristem in *Arabidopsis thaliana*.** *BMC Biol* 2018, **16**:20.

The authors describe the organ-wide distribution of PIPs in the *Arabidopsis* meristem and reveal a correlation with CMT and mechanical stress.

44. Hamant O, Haswell ES: **Life behind the wall: sensing mechanical cues in plants.** *BMC Biol* 2017, **15**:59.

45. Tran D, Galletti R, Neumann ED, Dubois A, Sharif-Naeini R, Geitmann A, Frachisse JM, Hamant O, Ingram GC: **A mechanosensitive Ca²⁺ channel activity is dependent on the developmental regulator DEK1.** *Nat Commun* 2017, **8**:1009.

This paper provides evidences for a role of DEK1 in plant mechanoperception as it shows that DEK1 is necessary for the activity of mechanosensitive Ca²⁺-permeable channel in the PM.

46. Johnson KL, Faulkner C, Jeffree CE, Ingram GC: **The phytoalpain defective kernel 1 is a novel *Arabidopsis* growth regulator whose activity is regulated by proteolytic processing.** *Plant Cell* 2008, **20**:2619-2630.

47. Heisler MG, Hamant O, Krupinski P, Uyttewaal M, Ohno C, Jonsson H, Traas J, Meyerowitz EM: **Alignment between PIN1 polarity and microtubule orientation in the shoot apical meristem reveals a tight coupling between morphogenesis and auxin transport.** *PLoS Biol* 2010, **8**: e1000516.

48. Zegzouti H, Anthony RG, Jahchan N, Bogre L, Christensen SK: **Phosphorylation and activation of PINOID by the phospholipid signaling kinase 3-phosphoinositide-dependent protein kinase 1 (PDK1) in *Arabidopsis*.** *Proc Natl Acad Sci U S A* 2006, **103**:6404-6409.

49. Fozard JA, King JR, Bennett MJ: **Modelling auxin efflux carrier phosphorylation and localization.** *J Theor Biol* 2013, **319**:34-49.

50. Benjamins R, Ampudia CS, Hooykaas PJ, Offringa R: **PINOID-mediated signaling involves calcium-binding proteins.** *Plant Physiol* 2003, **132**:1623-1630.

51. Landrein B, Kiss A, Sassi M, Chauvet A, Das P, Cortizo M, Laufs P, Takeda S, Aida M, Traas J *et al.*: **Mechanical stress contributes to the expression of the homeobox gene in *Arabidopsis* shoot meristems.** *Elife* 2015, **4**:e07811.

52. Vaten A, Dettmer J, Wu S, Stierhof YD, Miyashima S, Yadav SR, Roberts CJ, Campilho A, Bulone V, Lichtenberger R *et al.*: **Callose biosynthesis regulates symplastic trafficking during root development.** *Dev Cell* 2011, **21**:1144-1155.

53. Han X, Hyun TK, Zhang M, Kumar R, Koh EJ, Kang BH, Lucas WJ, Kim JY: **Auxin-callose-mediated plasmodesmal gating is essential for tropic auxin gradient formation and signaling.** *Dev Cell* 2014, **28**:132-146.

54. Wu S, O'Lexy R, Xu M, Sang Y, Chen X, Yu Q, Gallagher KL: **Symplastic signaling instructs cell division, cell expansion, and cell polarity in the ground tissue of *Arabidopsis thaliana* roots.** *Proc Natl Acad Sci U S A* 2016, **113**:11621-11626.

55. Daum G, Medzihradsky A, Suzaki T, Lohmann JU: **A mechanistic framework for noncell autonomous stem cell induction in *Arabidopsis*.** *Proc Natl Acad Sci U S A* 2014, **111**:14619-14624.

56. Perales M, Rodriguez K, Snipes S, Yadav RK, Diaz-Mendoza M, Reddy GV: **Threshold-dependent transcriptional discrimination underlies stem cell homeostasis.** *Proc Natl Acad Sci U S A* 2016, **113**:E6298-E6306.

The paper shows that the stem cell promoting transcription factor WUSCHEL (WUS) regulates CLAVATA3 transcription in a

concentration-dependent manner, activating its transcription at a low level in the central zone of the meristem and repressing it a higher level in the rib zone.

57. Chitwood DH, Nogueira FT, Howell MD, Montgomery TA, Carrington JC, Timmermans MC: **Pattern formation via small RNA mobility**. *Genes Dev* 2009, **23**:549-554.
58. Schwab R, Maizel A, Ruiz-Ferrer V, Garcia D, Bayer M, Crespi M, Voinnet O, Martienssen RA: **Endogenous TasiRNAs mediate non-cell autonomous effects on gene regulation in *Arabidopsis thaliana***. *PLoS One* 2009, **4**:e5980.
59. Skopelitis DS, Benkovics AH, Husbands AY, Timmermans MCP:
 - **Boundary formation through a direct threshold-based readout of mobile small RNA gradients**. *Dev Cell* 2017, **43**:265-273 e266.
 This paper shows that mobile small RNAs can have a morphogen activity through a sharp definition of the expression domain of their target genes.
60. Gruel J, Landrein B, Tarr P, Schuster C, Refahi Y, Sampathkumar A, Hamant O, Meyerowitz EM, Jonsson H: **An epidermis-driven mechanism positions and scales stem cell niches in plants**. *Sci Adv* 2016, **2**:e1500989.
61. Kawade K, Horiguchi G, Usami T, Hirai MY, Tsukaya H: **ANGUSTIFOLIA3 signaling coordinates proliferation between clonally distinct cells in leaves**. *Curr Biol* 2013, **23**:788-792.
62. Eldar A, Elowitz MB: **Functional roles for noise in genetic circuits**. *Nature* 2010, **467**:167-173.
63. Viney M, Reece SE: **Adaptive noise**. *Proc Biol Sci* 2013, **280**:20131104.
64. Angermueller C, Pärnamaa T, Parts L, Stegle O: **Deep learning for computational biology**. *Mol Syst Biol* 2016, **12**:878-894.
65. Arpòn J, Gaudin V, Andrey P: **A method for testing random spatial models on nuclear object distributions**. In *Plant Chromatin Dynamics. Methods in Molecular Biology*, 1675. Edited by Bemer M, Baroux C . Springer; 2018.
66. Biot E, Crowell E, Burguet J, Höfte H, Vernhettes S, Andrey P: **Strategy and software for the statistical spatial analysis of 3D intracellular distributions**. *Plant J* 2016, **87**:230-242.
67. Besson S, Dumais J: **Universal rule for the symmetric division of plant cells**. *Proc Natl Acad Sci U S A* 2011, **108**:6294-6299.
68. Refahi Y, Brunoud G, Farcot E, Jean-Marie A, Pulkkinen M, Vernoux T, Godin C: **A stochastic multicellular model identifies biological watermarks from disorders in self-organized patterns of phyllotaxis**. *Elife* 2016, **5**:e14093.

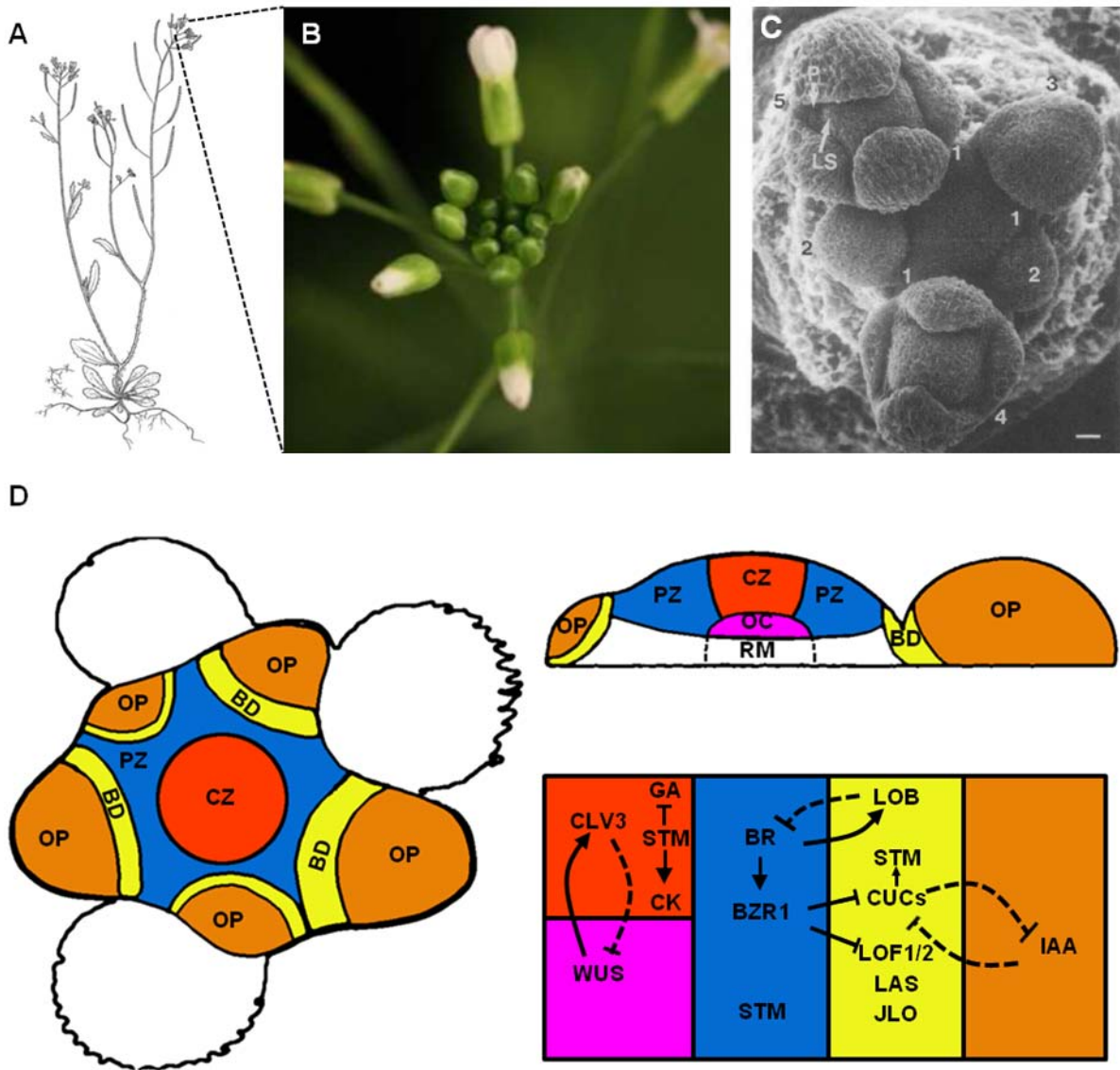


Figure 3: Shoot Apical Meristem (SAM) organization. The SAM located at the tip of the shoot (**A**) is the place of above ground lateral organ initiation like flower (**B and C**). SAM organization is highly stereotypic and is controlled by robust regulatory networks (**D**). OP: Organ Primordia; BD: Boundary Domain; PZ: Peripheral Zone; CZ: Central Zone; OC: Organizing Center; RM: Rib Meristem. CLV3: CLAVATA 3; WUS: WUSCHEL; STM: SHOOTMERISTEMLESS; BZR1: BRASSINAZOL RESISTANT 1; LOB: LATERAL ORGAN BOUNDARY; CUCs: CUP-SHAPED COTYLEDONS; LOF1/2: LATERAL ORGAN FUSION 1/2; LAS: LATERAL SUPPRESSOR; JLO: JAGGED LATERAL ORGAN; GA: Gibberellins; CK: Cytokinins; BR: Brassinosteroids; IAA: Indole Acetic Acid. (C) is from Smyth et al 1990

Differential growth shapes the above ground plant body plan.

Plants, like all living organisms, initiate from a single cell after fertilization, the subsequent increase in cell number results from cell division but the changes in size result only from growth (either cytoplasmic growth comprised in proliferation or true expansion). Changes in shapes result from spatial differences in growth at tissue, organ or whole plant levels, in other words: differential growth. After embryogenesis, all the above ground lateral organs are sequentially initiated on the periphery of a small dome-shaped group of cells located at the tip of the shoot: the Shoot Apical Meristem (SAM). After providing an overview of the functional organization of the SAM, I will introduce information on regulatory networks involved in this organization before presenting the contribution of auxin and CUP-SHAPED COTYLEDON transcription factor in shaping the plant body plan.

Meristem boundaries and primordia

The SAM is a highly stereotypical structure made of domains containing cells with distinct cell fates and functions which are spatially separated. The Central Zone (CZ) is made of slowly dividing cells renewing the stem cell pool; beside the CZ is the Organization Center (OC) which is important for maintaining the CZ identity. Below the CZ and OC lies the rib meristem which gives rise to the main stem and thus drives the formation of the main aerial growth axis of the plant. The Peripheral Zone (PZ) contains cells with higher division rate and is the place of organ primordia initiation. Within organ primordia, cells exhibit a higher growth rate than the surrounding cells and are the place of new growth axis formation resulting in the emergence of new lateral organs. The separation between fast growing organ primordia and the rest of the SAM is marked by a crease-shaped domain: the boundary domain (Figure 3).

The main transcription factors (TFs) sustaining the SAM organization have been intensively studied over the last decades. The CZ is defined by interplay between the WUSCHEL (WUS) mobile TF and the small peptide CLAVATA 3 (CLV3). WUS is expressed in the OC and moves to the CZ where it activates the

expression of CLV3, the binding of CLV3 to a complex made of CLAVATA1-2 triggers the restriction of WUS expression to the OC. This feedback loop prevents the expansion of stem cell identity outside of the CZ (Perales et al., 2016). In the same time, SHOOT MERISTEMLESS (STM) TF that belongs to the KNOTTED-like homeobox (KNOX) gene family is expressed in the CZ where it inhibits cell differentiation through induction of cytokinin (CK) synthesis and repression of gibberellin (GA) synthesis. Local repression of STM in the PZ is associated with initiation and differentiation of organ primordia. The boundary domain is marked by the expression of TFs belonging to distinct families. JAGGED LATERAL ORGAN (JLO) and LATERAL ORGAN BOUNDARY (LOB) (two LATERAL BOUNDARY DOMAIN TFs) are thought to regulate KNOX expression and to reduce growth by downregulating brassinosteroid (BR) synthesis, respectively (Bell et al., 2012). LATERAL SUPPRESSOR (LAS) a member of GIBBERELLIC ACID INSENSITIVE (GAI), REPRESSOR OF GAI (RGA) and SCARECROW (GRAS) TFs are expressed in the boundary and induces formation of axillary meristems (Greb et al., 2003). Another important group of TFs expressed in the boundary domains are the CUP-SHAPED COTYLEDON 1 to 3 (CUC1-3) belonging to NO APICAL MERISTEM (NAM)/ARABIDOPSIS ACTIVATOR FACTORS (ATAF)/CUC (NAC) TFs family, but since they have been of main interest in this project, their role in boundary domain formation will be discussed later in this introduction (see Figure 3 for a map of genetic actors involved in SAM patterning).

Beyond TFs, hormone distribution and signaling play a major role in SAM patterning. Among the hormones reported to have a role in SAM patterning CK, GA and BR are involved but auxin appears to be a master regulator in organ primordia initiation and I will focus on its contribution. Auxin corresponds to a class of molecules able to stimulate coleoptile or stem growth and having a chemical structure derived from tryptophan and exhibiting a short lateral chain ended by a carboxyl group. Indole Acetic Acid (IAA) the most abundant form in plants is a weak acid (pKa 4.85) and can be found as equilibrium between protonated (IAAH) and anionic (IAA⁻) forms depending on the pH. The protonated form can freely diffuse across the plasma membrane whereas the anionic form is unable to cross the membrane. In the apoplast, a weak proportion of IAA is protonated (IAAH) and reaches the cytosol where it dissociates. IAA can also enter the cell via auxin influx carriers belonging to

the AUX1/LAX family which are amino-acid permease-like proteins acting as H⁺ symports. In the cytosol, almost the entire pool of IAA is anionic and can only exit via efflux carriers either from the ABC MDR transporter family or the PIN-FORMED (PIN) family. PIN transporters are often polarly distributed at the PM and their polar localization is dynamically regulated through phosphorylations/de-phosphorylations (Figure 4). The multicellular patterns of PINs enable the dynamic and directional distribution of auxin, creating maxima and minima of auxin within organ and tissue that control cellular responses, differential growth and development. The underlying mechanisms responsible for coordinating PIN1 polarity across multiple cells enabling the formation of auxin fluxes across tissues are supported by various models. The “with the flux” model postulates that PINs polarize according to the flux direction, while the “up to the gradient” model postulates that PINs polarize toward the cell with highest auxin concentration. Both models lack of proposed mechanisms to explain them, the “with the flux” model miss a flux sensing mechanism, while the “up to the gradient” model would require cells to be able to sense the auxin concentration of their neighbors (Bhatia and Heisler, 2018). Auxin distribution via Polar Auxin Transport (PAT) mediated by PIN1 is at the heart of SAM patterning events since both naphthylphthalamic acid (NPA, inhibitor of polar auxin transport) treated plant or null mutant *pin1* exhibit a suppression of flower primordia initiation in PZ. This phenotype can be rescued by local application of IAA at the PZ indicating that local accumulation of IAA in the PZ is required to initiate OPs (Reinhardt et al., 2000; Reinhardt et al., 2003) (Figure 5). Conversely, imaging of auxin signaling input reporter (DII-VENUS based reporters) and auxin transcriptional output reporters (DR5 type reporters) show iterative formation of auxin responses in the PZ prior to organ primordia outgrow (Heisler et al., 2010; Brunoud et al., 2012)(Figure 5). As a consequence of differential growth between organ primordia and surrounding tissue, a circumferential pattern of tensile stress is formed around the growing organ primordia and since tensile stress has been shown to impact polarity of cells (Hamant et al., 2008), PIN1 reorients toward the initiating organ primordia. This particular orientation of PIN1 toward growing primordia contributes to deplete auxin from the rest of the SAM (Heisler et al., 2010), thus enabling the formation of an inhibitory field around the initiated organ primordia preventing any new auxin maxima from being formed. New auxin maxima and subsequent organ primordia will form sequentially at a distance from the previous organ primordia. The auxin depletion associated with

organ primordia initiation contributes to decrease auxin levels in the boundary domain and thus contributes to the activation of the expression of some TFs in the boundary domain, including CUC2 (Vernoux et al., 2000).

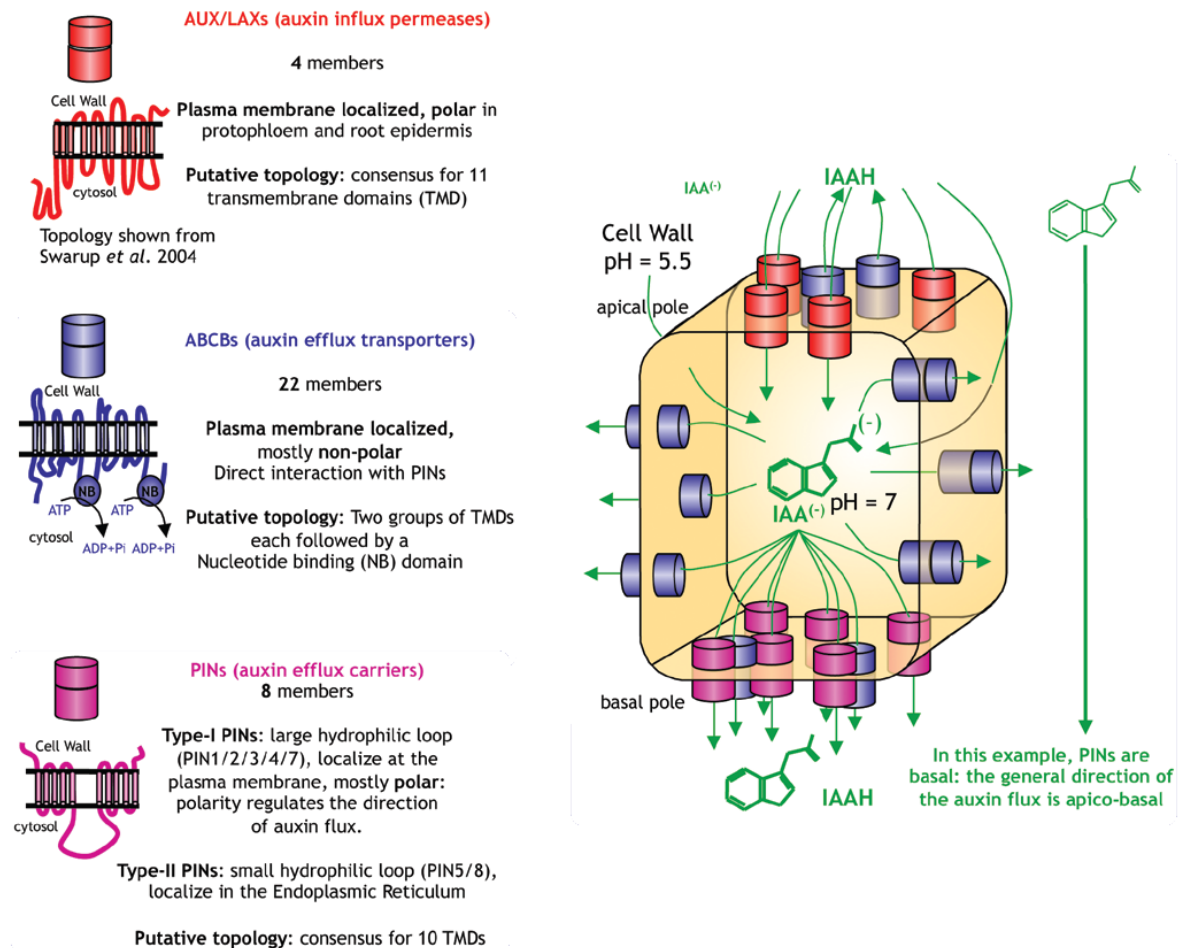


Figure 4: IAA mobility and transporters. Auxin is a weak acid with a pKa of 4.8, it can thus be found in either free anionic form (IAA⁻) or protonated one (IAAH) depending on the pH of the compartment. In the cytoplasm, where the pH is neutral, IAA is mainly found in the free form, while in the apoplasm (which is more acidic) IAA is found both as free and protonated forms. While IAAH can freely diffuse across the plasma membrane, IAA⁻ needs to be transported. Auxin efflux or influx transports are achieved by polarly distributed plasma membrane transporters PINs and AUX/LAX respectively. Other less polar auxin efflux transporters are members of the ABCBs transporters. The overall polarity of transporters allows the flux of auxin to be directional. This figure is adapted from Armengot et al JXB 2016.

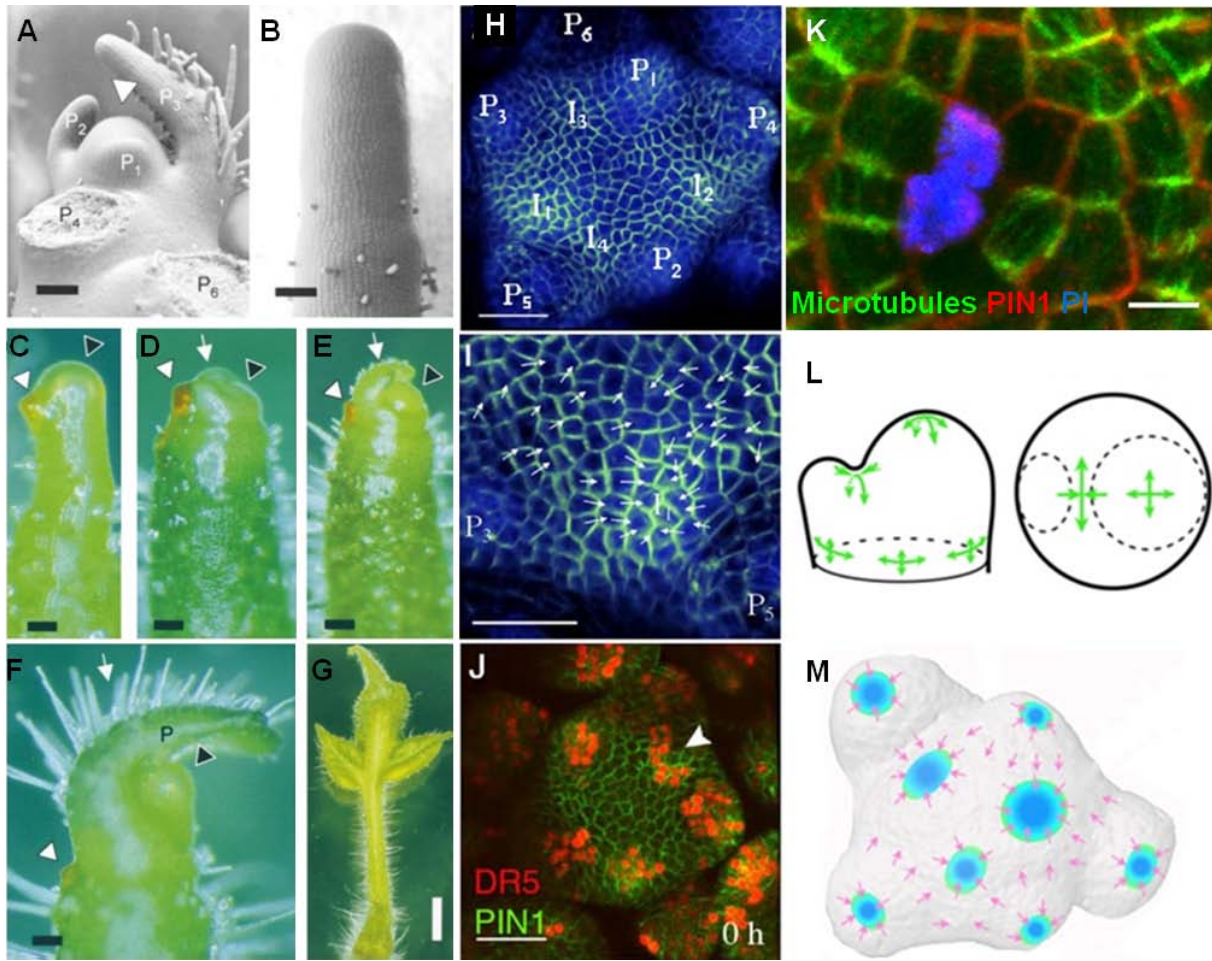


Figure 5: Polar auxin transport, auxin responses and mechanical stress sustain the reiterative organogenesis at the SAM. Organogenesis at Tomato SAM (A) is suppressed by the application of NPA, an inhibitor of polar auxin transport (B). Micro application of IAA in lanolin at the periphery of NPA treated shoot apices restores normal organogenesis (C to G). Arabidopsis SAM expressing PIN1 reporter shows local PIN1 convergence points associated with initiation of primordia (H and I), these local convergence points lead to transcriptional auxin responses visualized with DR5 reporter in red (J). Cell laser ablation induces circumferential pattern of tensile stress and influence polarity of PIN1 as well as the main direction of cortical microtubule array (K), ablated cells have internalized Propidium Iodide in blue, microtubules are in green and PIN1 in red. Schematic representation of mechanical stress pattern at the SAM (N). Simplified representation of auxin responses maxima associated with organogenesis at SAM (auxin in blue, PIN1 polarity in purple). Scale bar: (A to F) 100µm, (G) 0.5cm, (H and J) 30µm, (I) 20µm and (K) 10µm. (A to G) are from Reinhart et al Plant cell 2000, (H to J) are from Heisler et al 2005, (K and L) are from Hamant et al 2008, (M) is from Bhatia et al 2016,

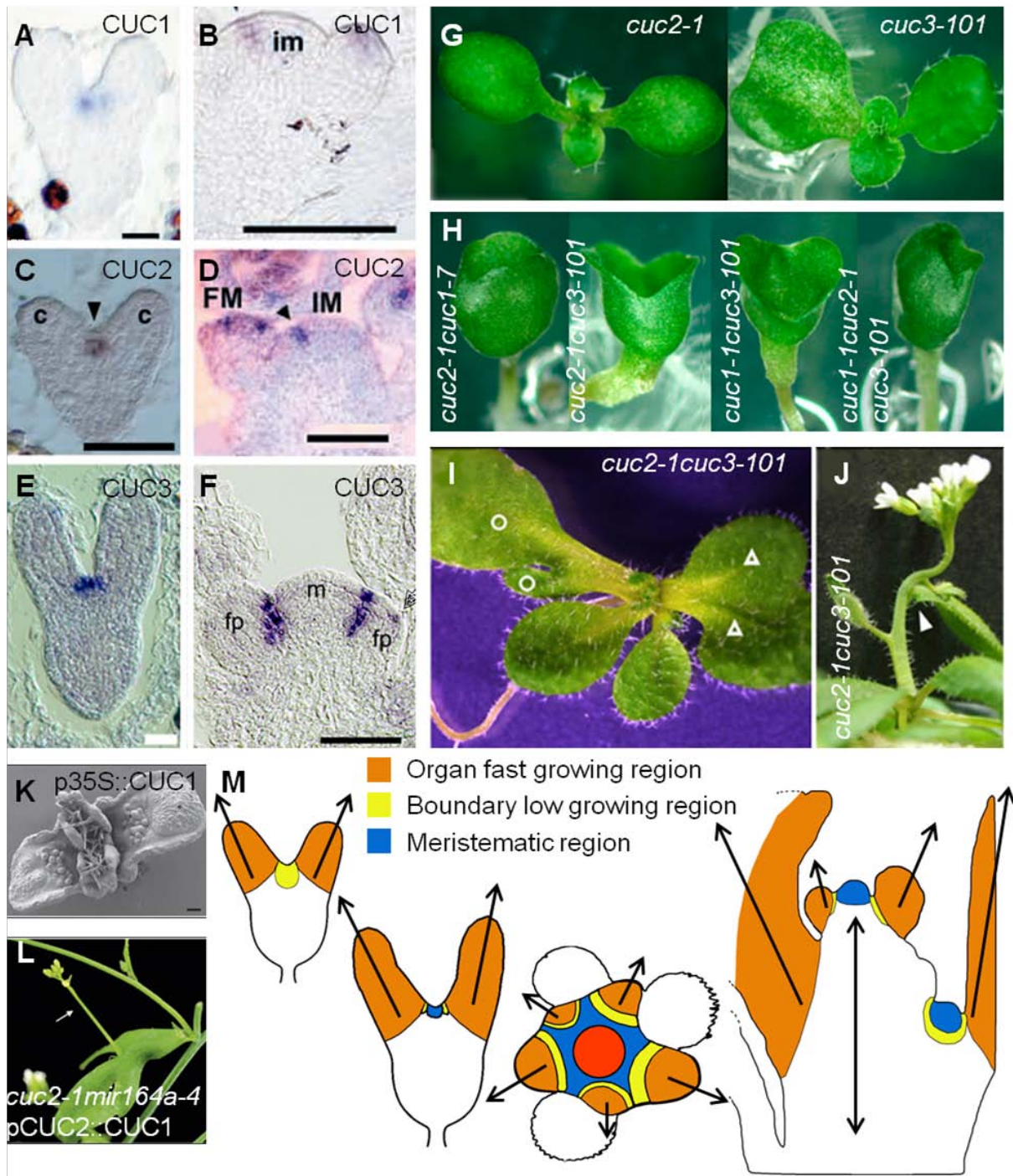


Figure 6: CUCs shape the aerial plant body plan. CUC TFs are expressed in boundary domains between cotyledons and between SAM and organ primordia as it has been revealed by mRNA in situ hybridization (A-F). Due to functional redundancy, *cuc1-7* and *cuc2-1* single mutants have no strong developmental defects (*cuc2-1* seedling in (G), *cuc1-1* not shown), *cuc3-101* mutant exhibit heart-shaped fused cotyledons (G). Double or triple mutants exhibit cup shaped fused cotyledons (H). *cuc2-1cuc3-101* mutant exhibits organ fusion (fused leaves in (I) and a cauline leaf fused with the stem in (J) Ectopic overexpression of CUC1 leads to the formation of ectopic meristem on cotyledons and cauline leaves (K and L).

Role of CUCs in shaping the plant body plan

CUC TFs are a subset of NAC TFs, they have been identified in the 90's and early 2000's in both *Petunia hybrida* and *Arabidopsis thaliana* using forward genetic screens searching for developmental defects (Souer et al., 1996; Aida et al., 1997). In petunia, the *no apical meristem (nam)* mutant has no apical meristem; this phenotype is also observed in the double mutants *cuc1cuc2* or *cuc1cuc3* of *Arabidopsis thaliana* (Figure 6). CUCs are expressed in numerous boundary domains in aboveground parts of the plant including cotyledon-cotyledon, SAM-organ primordia, sepal-sepal, petal-petal, stamen-stamen junctions, between carpels and between ovule primordia (Aida et al., 1999; Ishida et al., 2000; Takada et al., 2001; Vroemen et al., 2003; Goncalves et al., 2015). Except from STM and RAX that has been shown to induce CUC2 expression, rather little is known on the transcriptional regulation of CUC genes. Based on the use of *pCUC2::GUS* reporter, IAA treatment was reported to repress CUC2 expression; such regulation is to be correlated with the presence of auxin responsive elements within the promoter of CUC2 (Galbiati et al., 2013). The interplay between CUC2 and auxin is further supported by the fact that auxin is depleted from places where CUC2 is expressed and CUC2 has been proposed to impact PIN1 polarity, although direct evidences are lacking (Heisler et al., 2005; Bilsborough et al., 2011). In SAM, CUC3 expression has been shown to be induced by mechanical stresses whereas CUC1 is not altered in the same conditions suggesting that CUC genes are regulated through distinct pathways (Fal et al., 2016). Post-transcriptional regulation of CUC1 and CUC2 also affects their expression, their mRNAs being targeted by a microRNA. The MIR164 family comprises three members, *miR164a*, *miR164b* and *miR164c* that are largely functionally redundant. They differ by their expression pattern even if they exhibit overlapping patterns (Sieber et al., 2007). They negatively regulate CUC1 and CUC2 through cleavage of their transcripts thus modulating the level of their targets (Nikovics et al., 2006) (Figure 7) whereas CUC3 mRNA is not susceptible to these microRNAs.

CUCs are required to set differential growth between boundary and organ region (yellow and orange respectively) in embryo and shoots participating in the formation of growth axis (arrows) **(M)**. Through the initiation of meristems (blue) they participate in the formation of new growth axis (arrows). **(A)** and **(B)** are from Takada et al 2001, **(C)** is from Aida et al 1999, **(D)** is from Vernoux et al 2000, **(E)** and **(F)** are from Vreomen et al 2003, **(G) to (J)** are from Hibara et al 2006, **(K)** is from Takada et al 2001 and **(L)** is from Hasson et al 2011.

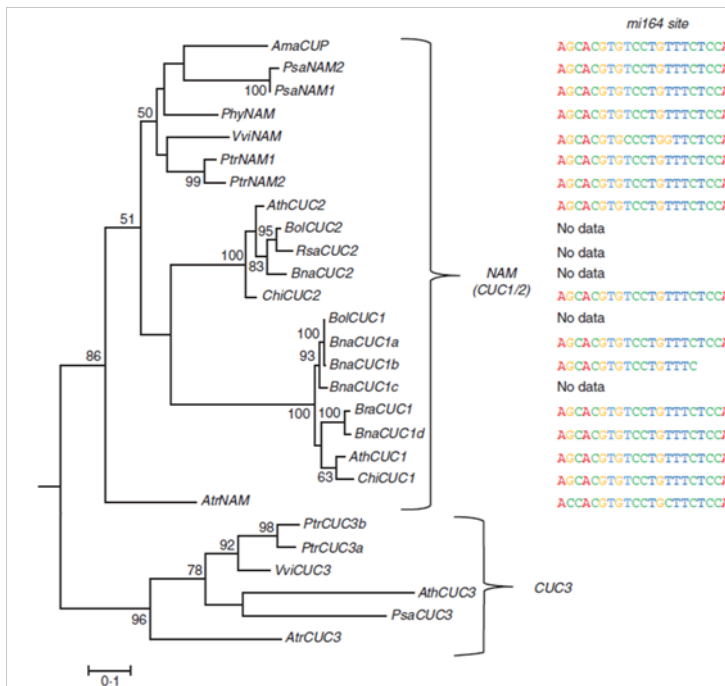


Figure 7: CUCs TF belong to the NACs TF family. Phylogenetic tree of the CUCs TF and their orthologs in some angiosperms show that CUC1 and CUC2 are closely related while CUC3 clade is separated from the NAM CUC1/2 clade. *CUC1* and *CUC2* mRNAs but not *CUC3* mRNA are targeted by the *miR164* whose binding site is given on the right of the tree. This figure is from Vialette Guiraud et al 2010.

Consistently with the localization of *CUC* expression in boundary domains, phenotypes of *cuc2cuc3* double mutants exhibit various organ fusions (cotyledons, leaves, ovules, sepals and stamen) indicating a conserved role of CUC TFs in establishing boundary domains for proper organ separation (Figure 7). Very little is known concerning CUC downstream targets; it has recently been shown that CUC2 indirectly induce the expression of CUC3. CUC2 was also reported to induce expression of KLUH, a Cytochrome P450 able to promote organ growth (Anastasiou et al., 2007; Eriksson et al., 2010; Maugarny-Cales et al., 2019). Boundary domains exhibit specific geometric, cellular and mechanical features. They are shaped in a saddle-way and thus have a negative Gaussian curvature; this result in anisotropic mechanical constraints namely compression. This compression impacts the orientation of cell division plane which are transverse to the main direction of the constraint (Kwiatkowska and Dumais, 2003; Kwiatkowska, 2008; Kwiatkowska and Routier-Kierzkowska, 2009; Landrein et al., 2015). Beside their roles in setting a separation between groups of cells with distinct growth properties (thus participating in differential growth), boundary domains are most of the times a place where new axes of growth appear. Indeed, the boundary between the two cotyledons is the place of SAM initiation, and accordingly, the expression of STM is lost between the two cotyledons in *cuc1cuc2* leading to a failure in SAM initiation (Hibara et al., 2003). Conversely ectopic expression of CUC1 in *Arabidopsis* leaves leads to the formation of ectopic meristems (Takada et al., 2001; Hasson et al., 2011). Lateral branches and flower primordia are initiated from the boundary domain since the axillary meristem and the floral meristem appear within the boundary between the leaf primordium and the SAM. CUCs can thus be considered as regulators of shoot architecture since they contribute to set differential growth and initiating new growth axis (Figure 6).

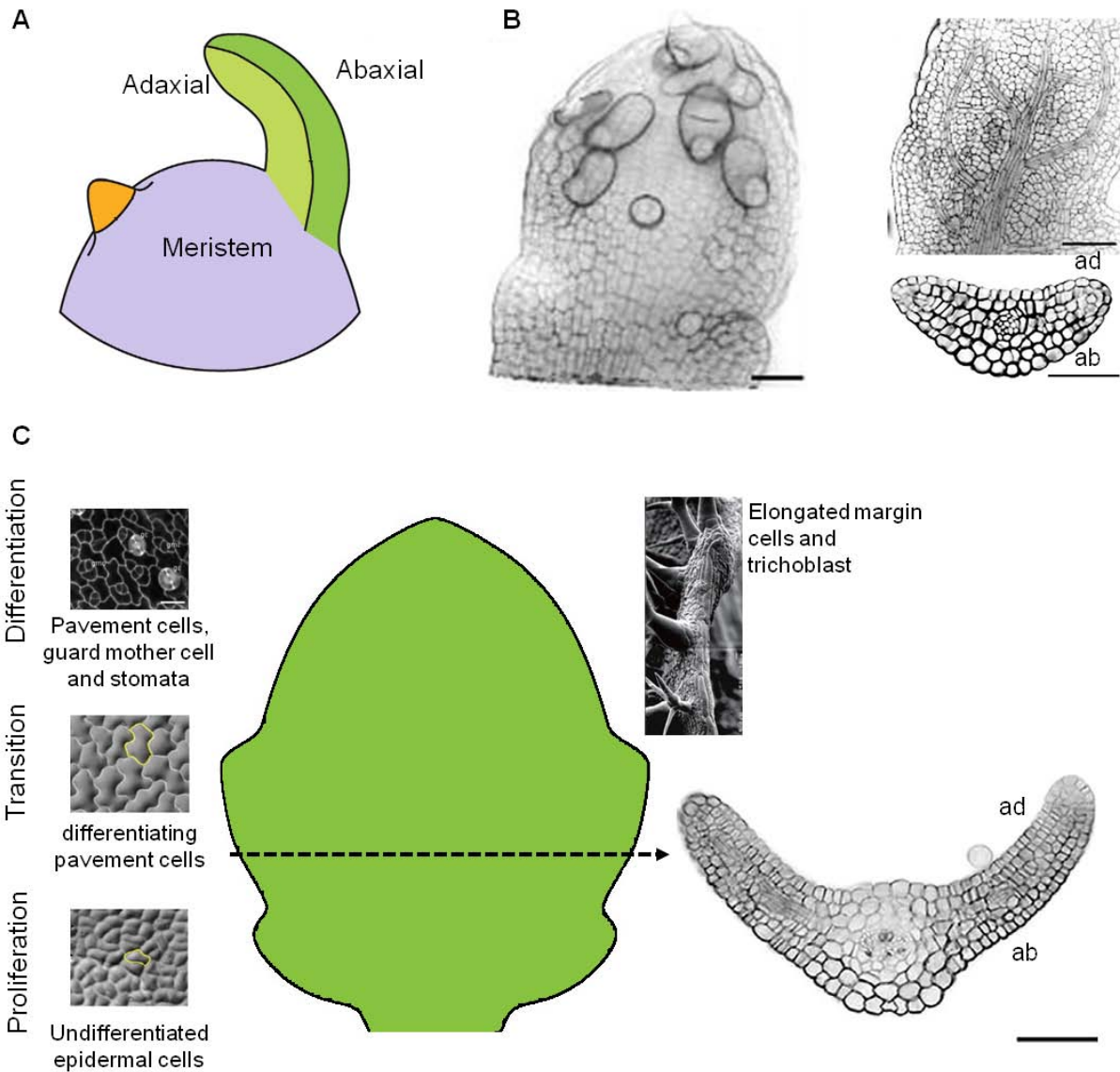


Figure 8: Leaf structural organization and cell types. After initiation in meristem PZ, leaf primordium acquires polarity, the face adjacent to the meristem is named adaxial while the other face is called abaxial (A). Adaxial view of leaf primordia stained with propidium iodide shows epidermal cells and differentiating trichoblasts (B) right. Single longitudinal optical section on the same leaf shows the vascular strands, transverse section shows adaxial epidermis, undifferentiated palisade and spongy mesophyll and abaxial epidermis (from top to bottom) and vascular strands located between the two mesophylls. As the leaf grows, cells progressively differentiate in distinct cell types illustrated around the leaf (C), transverse section show differentiated palisade and spongy mesophylls.

Leaf (margin): a model to study differential growth

Leaves are often the most visible part of plants, and leaf shapes can vary greatly between species. In fact, leaf shape belongs, together with flower features, to the main criteria used by botanists to identify species. Leaves can be simple or compound depending on the level of dissection between the iteratively formed new growth axes (serration or lobes in simple leaves, leaflets in compound leaves). As already mentioned before, leaves can be considered as archetypic organs from which all the aerial part of the plant derives (Goethe), thus understanding leaf development is somehow also understanding plant development (obviously it is an overstatement, but it might be true at least for shoot development). From a growth focused point of view, the Arabidopsis leaf represents a main growth axis (the proximo-distal axis of the blade) with new growth axis periodically initiated at the margin and resulting in serrations. Here, the structural organization of a leaf as well as the main cell types of a leaf will be introduced prior to the presentation of the major regulators and cellular events responsible for setting the leaf main growth axis and the iteratively formed new growth axes.

Structural organization of leaves and associated cell types

Leaves are polarized structures made of distinct cell layers: the adaxial epidermis (adjacent to the meristem), the palisade mesophyll, the spongy mesophyll and the abaxial epidermis and vascular strands developed at the interface between the two mesophylls. Each of these tissues is initially made of seemingly identical undifferentiated cells, then during differentiation, distinct cell types emerge. In Arabidopsis, the adaxial epidermis comprises undifferentiated isodiametric cells at the basis, elongated cells in the middle region, and then a patchy pattern of pavement cells, meristemoids (mother cells of stomata), stomata and trichomes. The abaxial epidermis comprises the same cell types as in the adaxial epidermis except trichomes that appear only on vegetative adult leaves. It also contains a higher number of meristemoids and stomata. Cells of the palisade mesophyll became elongated in the Z axis and cells from the spongy mesophyll increase in volume and some space arise between cells. The leaf contour is made of a file of cells which became elongated during differentiation: the marginal cells (Figure 8).

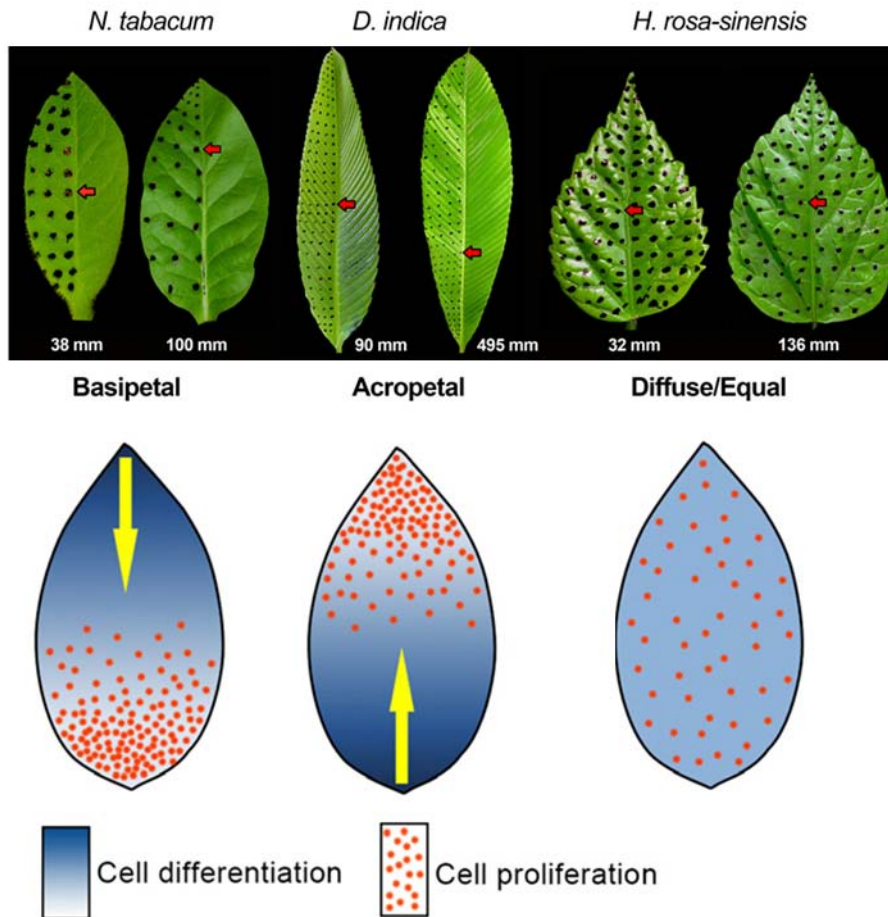


Figure 9: Leaf growth types. Leaf can have distinct gradient of growth as it can be revealed by the deformation of a gird of ink dots at the surface of leaves. *N.tabacum* like *A.thaliana* has basipetal growth gradient, *D.indica* has acropetal growth gradient and *H.rosa-sinensis* has a diffuse growth. Bidirectional growth gradient also exist but not illustrated here. This figure is from Das Gupta et al 2015

Main growth axis and control of leaf size

How a leaf grows has been a longstanding question for scientists studying leaf development, some of them believed leaves grow from the tips (August Trecul 1853), others argue it was from the basis. Like in most scientific controversies, both views were right it just depends on the species. While *Arabidopsis* leaves grow following a basipetal gradient, some other angiosperm species can exhibit acropetal, bidirectional or diffuse growth gradients (Das Gupta and Nath, 2015)(Figure 9). However, the first phase of leaf growth consists in the recruitment of cells from the peripheral zone of the meristem to the leaf primordia. This phase is followed by a proliferative phase which increases both the number of cells and the whole size of the leaf primordia, then cells progressively exit the cell cycle to enter into expansion (except for cells of the stomata lineage for which this is delayed). In *Arabidopsis*, this transition between cell proliferation and cell expansion occurs basipetally (from the tip to the basis of the leaf). Changes in either the number of founder cells recruited into the primordia or the rate of proliferation do not usually impact the final leaf size due to the existence of compensatory mechanisms. On the other hand, changes in timing of proliferation arrest affect the final organ size (Donnelly et al., 1999; Kazama et al., 2010; Andriankaja et al., 2012; Fox et al., 2018). The progression of proliferation arrest front is controlled by a set of regulatory modules, including TEOSINTE BRANCHED1/CYCLOIDEA/PROLIFERATING CELL NUCLEAR ANTIGEN FACTOR 1 (TCPs), GROWTH REGULATING FACTORS (GRFs) and micro RNAs (Kalve et al., 2014) (Figure 10). Class I TCPs promote proliferation and cell growth (Herve et al., 2009; Kieffer et al., 2011) while class II TCPs promote cell expansion by the indirect activation of Arabidopsis Responses Regulator 16 (ARR16, a negative regulator of Cytokinin signaling pathway) (Efroni et al., 2008; Efroni et al., 2013). Class II TCPs also up-regulate miR396 that restricts the expression of GRFs proliferation promoting factors to the basal part of the leaf. The entry into cell expansion is associated with endoreplication and plants with impaired capacity to enter into endoreplication are affected in both leaf cell size and leaf size (del Pozo et al., 2006). Relative to the duration of leaf development, the longer the proliferative phase will be the more complex the leaf will be. Indeed the transition from proliferation to differentiation has been shown to be delayed in compound leaves in

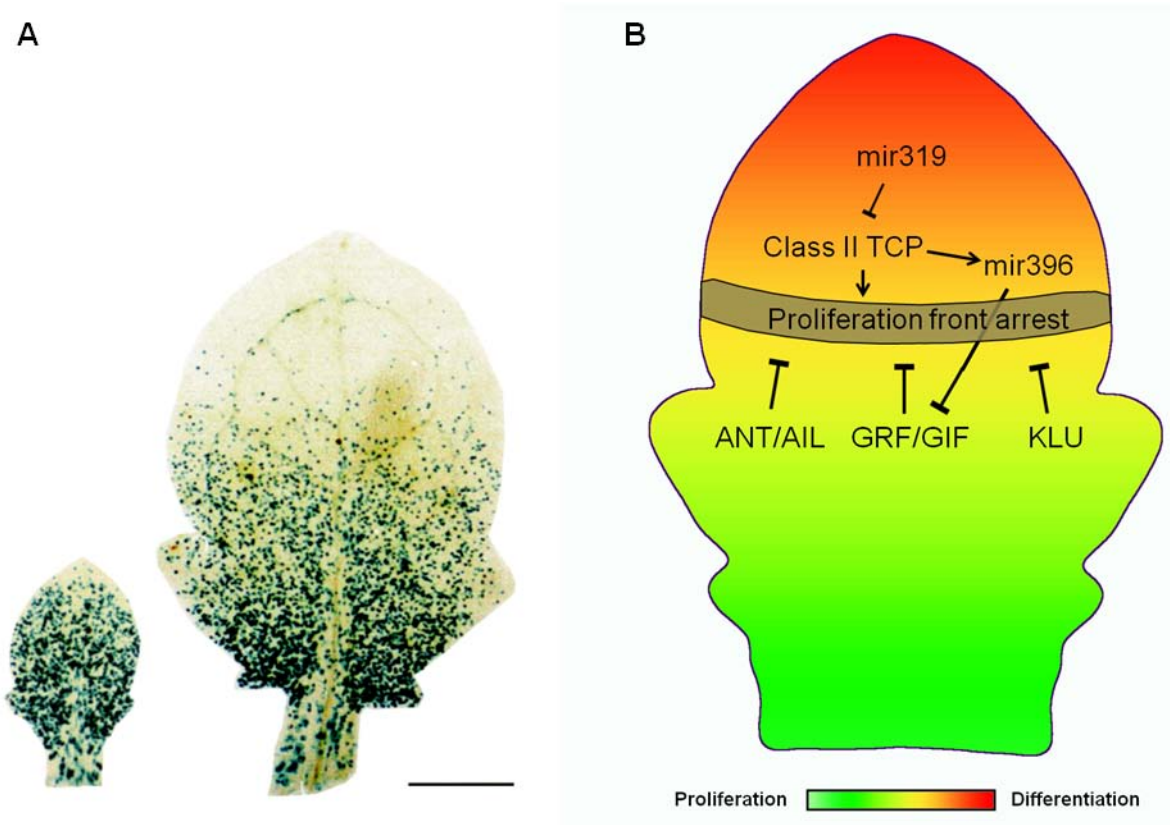


Figure 10: In *Arabidopsis* leaf the shift between proliferation and differentiation progresses basipetally. Cyclin B1: GUS reporter shows the proliferation zone in *Arabidopsis* leaves (A). The progression of the proliferation front arrest involves genetic actors, some of them are summarized in (B). TCP: TEOSINTE BRANCHED1/CYCLOIDEA/PROLIFERATING CELL NUCLEAR ANTIGEN FACTOR 1, ANT: AINTEGUMENTA, AIL: AINTEGUMENTA-LIKE, GRF: GROWTH REGULATING FACTORS, GIF: GRF-INTERACTING FACTORS, KLU: KLUH. (A) is from Donnelly et al 1999. Scale bar: 500 μ m

comparison to simple leaves. Conversely a down regulation of genes promoting the transition from proliferation to differentiation leads to a more complex leaf shape in *Arabidopsis* (Alvarez et al., 2016). In accordance with this view, some genetic actors involved in differentiation delay like STM and BREVIPEDICELLUS (BP) are expressed in *C. hirsuta* compound leaves but not in *A. thaliana* simple leaves (Rast-Somssich et al., 2015). Thus the regulation of proliferation and expansion impacts both leaf final size and leaf shape complexity, the latter relies on the iterative formation of new growth axis at the leaf margin; the actors and mechanisms associated with the formation of these new growth axis are developed in the following part.

New growth axis at the leaf margin

Leaves can display a range of various shapes depending on the number and orders of new growth axes formed. These new growth axes rely on differential growth and the intensity of this differential growth determines the nature of the new growth axis. To make it simpler, let's consider a conceptual leaf growing following the proximo-distal axis, let's now consider differential growth occurring at the margin, if the difference of growth is low, it will give rise to serration or lobe; if the difference is high, it will give rise to leaflets. For instance *Arabidopsis* leaves are simple with a serrated margin while in its close relative *Cardamine hirsuta*, differential growth is more pronounced and as a consequence, the leaves are composed of leaflets. These two leaves have one order of dissection (serrations or leaflets). Some leaves can have two or more orders of dissection, *Solanum lycopersicon* leaves for instance are composed of leaflets and each of these leaflets are serrated, they thus have two orders of dissection (leaflets being the first and serrations on leaflets the secondary) (Figure 11).

In *Arabidopsis*, serrations (called either tooth/teeth or serration/serrations hereafter) are flanked by grooves called sinuses. These serrations, representing new growth axis, are sequentially initiated in a basipetal way along the margin (the first

initiated pairs of teeth being distal to the following ones) and they tend to be progressively smoothed when the leaf grows and matures. Depending on the leaf

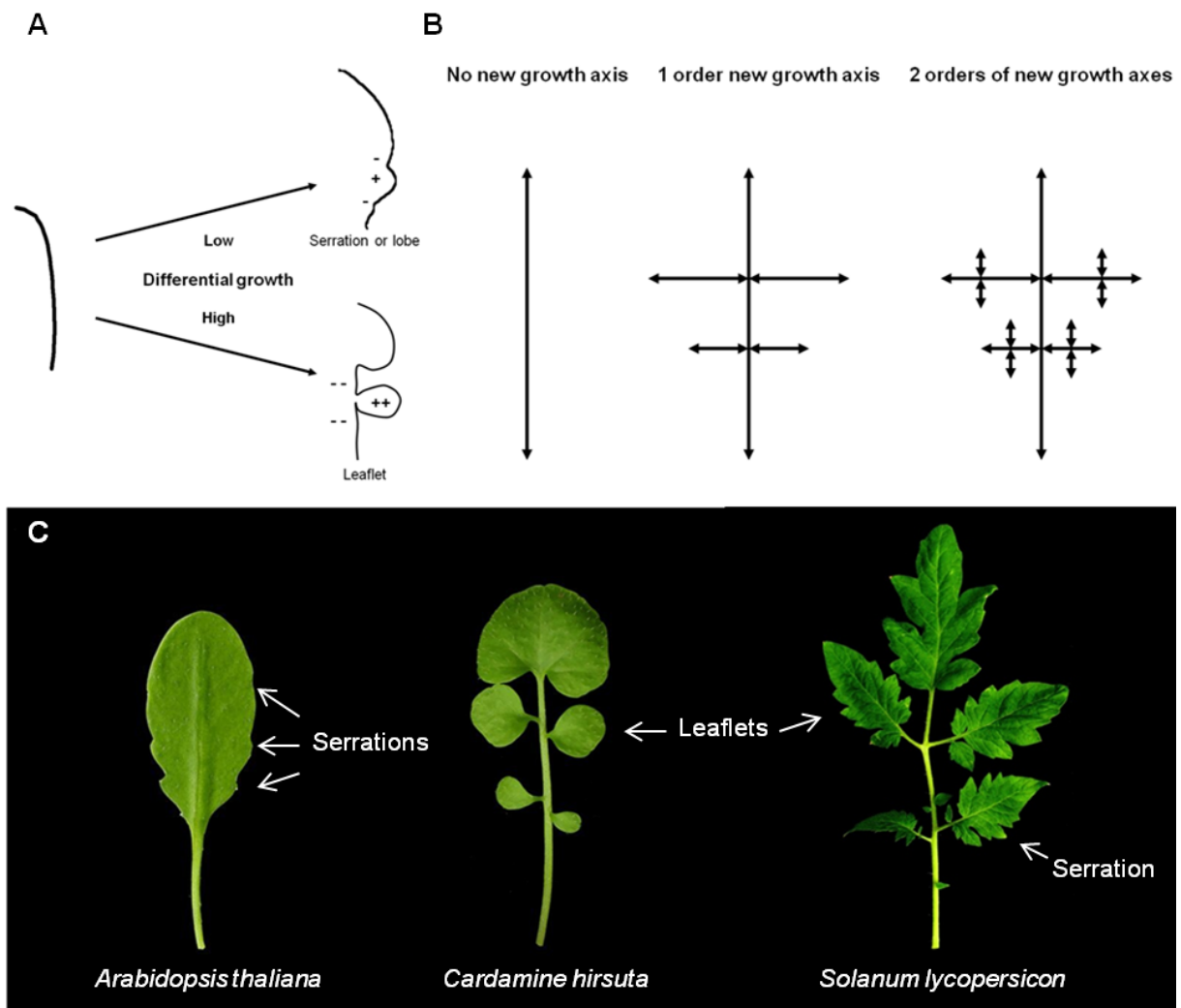


Figure 11: Intensity, number and order of differential growth shape the leaves. Differential growth generates new growth axes at the margin of leaves, depending on the differences between low and high growing regions the outgrowth will be a serration/lobe or a leaflet (**A**). The order of new growth axes formed by differential growth defines the level of complexity of the leaf (**B**). Differential growth produces serrations at the margin of *A.thaliana* leaves, more pronounced differential growth results in leaflet formation in *C.hirsuta* leaves and two orders of differential growth give rise to serrated leaflets in *S.lycopersicon* leaves (**C**).

rank, the positioning and the shape of the teeth vary, probably due to differences in the transition between proliferation and expansion. These differences sustain heteroblasty: the differences in leaf shape between distinct ranks of the same plant (Figure 12) (Biot et al., 2016). These new growth axes shaping the leaf resemble the formation of organ primordia and boundary domains at the PZ of SAM since they result from the interplay between CUC TFs and auxin. In *Arabidopsis*, only *CUC2* and *CUC3* are expressed in the leaf and are both located in sinuses. While the *cuc2-1* null mutant has a smooth margin indicating *CUC2* fundamental requirement for teeth initiation, *mir164a* mutant or transgenic lines expressing a *CUC2* miRNA insensitive form (*CUC2gm4*) both exhibit highly serrated margins. The *cuc3-105* mutant still initiates serrations but they tend to be smoothed very early and the adult leaf is nearly smooth (Figure 13) suggesting a role for *CUC3* in maintaining the differential growth at the leaf margin (Hasson et al., 2011).

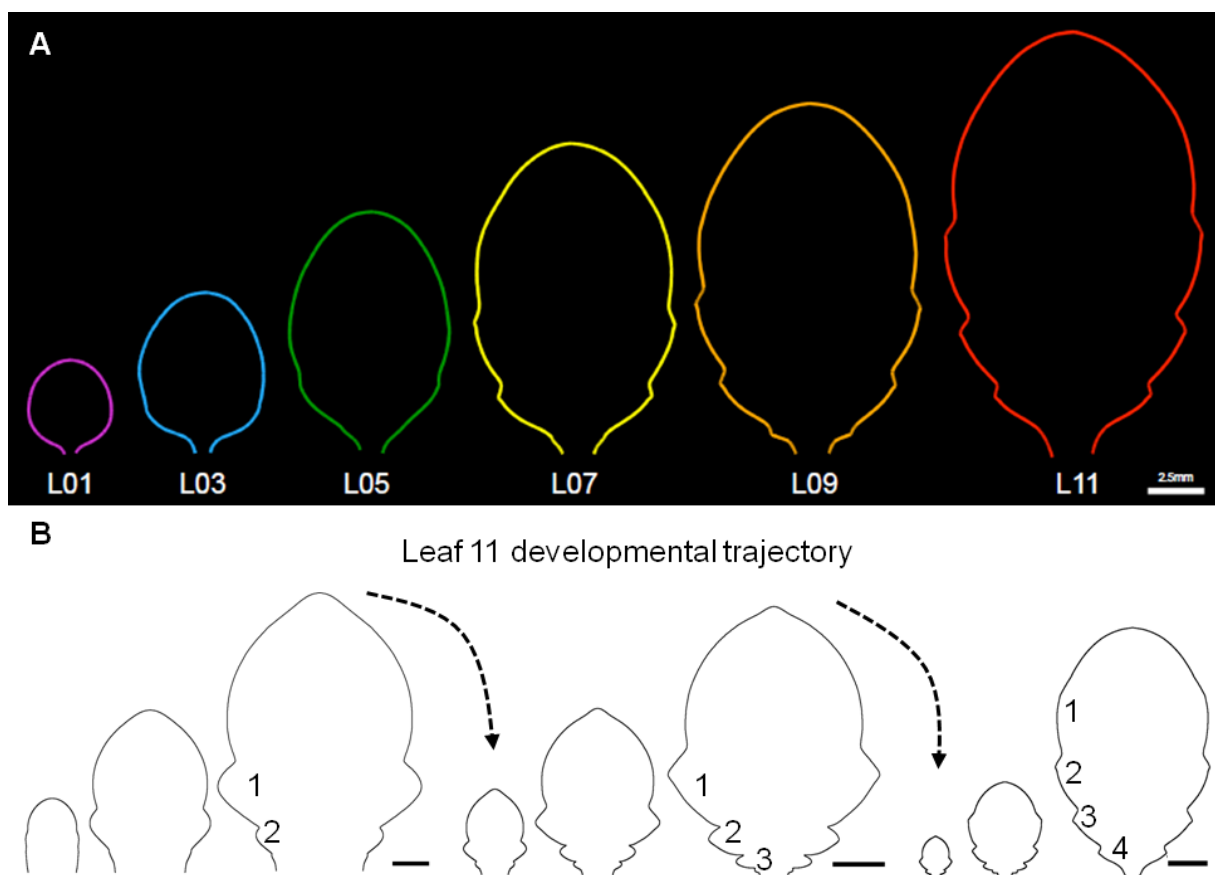


Figure 12: Arabidopsis heteroblasty and developmental trajectory of leaf 11. Mature leaf of distinct ranks exhibits distinct shapes (A). As leaf grows, its shape changes with the sequential initiation of teeth at its margin, these teeth themselves undergo changes in shape and the first pair of teeth becomes completely smoothed by the end of leaf development (B). (A) is from Biot et al 2016. Scales bars in (B): 100µm, 200µm and 1000µm from left to right.

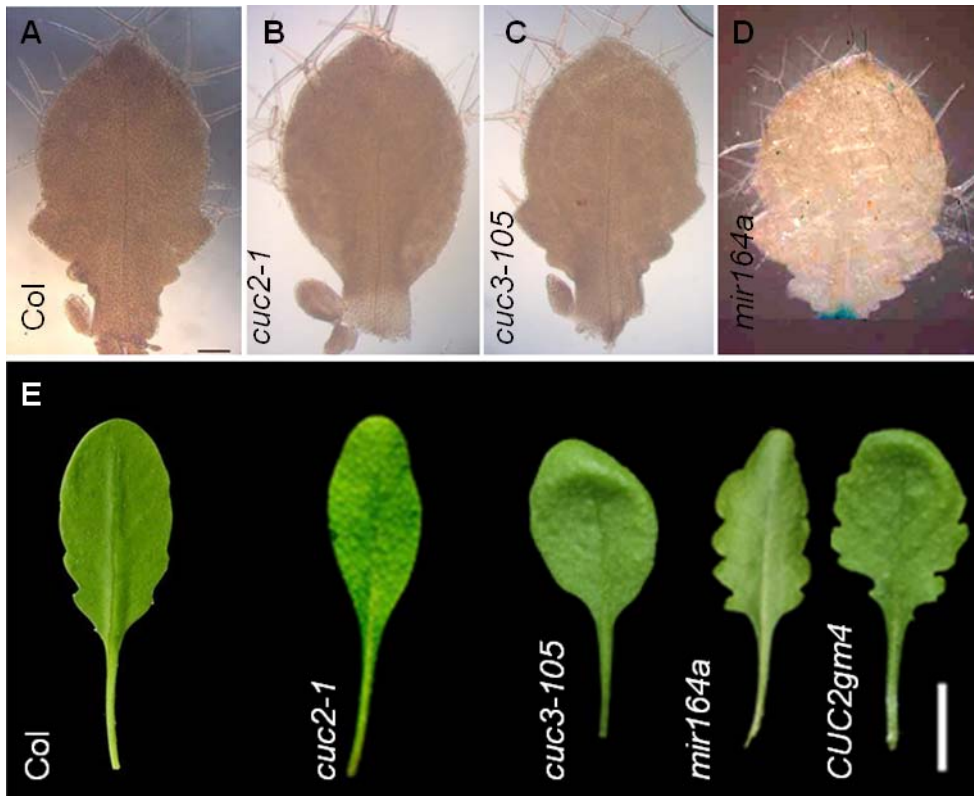


Figure 13: CUCs related leaf phenotypes. Phenotypes of young leaf primordial for Col-0, *cuc2-1*, *cuc3-105*, and *mir164a* (A to D). Phenotypes of matures leaves of the same genotypes and transgenic line expressing a miRNA insensitive version of CUC2 (*CUC2gm4*) (E). Images for this figure are from Hasson et al 2011.

Leaf margin morphogenesis is intimately linked with the patterning of vascular network since they both require tight control of the directional flux of auxin. PIN1 is initially expressed in epidermis and marginal cells with a polar localization toward the tip of the primordium; this broad expression pattern becomes restricted to the margin allowing a unidirectional flux of auxin from the basis to the tip of the primordium. As a consequence of auxin accumulation, an auxin response zone is set at the tip of the primordia and auxin is internalized from the tip of the primordia to the meristem. This auxin canalization precedes the differentiation of the mid vein (Scarpella et al., 2006; Marcos and Berleth, 2014; Verna et al., 2015). Local expression of CUC2 at the margin contributes to reverse PIN1 polarity at the leaf margin by an unknown mechanism, leading to the formation of a local auxin accumulation proximal to an auxin depleted zone. The local auxin accumulation leads to an auxin internalization from the margin toward the existing mid vein via PIN1 mediated PAT. Concomitantly the local auxin accumulation at the margin is translated in transcriptional responses including CUC2 repression thus creating an interspaced pattern of auxin responses and CUC2 expression along the margin. This pattern ultimately leads to growth promotion and growth restriction at least at initial stages (Bilsborough et al., 2011) (Figure 14). It should be noted that if local PIN1 polarity convergence points at the margin are always associated with auxin internalization toward the preexisting vein thus participating in leaf vascular patterning, these convergence points are not always associated with the formation of new growth axis. Accordingly, *pin1* mutant or plants treated with NPA exhibit strong leaf vascular defects as well as a range of leaf phenotypes. These phenotypes comprise leaf fusions, aberrant pattern of auxin responses at the leaf margin associated with small outgrowth: when they are not fused, mature leaves exhibit a smoothed margin (Kawamura et al., 2010; Bilsborough et al., 2011). The influence of CUC2 and CUC3 in shaping leaf dissection is conserved across species, since either mutations or decreased expression of their orthologues in other species (*C.hirsuta*, *Solanum lycopersicon*, *Aquilegia caerulea*, *Solanum tuberosa* and *Pisum sativum*) lead to simplification in leaf dissection (Blein et al., 2008). Additionally it has been shown that the same interplay between CUCs, PAT and auxin response described in *A.thaliana* is responsible for initiating new growth axis on leaves of other species (*Solanum* and *Cardamine*) (Koenig et al., 2009). To date the specific contribution of CUC3 on leaf serration and auxin has not been investigated. Beyond genetic understanding of leaf morphogenesis, very few

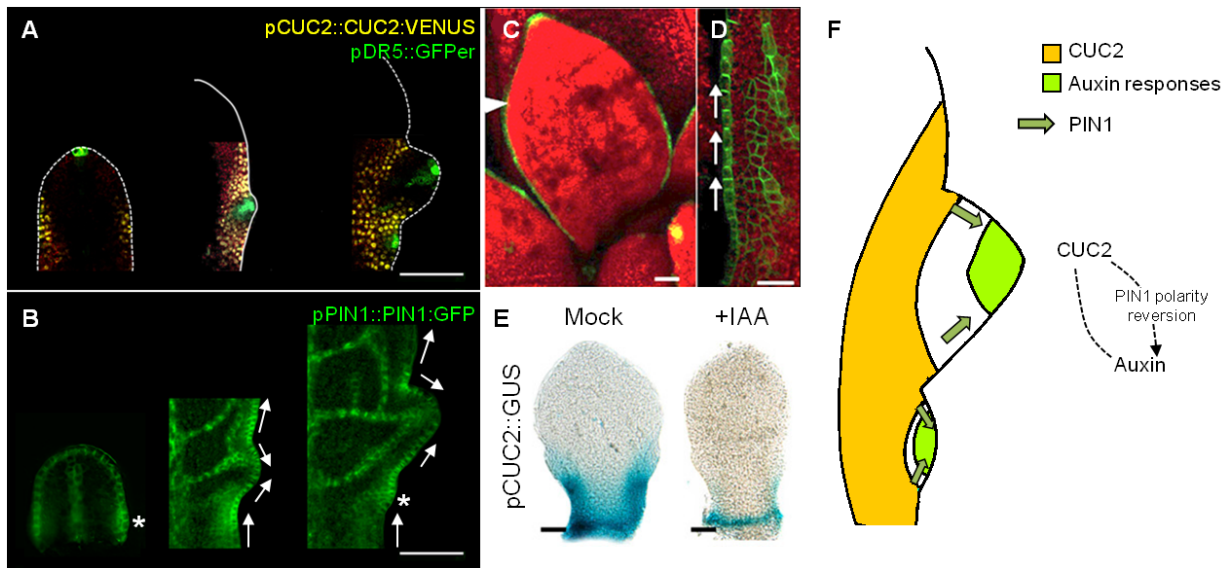


Figure 14: Interplay between CUC2 and auxin initiates serration at the leaf margin. CUC2 and auxin response form an interspaced pattern along the leaf margin, this pattern occurs iteratively during leaf development **(A)**. At the leaf margin, polarity of PIN1 initially allow an unidirectional flux of auxin from the basis to the tip of the leaf, then as leaf grows, PIN1 convergence points are sequentially set at the margin allowing local auxin accumulation and initiation of serrations **(B)**. Auxin responses are continuous along the smooth margin of *cuc2-1* **(C)** pDR5::GFP (in green), and auxin flux mediated by PIN1 is unidirectional from the basis to the tip of the leaf **(D)** pPIN1::PIN1:GFP (in green). IAA treatment ends in restriction of CUC2 expression pattern to the basis of the leaf **(E)**. Working model from these experimental evidences is that CUC2 expressed in sinuses indirectly reverts PIN1 polarity, locally depleting auxin and allowing the formation of local auxin maxima at the leaf margin, auxin in turn represses CUC2 expression (by a yet unknown mechanism); this interplay allows the formation of the above mentioned interspaced pattern and thus defines high growing (serrations) and low growing (sinuses) region. **(A, C, D and E)** are modified from Bilsborough et al 2011, **(B)** is modified from Alvarez et al 2016. In **(A),(B)** and **(D)**, images are single optical sections approximatively at the middle of the leaf, **(C)** is a 3D view.

studies have been focused on the cellular basis of differential growth shaping leaf margins. Static imaging of *Arabidopsis* leaves has revealed that some cell files seem to align with the main axis of the teeth (Kawamura et al., 2010). More recently comparative studies between *Cardamine hirsuta* (a close relative to *A.thaliana* with compound leaves) and *A.thaliana* using time lapse imaging on leaves have revealed a causal role for Reduced Complexity (RCO) TF of *C.hirsuta* in leaf dissection. RCO results from Late Meristem Identity 1 (LMI1) gene duplication which has been lost in *A.thaliana* and the mutation of RCO in *C.hirsuta* is sufficient to change its leaflets into lobes, the difference between these two morphologies was explained by an increase in both division event numbers and expansion area in the inter leaflet region of the mutant (Vlad et al., 2014). Leaves thus represent a model to study differential growth in plant shoots and more precisely the contribution of CUCs to differential growth.

Main objective of the project

Thanks to the many progresses in both live imaging and quantitative data processing, we are now entering a time where multiscale integrative understanding of plant development is accessible. Scientists of past centuries would not have dreamed of being able to follow the growth of an organ with a cellular resolution over several days. To date, we can have access to various information at the same time, including dynamics of gene expression, pattern of hormone responses or changes in physico-chemical properties of the cell wall. Anyway, the goal here was to take advantage of these technical advances to increase our knowledge on plant morphogenesis, in particular to determine the cellular basis of differential growth at the leaf margin. We used a combination of time-lapse and static imaging of the serrated margin of *A. thaliana* leaf to investigate the cellular basis of differential growth at the leaf margin of *Arabidopsis* from initiation to tooth outgrowth and later on tooth smoothing. The role of CUC3 in these responses was investigated using gene expression reporter and genetic tools and its influence on auxin responses was also explored. The corresponding data and quantitative analyses constitute the main part of my PhD work and are presented hereafter as a draft of a manuscript that we expect to submit soon in a peer-reviewed scientific journal after consolidation of the data with a set of

experiments using conditional *CUC3* overexpressing lines. A second chapter of results corresponds to the exploration of the implication of the TIR1/AFBs auxin co-receptors in leaf morphogenesis. Since auxin signaling was not described in details in this introduction, this chapter is including an overview of the present knowledge on auxin signaling and leaf development. We plan to combine these data with a set of data relative to mapping of ARFs during leaf serration that have been generated in the context of another thesis work. A global discussion on the outcomes of this thesis work and perspectives will be presented. To sustain some aspects of the discussion and perspectives, very preliminary results on apoplastic pH on leaf cells will be included in order to help proposing a model of the role of CUCs and auxin in shaping the leaf margin in particular and the aerial part of plant in general.

Chapter II: CUC3 mediates differential growth at the leaf margin by reducing cell growth

CUC3 mediates differential growth at the leaf margin by reducing cell growth.

Léo Serra^{1,2}, Patrick Laufs¹ and Catherine Perrot Rechenmann¹

¹ Institut Jean-Pierre Bourgin, INRA, AgroParisTech, CNRS, Université Paris-Saclay, RD10, 78026 Versailles Cedex, France.

² - -Saclay, 91405 Orsay, France

SUMMARY:

How a shape arises from the coordinated behavior of cells is one of the most fascinating questions in developmental biology. Here we used the early stages of development of serrated leaves in *Arabidopsis thaliana* as a model to study the tight relation between cellular behavior and morphogenesis. During *Arabidopsis thaliana* leaf development the fine control of cell proliferation and cell expansion sustains differential growth at the margin required for the formation of leaf outgrowth named teeth. In this model, differential growth is the result of interplay between auxin signaling and CUP SHAPED COTYLEDONS (CUCs) transcription factors that are involved in the maintenance of boundary domain identity. To clarify the interconnected relations between patterns of CUC TFs and auxin responses as well as the cellular events behind serrations we used time-lapse experiments on vegetative primordia of lines expressing developmental and/or auxin response reporters. Our results allowed us to describe the sequence of cellular events associated with leaf serration. In addition we showed that CUC3 TF is a negative regulator of cell growth and that its dynamic expression is tightly associated with the control of differential growth at the leaf margin.

INTRODUCTION:

Cells of multicellular living organisms are, roughly speaking, quite similar, and yet all organisms exhibit a range of various shapes. In plants, since there is no cell migration and very little cell death, cells can thus undergo only two types of processes: cell proliferation, that combines cell division which is the partitioning of one cell into two daughter cells and cell growth which is the increase in cell volume, and cell expansion that consists in an increase in size of cells that have exited cell division and is often associated with endoreplication and differentiation processes. At tissue, organ and whole plant levels, growth results from the combination of proliferation and expansion; spatial and temporal regulations of growth then sustain

differential growth across the body plant, which are the basis for morphogenesis. In the above ground parts of a plant, organogenesis takes place in the Shoot Apical Meristem (SAM). Small groups of cells within the SAM peripheral zone exhibit high level of growth and give rise to organ primordium. These cells are spatially isolated from the rest of the meristem by a small group of low dividing and growing cells forming the boundary domain (Dumais and Kwiatkowska, 2002; Kwiatkowska, 2004). Genetic approaches have shown that CUP-SHAPED COTYLEDONS (CUCs) transcription factors are involved in the initiation and maintenance of these boundary domains, disruption of two of the three CUCs ends in various organ fusions (Aida et al., 1997; Aida et al., 1999; Vroemen et al., 2003). In addition to expressing CUC TFs, the boundary domain has been shown to be depleted in the “growth promoting” hormone auxin. Apart from the SAM, boundary domains are found in numerous sites in plants separating organs between them (Aida and Tasaka, 2006). Expression of CUCs is found in each of these sites, indicating a conserved role for CUCs in the establishment of the boundary domains in the aerial part of the plant.

CUCs are also expressed in leaves between leaflets in compound leaves or in sinuses between serrations in simple leaves. Regardless of the species when CUCs are mutated the resulting phenotype is always a simplification of leaf dissection indicating that their roles in leaf morphogenesis is conserved across species (Blein et al., 2008). The formation of new growth axis at the leaf margin, serration in simple leaf or leaflet in compound leaf, is the result of interplay between CUCs and auxin, CUC2 being expressed in a discontinuous pattern at the leaf margin interspaced with sites of transcriptional auxin responses. It has been shown that CUC2 is required to form local convergence point of the auxin efflux transporter PIN1 at the leaf margin and subsequent local accumulation of auxin leading to transcriptional responses including repression of CUC2 ending in the above mentioned interspaced pattern (Bilsborough et al., 2011). In *Arabidopsis thaliana* simple leaf, apart from CUC2, CUC3 is the only other CUC being expressed although with a slightly different pattern. CUC2 has a broad expression at the leaf margin and in the inner tissues with a maximum in the region of sinuses whereas CUC3 is expressed only in few cells of the epidermis at the sinuses. While *cuc2-1* loss of function leads to a smooth margin, *cuc3-105* mutant still initiates serrations but they tend to be smoothed earlier during leaf development. This is reminiscent to the smoothing of the first pair of teeth at the end of wild-type leaf development (Hasson et al., 2011; Biot et al., 2016). This particularity makes leaf serrations a unique model to study the relative contribution of CUCs to the regulation of differential growth within an organ with determinate growth. Except from one study in *Cardamine hirsuta* where it was shown that REDUCE COMPLEXITY transcription factor (RCO) was responsible for reducing growth between leaflet by acting on both cell growth and division (Vlad et al., 2014), the cellular basis for differential growth at the leaf margin is still scarcely described.

In plants, the epidermis has been shown to play a preeminent role in morphogenesis and development, since it represents the outermost layer of organs

(Malivert et al., 2018). As a consequence epidermis is under tension due to the containments of the inner compressed tissues. Changes in its mechanical properties can thus underlie changes in organ morphologies. In addition numerous mutants with aberrant morphogenesis can be complemented by restoring the expression of the impacted genes only on the epidermis (Reinhardt et al., 2007; Billsborough et al., 2011). Here using a combination of 3D imaging and time lapse experiments on leaf primordia of *Arabidopsis thaliana* we analyzed cellular behaviors at the abaxial epidermis and leaf margin at early stages of leaf development. We revealed that local reduction of cell growth mediated by CUC3 is required to maintain a differential growth at the leaf margin sustaining the growth of serrations. We further showed that CUC3 influences the pattern of auxin response and that repression of growth is released when CUC3 expression decreases.

RESULTS:

Spatial differences in cell growth sustain differential growth at the leaf margin.

In order to answer the longstanding question of cellular events occurring behind differential growth at the leaf margin, we used 3D imaging and time lapse experiments on lines expressing *p70::PIP2-GFP*, a plasma membrane marker (Luu et al., 2012) (Figure 1A) to analyze cell behavior during early stages of teeth formation. Cell segmentation and growth analyses were performed using MorphoGraphX software (Barbier de Reuille et al., 2015) completed by homemade pipelines aiming at identifying and analyzing cellular or clonal parameters (see Figure S1 for image analyses pipeline). For each experiment, the first step was to determine, in a reproducible manner, cells of the abaxial epidermis belonging to sinus and tooth, respectively. To do so we took advantage of geometric features of the leaf margin. Teeth are dome-shaped whereas sinuses are saddle-shaped; they thus exhibit positive and negative gaussian curvature, respectively. Once sinuses belonging cells have been identified based on the mean gaussian curvature of the leaf surface (measured per cell), we then defined the teeth as the portion of epidermis comprises between two successive sinuses on the margin side. For time lapse experiments, we identified these two cell populations at the beginning of the experiment (time zero) to further define sinuses and teeth derived clones at the following time points (at 24 and 48 hours, Figure 1B). We then performed quantitative measurements on size, division and growth on these two types of clones (Figure 1). As anticipated, differences in clone size increase between sinus and tooth during tooth outgrowth, with sinus derived clones being smaller than the tooth derived ones (Figure 1C and 1F). To determine whether this difference results from reduced division or reduced cell growth we analyzed the number of division events occurring per clone from time zero to 48h and computed the Relative Surface Increase (RSI) over the same time frame. The number of cell division event was not significantly different in sinus in

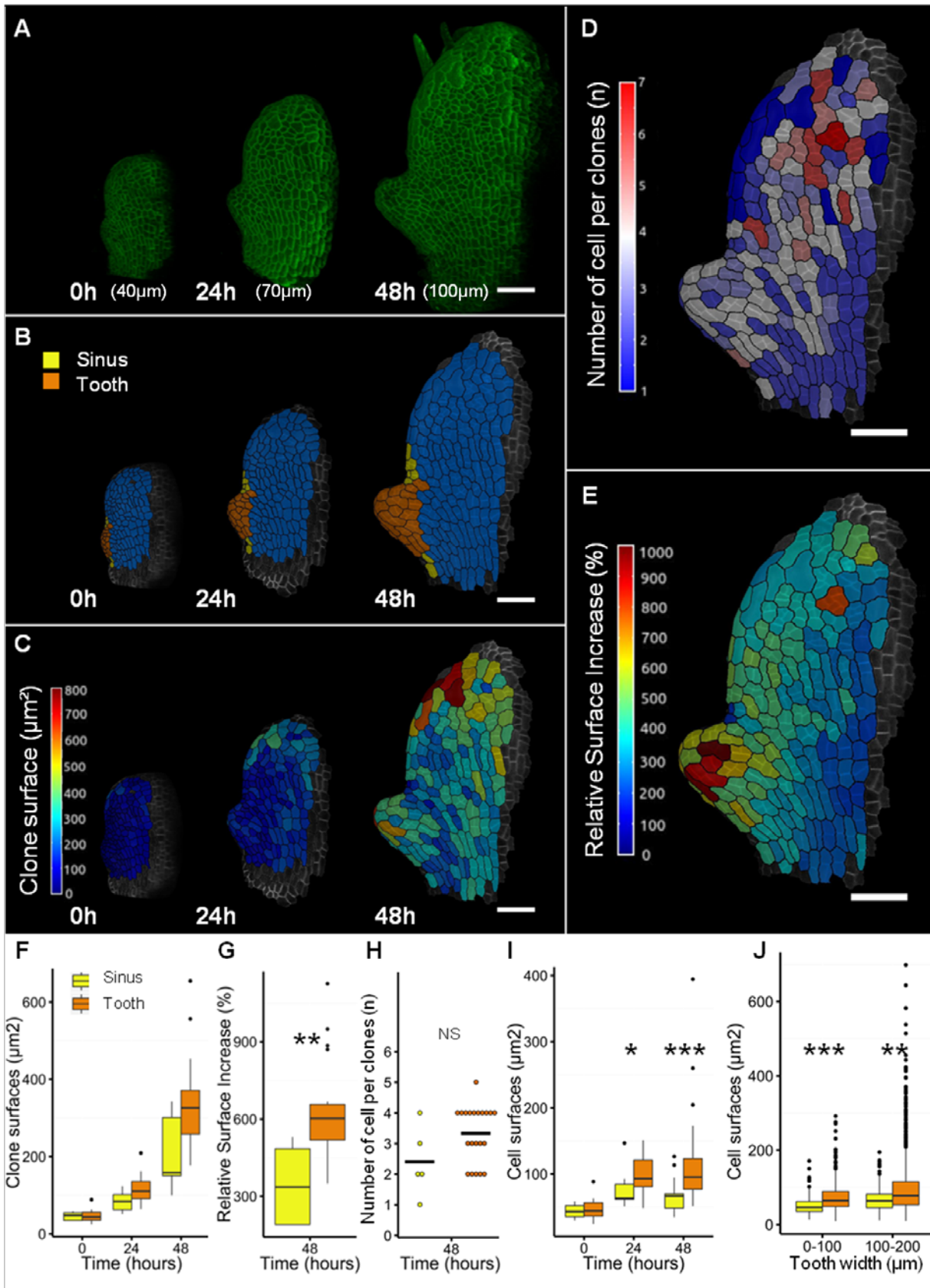


Figure 1: Low cell growth at sinuses is responsible for tooth arising at leaf margin.

comparison to the tooth (2-3 cells per clones in sinus, 3-4 in tooth Figure 1H), indicating that spatial differences in number of cell division events is not responsible for differential growth during this developmental window (Figure 1D). During this developmental frame (40µm to 100µm in tooth width) clones resulting from a single cell within the tooth area exhibit an average increase in surface area over 48h that is twice the one of a sinus clone over the same time frame (Figure 1E and 1G). To complete these analyses, we measured cell surfaces in sinuses and tooth at each time point and found significantly smaller cells in sinuses (Figure 1I). To further confirm these results and avoid potential bias resulting from time lapse experiments, we looked at the distribution of cell surfaces in sinuses and tooth and plotted the results according to the width of the teeth (20 leaves were used per classes of measurements). We found that there is always a significant difference in cell surfaces between sinuses and teeth (Figure 1J). Altogether these results indicate that during the early stages of teeth formation, serration results from cell growth reduction of dividing cells.

CUC3 expressing cells of the CUC2 expression domain exhibit reduced cell growth.

To figure out the link between expression patterns of CUCs and differential growth occurring during leaf morphogenesis, we combined live-imaging and time lapse experiments on lines carrying transcriptional reporters for CUC2 and CUC3. We first normalized mean projected signal intensities of CUC2 and CUC3 reporters then applied a threshold on these normalized signals to classify cells into three domains: CUC2 expressing cells, CUC2 and CUC3 expressing cells named CUC2 and CUC2/3 hereafter and cells expressing neither CUC2 nor CUC3 assigned as noCUC cells (Figure 2A-D). We then measured the area of CUC2 and CUC2/3 domains as well as the surfaces of cells within these domains on 29 independent leaves. These measurements show that CUC2/3 domain is more restricted to the sinuses than the CUC2 domain and is composed of smaller cells (Figure 2D, G-H).

(A) Leaf primordia of a plasma membrane marker expressing line (p70s::PIP2:GFP) at three time points of a time lapse experiment (tooth 1 width is indicated under each image). **(B)** Segmented abaxial epidermis with clones deriving from cells at 0h outlined in black and colored according to the type of clones (Sinus in yellow and Tooth in orange) see figure S1 for the detailed method of clone type assessment. **(C)** Heatmaps of clone surface at each time point of the experiment. **(D)** Heatmap of proliferation over the 48h of the experiment (number of cells per clone at the end of the experiment). **(E)** Heatmap of the Relative Surface Increase over the 48h of the experiment (define as follow: $[(\text{clone surface at 48h} - \text{clone surface at 0h}) / \text{clone surface at 0h}] * 100$). **(F)** Distribution of clone surfaces by clone type for each time point of the experiment. **(G)** Relative Surface Increase over the 48h of the experiment for sinus and tooth clones. **(H)** Numbers of cells formed per clones at the end of the experiment (individual data are represented by dots and mean is represented by black line). **(I)** Distribution of cell surfaces in sinus and tooth at each time point of the experiment. **(J)** Distribution of cell surfaces in sinus and tooth according to the width of the tooth (data for this panel came from more than 20 independent experiments for each class of tooth width). Scale bars, (A-E) 50µm, asterisks represent statistical differences according to t-test: *p<0.05, **p<0.02, ***p<0.001

Cell surfaces of the CUC2 domain are however a smaller than surrounding cells from the leaf. (Figure 2H). For time lapse experiments, respective domains were defined at the first time point as described above and derived clones were considered belonging to the same domains as their initial mother cells. Quantifications reveal that both clone surfaces and RSI over 48h are significantly different between CUC2 and CUC2/3 domains, clones of the latter being smaller than the CUC2 ones and exhibiting lower RSI. These results indicate that even if CUC2 is required for initiating serration and contributes to the limitation of cell growth, CUC3 is likely to be responsible for the local inhibition of cell growth at the margin in the following stages of serrations.

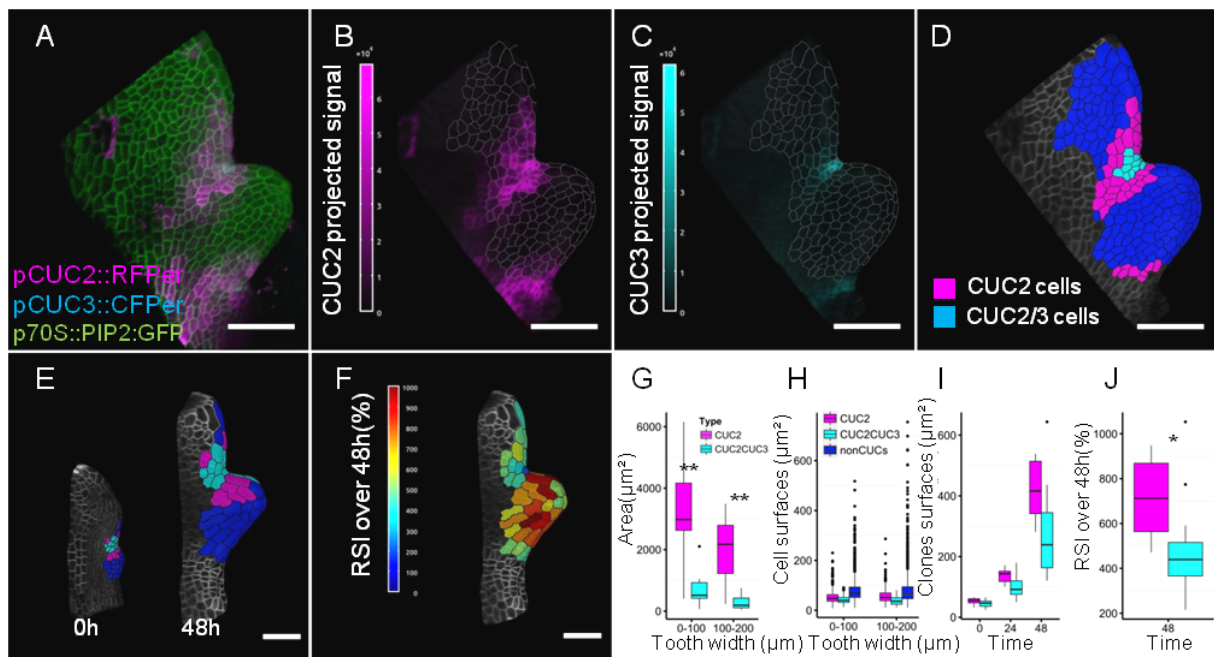


Figure 2: CUC3 expression domain is associated with reduced cell growth. (A) 3D view of a leaf carrying reporters for CUC2 and CUC3 expression (in magenta and cyan respectively). **(B)** CUC2 signal from the abaxial epidermis projected on the leaf surface. **(C)** CUC3 signal from the abaxial epidermis projected on the leaf surface. **(D)** Map of cell expression types, based on the normalized projected signal of CUC2 and CUC3, cell are classified in CUC2 or CUC2 and CUC3 expressing cells (CUC2 in magenta and CUC2/3 in cyan, remaining cells in blue). **(E)** First and last time points of a time lapse experiment showing cells at 0h and clones derived from these cells at 48h (cells and derived clones are colored according to CUCs expression level at 0h following the same color code as in D). **(F)** Map of the Relative Surface Increase over the 48h of the experiment. **(G)** Distribution of CUC2 and CUC2/3 expression domain areas according to width of the tooth1. **(H)** Distribution of cell surfaces in CUC2 and CUC2/3 expression domains as well as cells expressing neither CUC2 nor CUC3 according to width of the tooth1. **(I)** Evolution of clone surfaces distribution in CUC2 and CUC2/3 expression domains at each point of time lapse experiment shown in (E). **(J)** Distribution of Relative Surface Increase over the 48 h of the time lapse experiment for CUC2 and CUC2/3 derived clones. Data presented in G and H came from 18 and 11 independent acquisitions on leaves with tooth 1 width ranging between 0-100µm or 100-200µm. All these acquisitions were treated as presented in (A-D). *p-value <0.05; **p-value<0.02

The local reduction of cell growth at the sinuses is mediated by CUC3

Given that serrations become smoothed earlier during leaf development in *cuc3-105* than in wild-type (Hasson et al., 2011) and that CUC3 expressing cells are more restricted to sinuses and smaller than the rest of the CUC2 expressing cells, we hypothesized that CUC3 may be involved in local cell growth reduction at the leaf margin. To test this hypothesis we introduced a plasma membrane marker in the *cuc3-105* mutant background and performed 3D imaging and time lapse experiments on leaf primordia. We applied the previously described pipeline (FigureS1) to identify cells or derived clones from tooth and its relative distal sinus. Time lapse experiments no longer reveal any significant differences in clone RSI at sinuses and tooth (Figure 3A, C and G), but they reveal that whereas division occurred in tooth, no division was observed in sinuses (Figure 3B and F). In addition, measurements of cell surface at each point of the time lapse show an increase in cell surfaces at the sinus while the mean cell surfaces remain constant in the tooth (Figure 3H). Performing cell surfaces analyses on 31 independent acquisitions we confirmed the differences in cell surfaces between sinuses and teeth (Figure 3I). Comparison of the distribution of cell surfaces in sinuses and tooth of *cuc3-105* with the ones in Col-0 indicates that while cell size in sinuses of *cuc3-105* are significantly higher than in Col, there is no significant differences concerning tooth cell surfaces (Figure 3 J-K). These data strongly suggest that CUC3 is involved in local cell growth reduction at the sinus.

To confirm that CUC3 mediates cell growth reductions, we generated an inducible overexpressing line for CUC3 (*p35S::CUC3-GR* in a *cuc3-105* background). We performed continuous Dexamethasone (DEX) induction on seedling cultivated in vitro or on 2 weeks old soil grown plants (Preliminary Figure 4). In vitro induction results in a very strong reduction of growth at the level of whole seedling (please compare seedlings in figure 4 A to B and C). Induction on soil grown plants restores the formation of serrations at the leaf margin. These serrations are even more pronounced than in wild type leaves (Figure 4 D, E and F). These results indicate that CUC3 is very likely to be a negative regulator of cell growth. Additional experiments aiming at comparing leaf cell surfaces in induced and non-induced conditions will be achieved on samples stained with Calcofluor (Cell wall staining dye) that will provide the cellular resolution. (in progress)

CUC3 influences pattern of auxin response during leaf margin development.

Auxin is also known to be involved in setting the differential growth at the leaf margin in addition to CUCs. We thus wondered whether the growth defect observed in *cuc3-105* could be linked with a change in the pattern of transcriptional responses mediated by auxin (termed auxin responses hereafter). In order to compare the area of auxin responses as well as the number and size of cells in the abaxial epidermis exhibiting such a response in *cuc3-105* and Col-0, we compared the profile of the auxin transcriptional response reporter *pDR5rev::VENUS:NLS* (called DR5 hereafter)

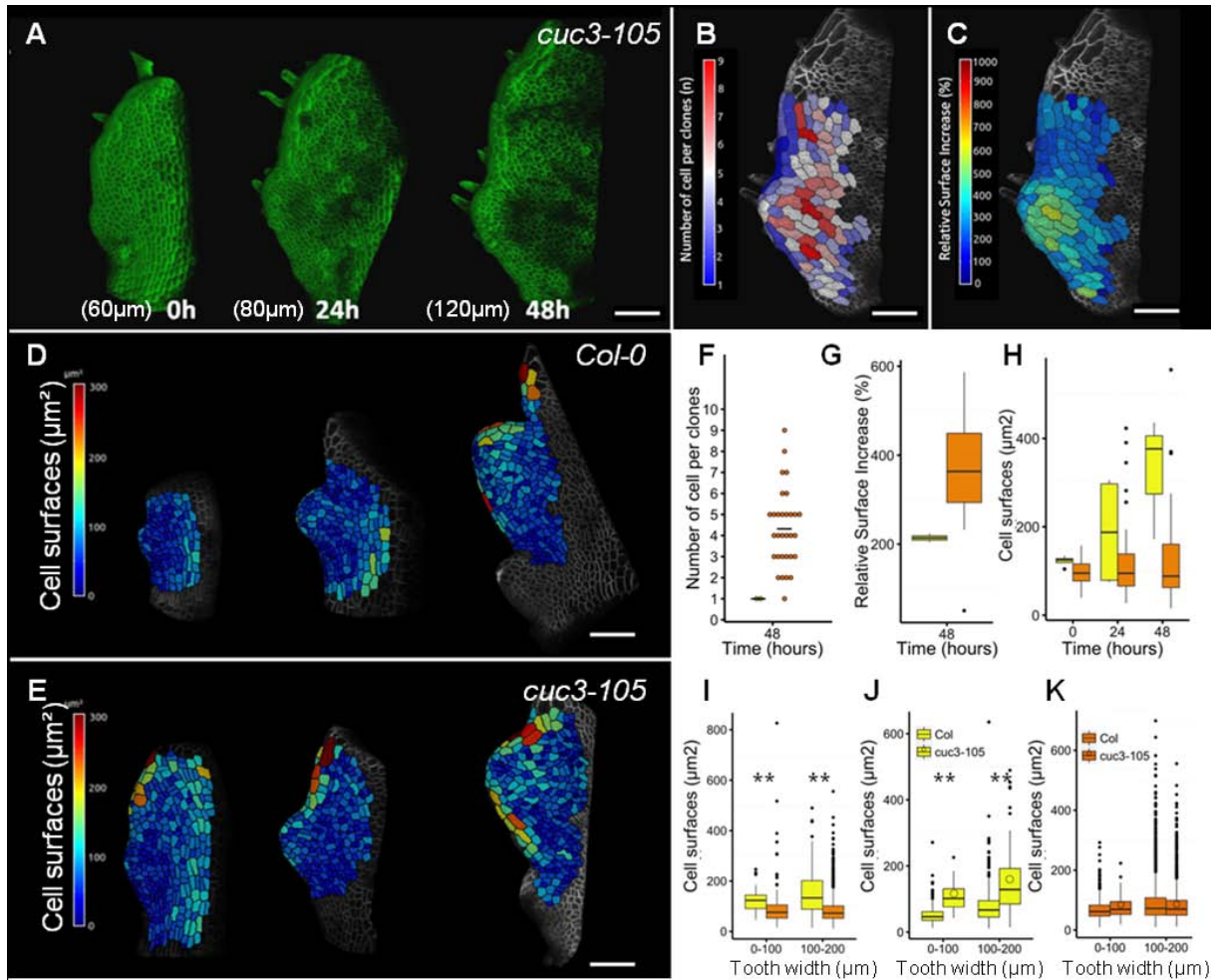


Figure 3: CUC3 mediates local cell growth reduction at the leaf margin. (A) 3D images of the same *cuc3-105* leaf primordia at 3 time points of a time lapse experiment (tooth 1 width is indicated under each images). (B) and (C) Maps of numbers of cells per clones and Relative Surface Increase over the 48h of the experiment (represented on the last time point of the experiment). (D) and (E) Maps of cell surfaces for three representative leaves of *Col-0* and *cuc3-105* (tooth width from left to right are about: 50μm, 100μm and 150μm). (F) Number of cells per clone at the end of the experiment in sinus (yellow) and tooth region (orange) (related to(B)). (G) Relative surface increase over the experiments in sinuses and tooth clones (related to (C)). (H) Evolution of cell surface distributions in sinuses and tooth over the experiment. (I) Distribution of cell surfaces in *cuc3-105* sinuses and tooth according to the width of the tooth (data from 8 and 23 independent acquisition on *cuc3-105* leaves with tooth1 width ranging between 0-100μm or 100-200μm has been pooled for this plot). (J) Distribution of cell surfaces in sinus of *Col-0* (yellow) and *cuc3-105* (yellow with a circle) leaves according to the width of the tooth (data for *cuc3-105* sinuses cells are the same as in (I), data from 32 and 23 independent acquisitions on *Col-0* leaves with tooth1 width ranging between 0-100μm or 100-200μm has been pooled for this plot (data used in Figure 1)). (K) Distribution of cell surfaces in teeth of *Col-0* (orange) and *cuc3-105* (orange with a circle) according to the width of the tooth (data for this plot came from the same acquisitions used in (I) and (J)). scale bars: 50μm. When relevant, statistical analysis has been done. Statistical differences according to t-test: **p-value<0.001

in both genotypes, (Figure 5). To discriminate in an automatic manner the cells expressing DR5 from the others, we applied a threshold on the mean intensities of the projected signal then measured the global area, number and surfaces of cells expressing DR5. For teeth ranging from 0 to 100 micrometers in width, although auxin responses in the abaxial epidermis seem to be slightly broader in *cuc3-105* than in wild type, the difference was not significant. However for teeth ranging from 100 to 200 micrometers in width, the difference in auxin response area became significant with a broader area in the mutant. This difference results in a higher number of DR5 expressing cells in *cuc3-105* compared to Col0 with no differences in cell surfaces. These results suggest that CUC3 expressed at sinuses has a non-cell autonomous effect on auxin response pattern in the abaxial epidermis by restricting its area.

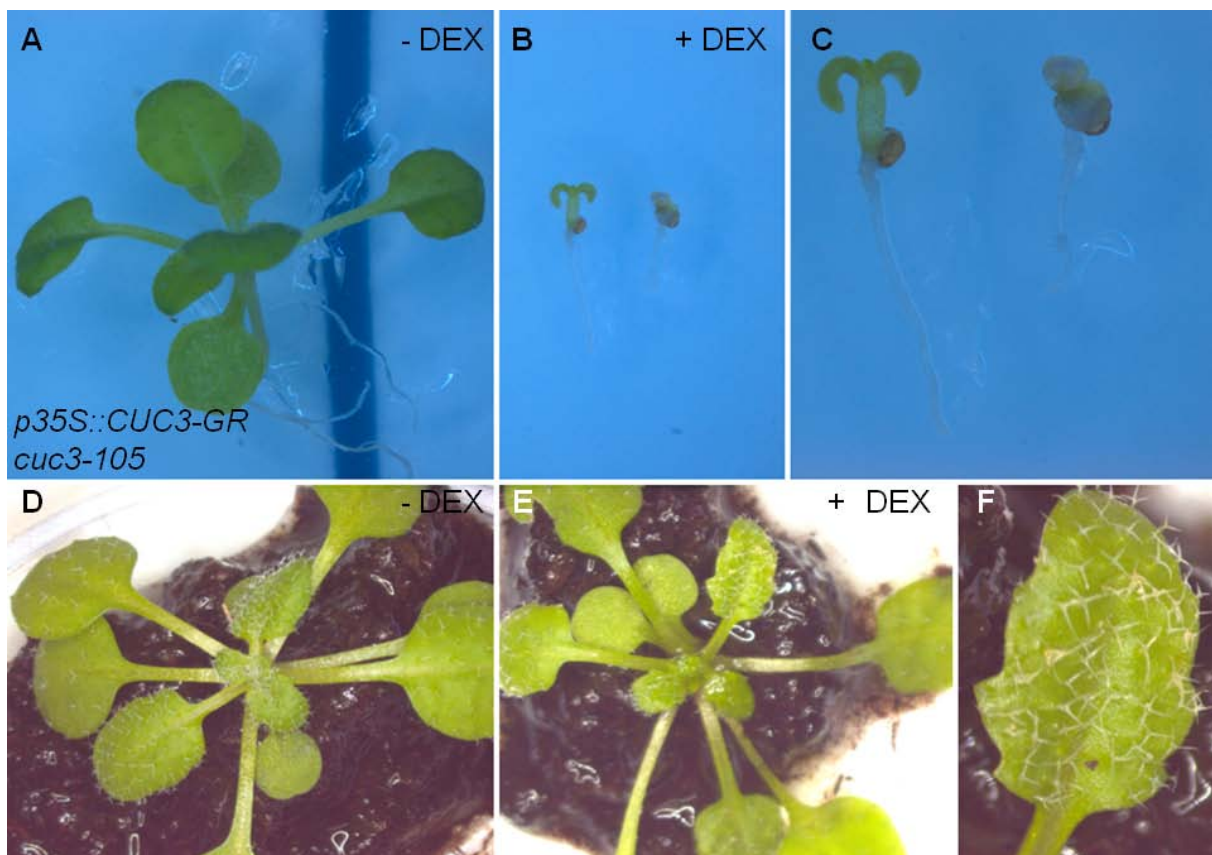


Figure 4 (preliminary): CUC3 represses growth. Inducible overexpression of CUC3 leads to strong reduction of growth upon continuous *in vitro* Dexamethasone induction (**A-C**) (compare **(A)** and **(B)**, pictures are at the same scale, see **(C)** for higher magnification of seedlings in **(B)**). In soil induction on 2 weeks old plants of the same line restores the formation of serration at the margin of *cuc3-105* mutant (**D-F**).

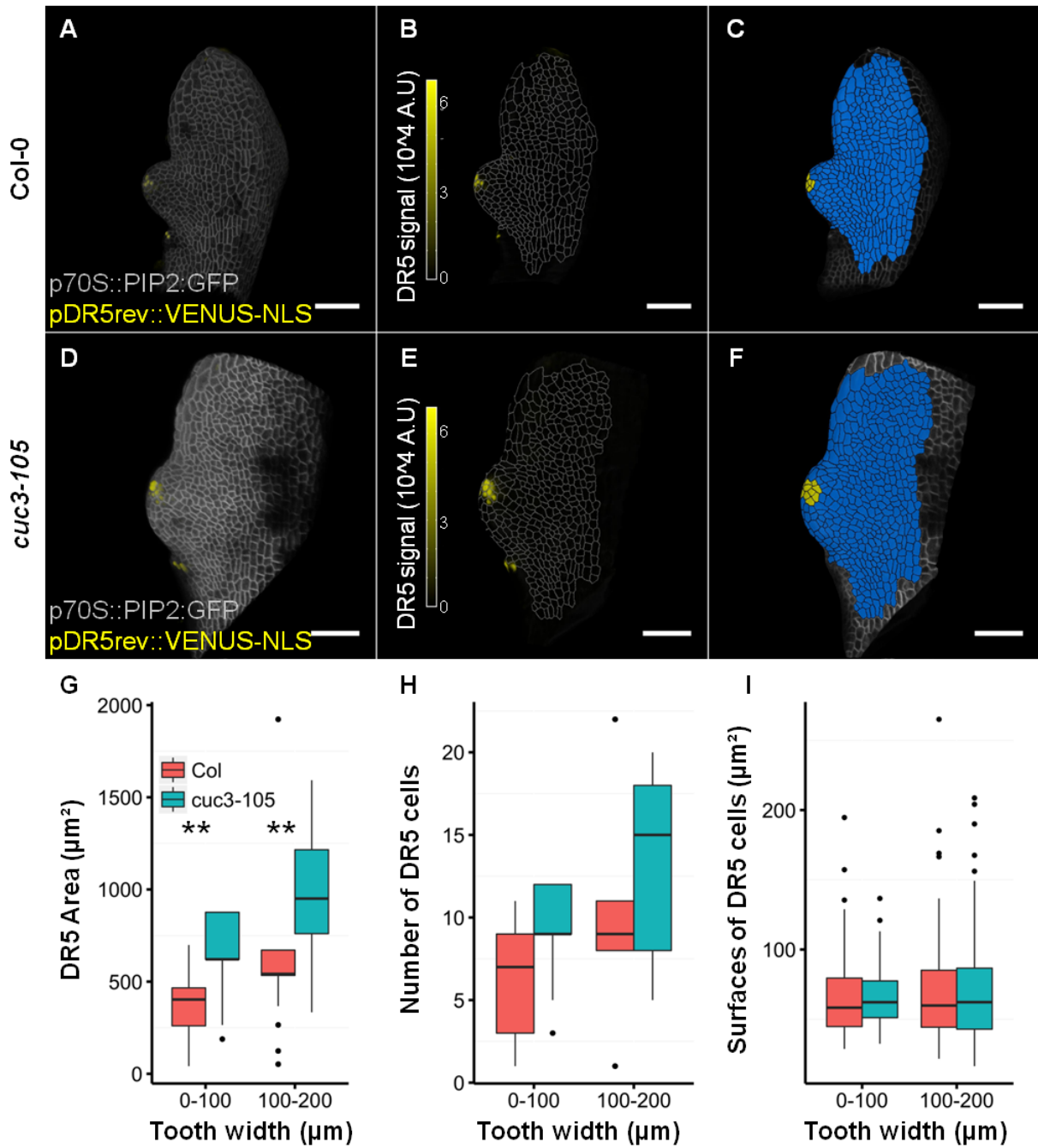


Figure 5: CUC3 narrows the area of auxin responses at the tip of the tooth. 3D view of leaf expressing DR5 auxin response reporter (**A, D**) DR5 signal from the epidermis projected on the leaf surfaces (**B, E**). Maps of Auxin responses (cells mean DR5 signal over 10000 A.U are colored in yellow) (**C, F**). (**A**), (**B**) and (**C**) are in Col-0 and (**D**), (**E**) and (**F**) are in *cuc3-105* background. Distribution of DR5 area (**G**), numbers of DR5 cells (**H**) and surfaces of DR5 cells (**I**) in Col-0 and *cuc3-105* according to the width of the tooth. Col-0 related data came from 18 and 11 independent acquisitions on leaves with tooth 1 width ranging between 0-100 μm or 100-200 μm ; *cuc3-105* related data came from 4 and 14 independent acquisitions on leaves with tooth 1 width ranging between 0-100 μm or 100-200 μm . Scale bars: 50 μm . **p-values<0.02 based on t-tests

Smoothing of tooth1 at later stages of leaf development is associated with a release of CUC3 mediated cell growth reduction at the sinuses.

Later in leaf development, the first pair of teeth tends to be smoothed in wild – type plants indicating that the initial differential growth is not further maintained but on the contrary there might be more growth at the sinus than in the tooth that can be considered as the implementation of a new differential growth. To get insights onto the cellular bases of this smoothing and further investigate the potential role of CUC3 in this process, we performed time lapse experiments at late stages of teeth development in Col0 co-expressing a plasma membrane marker and a transcriptional reporter for CUC3 (p70S::PIP2:GFP/pCUC3::CFPer). We focused our analyses on sinus cells identified as described above (figure S1), we measured cell surfaces and CUC3 projected signal per cell distribution at each time of the experiment (Figure 6). Leaf abaxial surfaces with cell type, CUC3 projected signal, signal quantification and cell surface measurements at first (Figure 6A-C) and last time points (Figure 6D-F) of a time lapse experiment were used to quantify the evolution of these parameters during tooth smoothing. These quantifications indicate that late growth at the sinus results from an increase in cell surfaces (Figure 6G). Measurements of the projected CUC3 signal indicate a decrease in CUC3 expression in sinus cells that tightly correlates with the release of repression of cell expansion (Figure 6H). Together these results show a correlation between an increase in cell size at the sinus and a decrease in CUC3 expression during the release of growth in later stages of teeth development.

DISCUSSION:

Spatial and temporal control of cell growth directs leaf serration

Serration initiation at the leaf margin is a case of differential growth. Since this process takes place in the basal half of the leaf below the front of proliferation arrest, the spatial differences in growth might rely on spatial differences in cell division or in cell growth. It can also results from spatial differences in the number of cells contributing to growth. Time lapse analyses gave us information at several levels: Relative Surface Increase (RSI) and clone surfaces informed us on clone growth whereas the map of the number of cells per clones is directly related to cell division events. The combination of time lapse experiments with the analysis of cell surfaces from numerous independent static acquisitions allowed us to draw the sequence of cellular events occurring from the initiation of the first tooth to its smoothing at a later stage of leaf development. In the first steps of tooth development (less than 100µm in width) an equivalent number of cells are formed per clone in sinus and tooth whereas RSI and clone surfaces are higher in tooth than in sinuses (Figure 1 and S2-1). These results, confirmed by the measurement of smaller cells in sinus on

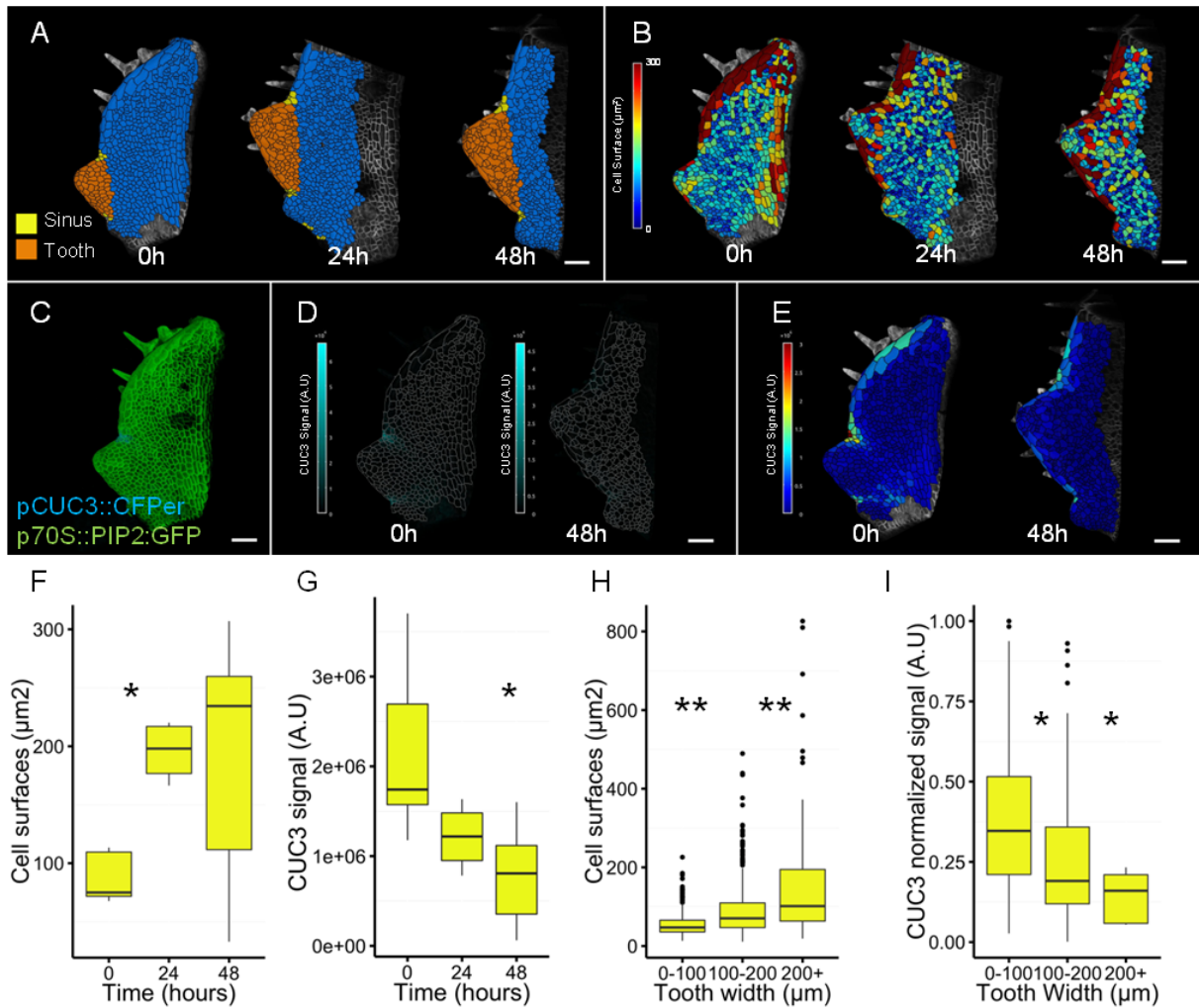


Figure 6: Decrease in CUC3 expression release local restriction of sinuses cell growth in late stage of teeth development. (A) Sinus and tooth cells on segmented leaf abaxial epidermis at 3 time points of a time lapse experiment. (B) Heatmap of cell surfaces over the course of the time lapse. (C) 3D view of leaf expressing CUC3 reporter. CUC3 signal from the epidermis projected on the leaf surface (D) and corresponding heatmaps (E) at the beginning and end of the time lapse. Distribution of cell surfaces (F) and CUC3 signal (G) over the time of the experiment. Distribution of cell surfaces (H) and CUC3 normalized signal (I) from sinuses of teeth 1 of distinct width (N independent acquisitions). Scale bars: 50 μm , *p-values<0.05 ; **p-values<0.01 based on t-test.

static acquisitions clearly indicate that differences of cell growth between sinus and tooth are responsible for the differential growth in the initial phase of tooth outgrowth. Later on (between 100 and 200 μ m in tooth width), the number of cell divisions is reduced and stops in the region of the sinus. At this stage, growth of clones is not different anymore between sinus and tooth. However since a homogeneous growth takes place on cells of different surfaces, the difference of cell surface between sinus and serration is maintained (Figure S2-2). When the tooth reaches more than 200 μ m in width, cell growth and probably cell expansion take place in the distal sinus (figure 6).

Our observation of reduced cell growth in sinus cells is in accordance with the previously reported data showing reduced cell expansion in *Anagallis arvensis* leaf axils (Kwiatkowska and Dumais, 2003) or smaller cells in inter-leaflets boundaries of Tomato and Cardamine leaves (Rossmann et al., 2015). Time lapse experiments on *rco* and WT *Cardamine hirsuta* leaves pointed RCO as a regulator of both proliferation and growth in the inter-leaflets region (Vlad et al., 2014). Proliferation has been reported in the sepal-sepal boundary in early stage of flower meristem development (Laufs et al., 2004). On the other hand, some studies reported a lower rate of cell division in the boundary domains in contrast to surrounding tissues (Breuil-Broyer et al., 2004) that appears to differ from our data on leaf serration in Arabidopsis. Previous data were however based on the analyses of expression of cell cycle related genes and BrdU labelling providing a static view of the process at one time, thus these differences might just be the reflect of a specific developmental window as we showed that cellular behavior evolve over time. We observed a decrease in the number of cell divisions but only at a late stage in tooth development (figure S2-2). Such decrease and even arrest of cell division at the latest stages might be correlated with the progressive retreat of the front of cell division competence of the whole leaf (Andriankaja et al., 2012). Even if cell growth is impaired at the sinus during the previous phase, the mean cell size reached by the daughter cells at the time of the decrease in cell division is greater than that of the initial mother cell and should therefore not represent an intrinsic constraint on the ability to divide (Hisanaga et al., 2015; Sablowski, 2016).

Interestingly, the release of growth repression in sinus at the latest stage of tooth development occurs on cells that have stopped to divide, it is thus likely that the increase in cell size at this late stage corresponds to a post-mitotic cell expansion. This late process at the leaf sinuses that results in a smoothing of the teeth differs from what is happening in other boundary domains and makes the dynamics of leaf serrations rather unique. For examples, the boundaries located between floral organs and floral meristem give rise to differentiated cells required for organ abscission (McKim et al., 2008). The boundaries between ovule primordia are kept in a low growing state allowing proper separations of ovules and then seeds (Goncalves et al., 2015). The boundaries between leaf and meristem undergo meristematic activity associated with axillary meristem initiation (Grbic and Bleecker, 2000; Long and

Barton, 2000). These differences might rely on distinct developmental contexts (e.g. meristematic identity) and involvement of other molecular actors.

CUC2 and CUC3 have distinct contributions to differential growth at the leaf margin

Our results show that CUC3 expression is restricted to sinus cells, and these cells grow less than the surrounding cells (Figure 2). Although the *miR164* regulation on CUC2 mRNA is thought to narrow the pattern of CUC2 (Sieber et al., 2007), CUC2 expressing cells are a little smaller than surrounding cells suggesting that to some extent CUC2 is also able to affect cell growth. The stronger reduction of cell growth at the sinus might thus result from the additive effect of CUC2 and CUC3. Our results suggest however that CUC2 and CUC3 have distinct contributions to the differential growth at the leaf margin at least from a quantitative and temporal point of view. CUC3 involvement in the control of cell growth in sinus cells is confirmed by bigger cell surfaces in *cuc3-105* sinuses (Figure 3). It is further confirmed by global and local growth restriction in plants overexpressing CUC3 (Figure 4). It has been shown previously that CUC2 is only transiently required at the initiation of the tooth and that it is sufficient to trigger the entire developmental program of tooth outgrowth suggesting that other genes take care of tooth growth and development after the initiation has occurred (Maugarny-Cales et al., 2019). Lines with an increased level of CUC2 usually exhibit over-dissected leaves but in a *cuc3-105* background the leaf phenotype is always a smoothing of the leaf margin (Hasson et al., 2011; Maugarny-Cales et al., 2019). Altogether these data indicate that CUC2 is required to initiate differential growth potentially through its effect on polar auxin transport (Bilsborough et al., 2011) whereas CUC3 is required to maintain the differential growth by repressing cell growth. Furthermore we showed that decrease in CUC3 expression in late stage of teeth development correlates with an increase in cell size at the sinus. Conditional overexpression of CUC3 prevents tooth smoothing (Figure 4) indicating that CUC3 is sufficient to maintain the repression of cell growth/expansion at the sinus. CUC3 expression was reported to be induced upon mechanical stress (Fal et al., 2016), and the initiation of differential growth mediated by CUC2 produces per se a mechanical stress at the leaf margin. These two mechanisms provide an efficient combination to induce very locally expression of CUC3 at the sinus at a very early stage of tooth initiation and an effective feedback to reinforce and maintain differential growth. Even if growth and mechanical properties of sinus cells are mainly controlled at a local scale, organ scale growth pattern is likely to interfere with local mechanical stress. Global growth of the leaf could thus influence the mechanical stress in sinus cells and trigger the decrease in CUC3 expression in late stage of teeth development.

In conclusion we described a differential growth process occurring in a population of proliferating cells. Like differential growth occurring in apical hook

formation or tropic responses it requires the temporal and spatial control of cell growth. It also involves differential repartition of the CUC3 transcription factor that negatively controls cell growth. This negative control necessarily involves a modulation in the expression of growth related genes. Identification of these genes will require transcriptional analyses of sinus cells compared to others, that might be very tricky to perform, however single cell analysis are now emerging and might open novel perspectives. Identifying CUC3 targets in the context of leaf serrations would be an important step toward the understanding of differential growth at the leaf margin.

MATERIAL AND METHODS:

Plant materials and growth conditions:

All lines are in the Columbia-0 (Col-0) ecotype, the *cuc3-105* mutant was described in (Hibara et al., 2006), *pCUC3::CFPer* and *pCUC2::RFP* were described in (Goncalves et al., 2015), *pDR5rev::3xVENUS-NLS* was described in (Heisler et al., 2005), *35S::CUC3-GR* was described in (Bennett et al., 2010), and *p70s::PIP2-GFP* was described in (Luu et al., 2012). Seeds were surface sterilized (10 min in etOH 70%, SDS 0.5%, then washed few seconds in etOH 95%) prior to be sown on half Murashige and Skoog medium in agar 0.8% ,pH adjusted at 5.7. All plates were stratified at 4°C for 48h. All plants were grown 7 days in vitro in long day photoperiods [16h light / 8h dark at 21 °C] prior to be transferred in soil under short-day photoperiods [1 h dawn (19°C, 65% hygrometry, 80 $\mu\text{mol.m}^{-2}.\text{s}^{-1}$ light), 6 h day (21°C, 65% hygrometry, 120 $\mu\text{mol.m}^{-2}.\text{s}^{-1}$ light), 1 h dusk (20°C, 65% hygrometry, 80 $\mu\text{mol.m}^{-2}.\text{s}^{-1}$ light), 16 h dark (18°C, 65% hygrometry, no light)] for 14 days.

Culture condition for time-lapse imaging:

Plants were carefully removed from soil, and cotyledons and leaf 1 to 10 were removed using fine tweezers and surgical syringe needle under a stereo microscope. Seedlings were then transferred on plate containing half Murashige and Skoog media supplemented with 1% sucrose and 0.8% agarose. Dissected seedlings were glued to the media by careful deposition of melt agarose droplets on the hypocotyls. Samples were then imaged every 24h and grown under long day conditions between imaging sessions.

Confocal Imaging:

All samples were prepared as for time lapse experiments. Prior to imaging, samples were immersed in water for 5 minutes in order to saturate the agarose gel and avoid uncontrolled movement during imaging. Acquisitions were performed on an upright Leica TCS SP8 laser scanning confocal microscope equipped with a long distance water immersion lens (Leica, 40X0, 8NA water HCX APO L). CFP was excited at 405 nm, GFP at 488nm, VENUS at 514nm and RFP at 560nm. CFP signal were collected

from 415 to 480 nm, GFP from 498nm to 510nm, VENUS from 524nm to 554nm and RFP from 570nm to 650nm. GFP was collected on a Hyd detector, all the others fluorochromes were collected on PMT detectors. Sequential image settings were used when required. All samples were acquired as a stack of images with a voxel resolution of about 0.5X0.5X0.5 μm .

Image analyzes:

All stack files were processed using MorphoGraphX software (Barbier de Reuille et al) to segment cells, perform lineage tracking and measure grow parameters, then quantitative data were exported to R as .csv files to perform further analyses.

For the classification of cells into CUC2, CUC2/3 or no CUCs categories in figure 2 we proceeded as follow: 1) signal from pCUC2::RFP or pCUC3::CFP were projected onto a segmented mesh using MorphoGraphX project signal function in a range of 2 to 6 μm from the surface. 2) Mean signal intensities were collected for both reporters in each cells, a .csv files containing these data and exported to R software .3) Cell signal intensities from all the acquisitions on lines expressing these reporters were pooled together in order to plot the overall distribution of signal intensities according to the surface of cells for both reporters. 4) Signal intensities have been normalized in order to range the signal intensities value between 0 and 1. 5) A threshold has been applied for both signals: all cells with a normalized signal over 0.2 were considered as expressing the reporter. 6) Cells were then classified into CUC2, CUC2/3 or noCUCs according to the reporter they expressed after the previous steps of the pipeline.

A similar pipeline was used to identify cells expressing DR5 in figure 5. After cell classification, cell surfaces, area of domain (CUC2, CUC2/3, no CUCs, DR5) as well as number of cells per domain were computed from the data files on R.

For each acquisition, a single .csv file was generated as an output of R data analyses pipelines. It contains all the relevant information on cells: classification into marker domains, cell surface, mean gaussian curvature, localization (sinus, tooth, and leaf). These files can be read in MorphoGraphX in order to visualize any quantified information on the surface mesh of the acquisition.

For time lapse experiments, additional .csv files were generated. They contain additional information on: clones surface, numbers of cells per clones, Relative Surface Increase, clone type (CUC2, CUC2/3, noCUCs), clone position (Distal sinus, Tooth, Leaf).

Author contributions:

L.S. performed all experiments, image and quantitative analyses, L.S. and C.P.-R. designed the research, analyzed the data and wrote the ms, L.P. provided genetic material and contributed to discussions.

Acknowledgments:

We thank Jasmine Burguet (MIN team IJPB, Versailles) Pradeep Das, Anna-Maria Kiss and C. Godin (RDP, Lyon) and members of the FTA team for helpful discussions. We would also like to pay tribute to Olivier Grandjean whose skills and advice were invaluable in setting up the experiments in real time. We warmly thank Ben Scheres who kindly provided us the p35S::CUC3-GR construct. We are grateful to the members of the IJPB plant culture service who took care of the plants. This work and L.S. were supported by the ANR project ANR-14-CE11-0018.

REFERENCES:

Aida, M., Ishida, T., Fukaki, H., Fujisawa, H., and Tasaka, M. (1997). Genes involved in organ separation in Arabidopsis: an analysis of the cup-shaped cotyledon mutant. *Plant Cell* 9, 841-857.

Aida, M., Ishida, T., and Tasaka, M. (1999). Shoot apical meristem and cotyledon formation during Arabidopsis embryogenesis: interaction among the CUP-SHAPED COTYLEDON and SHOOT MERISTEMLESS genes. *Development* 126, 1563-1570.

Aida, M., and Tasaka, M. (2006). Morphogenesis and patterning at the organ boundaries in the higher plant shoot apex. *Plant Mol Biol* 60, 915-928.

Andriankaja, M., Dhondt, S., De Bodt, S., Vanhaeren, H., Coppens, F., De Milde, L., Muhlenbock, P., Skiryecz, A., Gonzalez, N., Beemster, G.T., et al. (2012). Exit from proliferation during leaf development in Arabidopsis thaliana: a not-so-gradual process. *Dev Cell* 22, 64-78.

Barbier de Reuille, P., Routier-Kierzkowska, A.L., Kierzkowski, D., Bassel, G.W., Schupbach, T., Tauriello, G., Bajpai, N., Strauss, S., Weber, A., Kiss, A., et al. (2015). MorphoGraphX: A platform for quantifying morphogenesis in 4D. *Elife* 4, 05864.

Bennett, T., van den Toorn, A., Sanchez-Perez, G.F., Campilho, A., Willemsen, V., Snel, B., and Scheres, B. (2010). SOMBRERO, BEARSKIN1, and BEARSKIN2 regulate root cap maturation in Arabidopsis. *Plant Cell* 22, 640-654.

Bilsborough, G.D., Runions, A., Barkoulas, M., Jenkins, H.W., Hasson, A., Galinha, C., Laufs, P., Hay, A., Prusinkiewicz, P., and Tsiantis, M. (2011). Model for the regulation of Arabidopsis thaliana leaf margin development. *Proc Natl Acad Sci U S A* 108, 3424-3429.

Biot, E., Cortizo, M., Burguet, J., Kiss, A., Oughou, M., Maugarny-Cales, A., Goncalves, B., Adroher, B., Andrey, P., Boudaoud, A., et al. (2016). Multiscale quantification of morphodynamics: MorphoLeaf software for 2D shape analysis. *Development* 143, 3417-3428.

- Blein, T., Pulido, A., Vialette-Guiraud, A., Nikovics, K., Morin, H., Hay, A., Johansen, I.E., Tsiantis, M., and Laufs, P.** (2008). A conserved molecular framework for compound leaf development. *Science* 322, 1835-1839.
- Breuil-Broyer, S., Morel, P., de Almeida-Engler, J., Coustham, V., Negrutiu, I., and Trehin, C.** (2004). High-resolution boundary analysis during *Arabidopsis thaliana* flower development. *Plant J* 38, 182-192.
- Dumais, J., and Kwiatkowska, D.** (2002). Analysis of surface growth in shoot apices. *Plant J* 31, 229-241.
- Fal, K., Landrein, B., and Hamant, O.** (2016). Interplay between miRNA regulation and mechanical stress for CUC gene expression at the shoot apical meristem. *Plant Signal Behav* 11, e1127497.
- Goncalves, B., Hasson, A., Belcram, K., Cortizo, M., Morin, H., Nikovics, K., Vialette-Guiraud, A., Takeda, S., Aida, M., Laufs, P., et al.** (2015). A conserved role for CUP-SHAPED COTYLEDON genes during ovule development. *Plant J* 83, 732-742.
- Grbic, V., and Bleecker, A.B.** (2000). Axillary meristem development in *Arabidopsis thaliana*. *Plant J* 21, 215-223.
- Hasson, A., Plessis, A., Blein, T., Adroher, B., Grigg, S., Tsiantis, M., Boudaoud, A., Damerval, C., and Laufs, P.** (2011). Evolution and diverse roles of the CUP-SHAPED COTYLEDON genes in *Arabidopsis* leaf development. *Plant Cell* 23, 54-68.
- Hibara, K., Karim, M.R., Takada, S., Taoka, K., Furutani, M., Aida, M., and Tasaka, M.** (2006). *Arabidopsis* CUP-SHAPED COTYLEDON3 regulates postembryonic shoot meristem and organ boundary formation. *Plant Cell* 18, 2946-2957.
- Hisanaga, T., Kawade, K., and Tsukaya, H.** (2015). Compensation: a key to clarifying the organ-level regulation of lateral organ size in plants. *J Exp Bot* 66, 1055-1063.
- Kwiatkowska, D.** (2004). Surface growth at the reproductive shoot apex of *Arabidopsis thaliana* pin-formed 1 and wild type. *J Exp Bot* 55, 1021-1032.
- Kwiatkowska, D., and Dumais, J.** (2003). Growth and morphogenesis at the vegetative shoot apex of *Anagallis arvensis* L. *J Exp Bot* 54, 1585-1595.
- Laufs, P., Peaucelle, A., Morin, H., and Traas, J.** (2004). MicroRNA regulation of the CUC genes is required for boundary size control in *Arabidopsis* meristems. *Development* 131, 4311-4322.
- Long, J., and Barton, M.K.** (2000). Initiation of axillary and floral meristems in *Arabidopsis*. *Dev Biol* 218, 341-353.

- Luu, D.T., Martiniere, A., Sorieul, M., Runions, J., and Maurel, C. (2012).** Fluorescence recovery after photobleaching reveals high cycling dynamics of plasma membrane aquaporins in Arabidopsis roots under salt stress. *Plant J* 69, 894-905.
- Malivert, A., Hamant, O., and Ingram, G. (2018).** The contribution of mechanosensing to epidermal cell fate specification. *Curr Opin Genet Dev* 51, 52-58.
- Maugarny-Cales, A., Cortizo, M., Adroher, B., Borrega, N., Goncalves, B., Brunoud, G., Vernoux, T., Arnaud, N., and Laufs, P. (2019).** Dissecting the pathways coordinating patterning and growth by plant boundary domains. *PLoS Genet* 15, e1007913.
- McKim, S.M., Stenvik, G.E., Butenko, M.A., Kristiansen, W., Cho, S.K., Hepworth, S.R., Aalen, R.B., and Haughn, G.W. (2008).** The BLADE-ON-PETIOLE genes are essential for abscission zone formation in Arabidopsis. *Development* 135, 1537-1546.
- Reinhardt, B., Hanggi, E., Muller, S., Bauch, M., Wyrzykowska, J., Kerstetter, R., Poethig, S., and Fleming, A.J. (2007).** Restoration of DWF4 expression to the leaf margin of a *dwf4* mutant is sufficient to restore leaf shape but not size: the role of the margin in leaf development. *Plant J* 52, 1094-1104.
- Rossmann, S., Kohlen, W., Hasson, A., and Theres, K. (2015).** Lateral suppressor and Goblet act in hierarchical order to regulate ectopic meristem formation at the base of tomato leaflets. *Plant J* 81, 837-848.
- Sablowski, R. (2016).** Coordination of plant cell growth and division: collective control or mutual agreement? *Curr Opin Plant Biol* 34, 54-60.
- Sieber, P., Wellmer, F., Gheyselinck, J., Riechmann, J.L., and Meyerowitz, E.M. (2007).** Redundancy and specialization among plant microRNAs: role of the MIR164 family in developmental robustness. *Development* 134, 1051-1060.
- Vlad, D., Kierzkowski, D., Rast, M.I., Vuolo, F., Dello Iorio, R., Galinha, C., Gan, X., Hajheidari, M., Hay, A., Smith, R.S., et al. (2014).** Leaf shape evolution through duplication, regulatory diversification, and loss of a homeobox gene. *Science* 343, 780-783.
- Vroemen, C.W., Mordhorst, A.P., Albrecht, C., Kwaaitaal, M.A., and de Vries, S.C. (2003).** The CUP-SHAPED COTYLEDON3 gene is required for boundary and shoot meristem formation in Arabidopsis. *Plant Cell* 15, 1563-1577.

SUPPLEMENTAL INFORMATION:

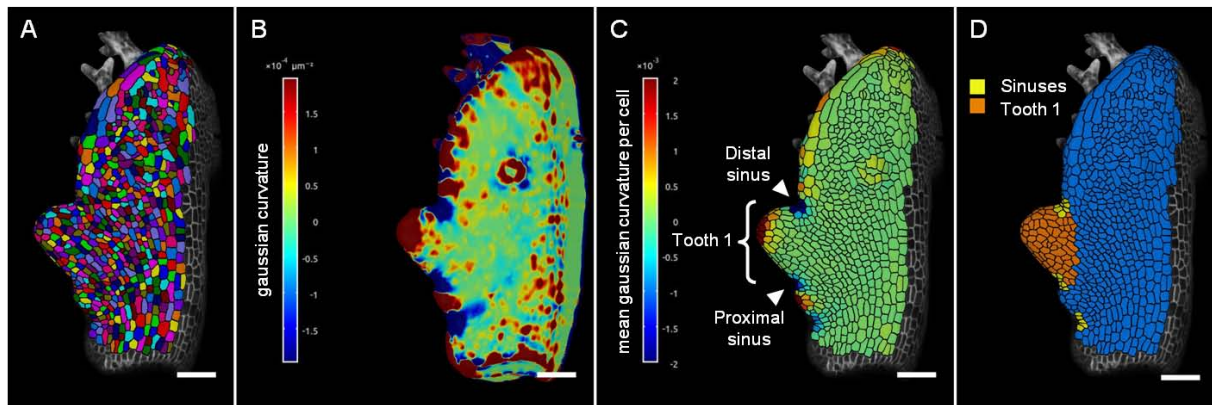


Figure S1: Pipeline for cell type determination. Abaxial epidermis cells are manually segmented on the leaf surface using MorphoGraphX **(A)**. The gaussian curvature of the surface is calculated within a $15\mu\text{m}$ neighborhood **(B)**. The mean gaussian curvature of the surface is then measured for each cell **(C)**. All cells with a mean gaussian curvature value under $-5.10\text{e-}4$ are considered belonging to sinuses. The first tooth is then defined as the region comprised between the two successive first sinuses, named distal and proximal sinuses, respectively. Combining these information with the relative localization of cells, they are assigned to distal sinus, proximal sinus, first tooth or leaf (yellow, orange and blue respectively) **(D)**. This pipeline was used in most of the presented analyses. For time lapse experiments, cell types defined at time 0 were used to determine sinus and tooth derived clones. Note that all sinuses are colored in yellow but quantifications were performed on cells from the distal sinus of the first tooth. Scale bars: $50\mu\text{m}$.

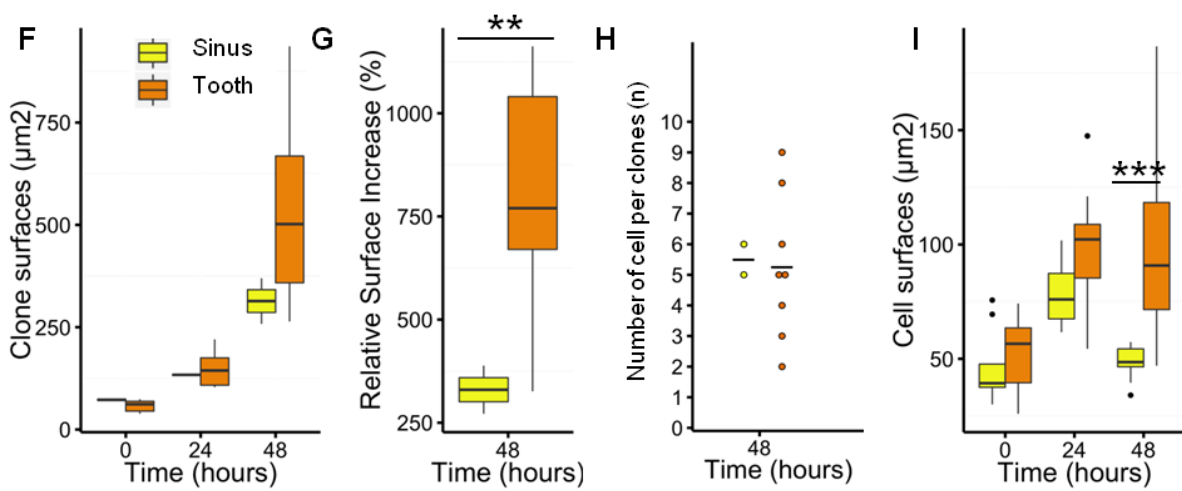
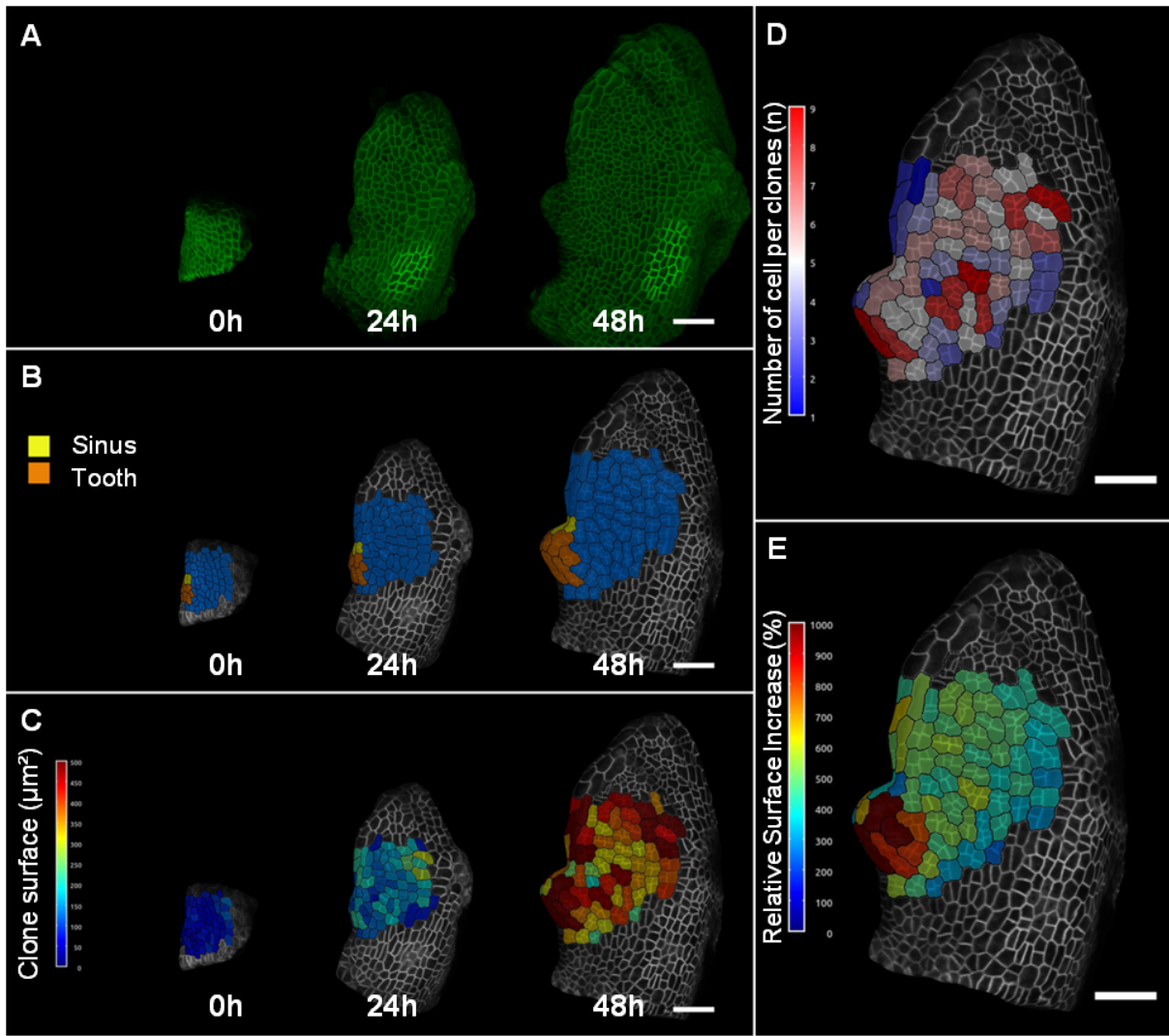


Figure S2-1: Additional time lapse experiment on tooth initiation stage.

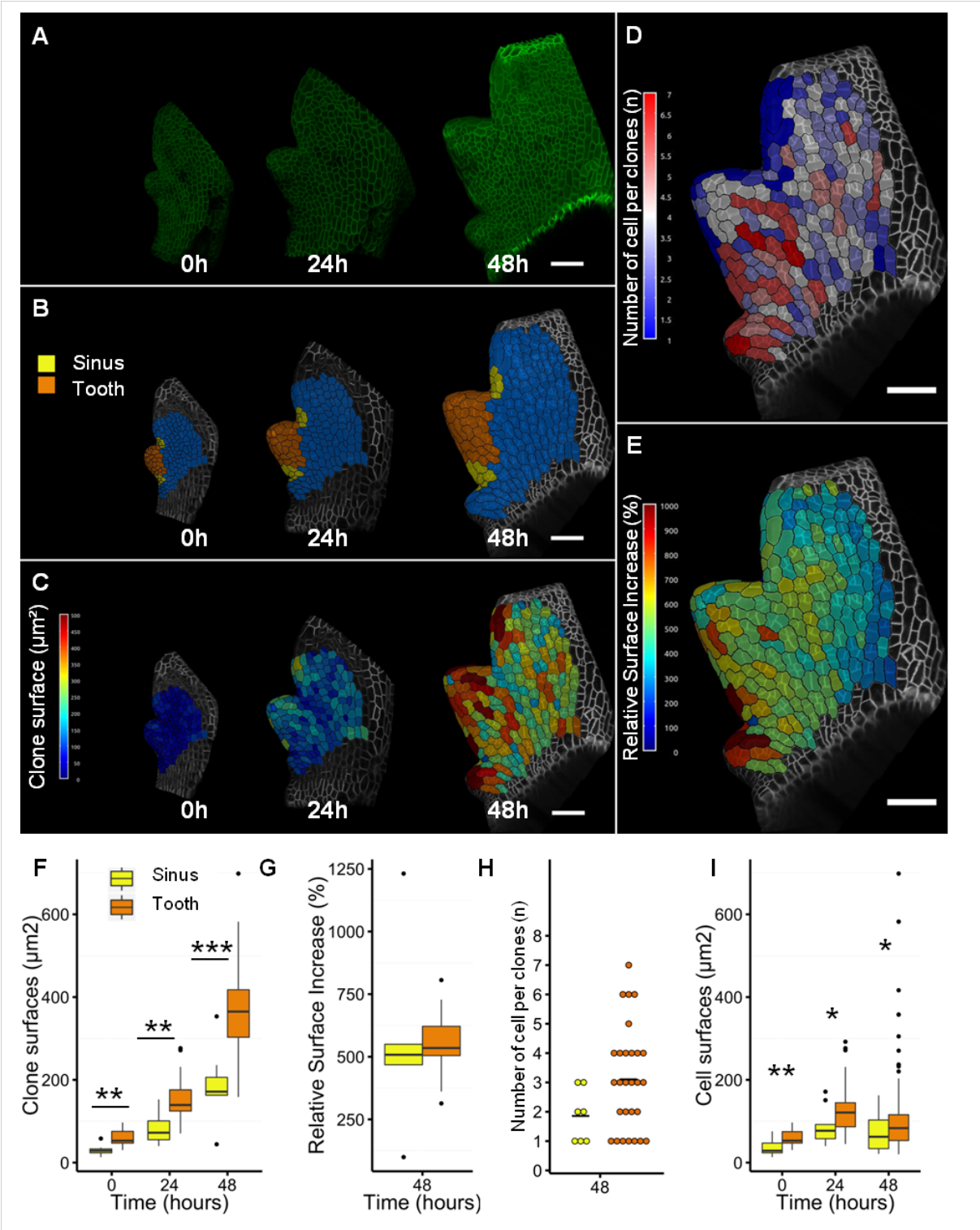


Figure S2-2: Additional time lapse experiment 80-180µm in width tooth.

Chapter III: Auxin responses and mapping of TIR1/AFB during leaf serration

This part of the thesis project was a part of a bigger project aiming at mapping auxin responses and auxin signaling components during leaf serration. While I focused on the mapping of early auxin response and pattern of members of the TRANSPORT INHIBITOR RESPONSE1/AUXIN SIGNALING F-BOX PROTEINS (TIR1/AFB) subgroup family, a former Ph.D student in the lab (M.Boudin) investigated the pattern of expression of AUXIN RESPONSE FACTORS (ARFs) and few AUXIN/INDOLE-3-ACETIC ACID (Aux/IAAs) during leaf serration. In the following part, I will present the results that I obtained on the mapping of auxin responses using different types of reporters, of some members of TIR1/AFBs as well as the description of leaf phenotypes of mutants affected in various combinations of TIR1/AFB genes. These results combined with some others obtained during the thesis of M.Boudin will be compiled in an article that we will submit in the coming months in the context of a special issue of *Plants*. Since the auxin signaling pathway was only briefly evoked in the main introduction I will introduce it here in more details as well as an overview of the present knowledge on auxin signaling components in leaf development.

Core auxin signaling pathway: from perception to transcriptional outputs.

Auxin has the ability to be transported away from its synthesis site and to act at very low concentration to trigger a vast array of specialized responses. This particularity has pushed some scientists to argue that auxin was the main plant hormone and that it was virtually involved in every aspects of a plant life. The versatility of auxin responses relies to some extent on its signaling pathway.

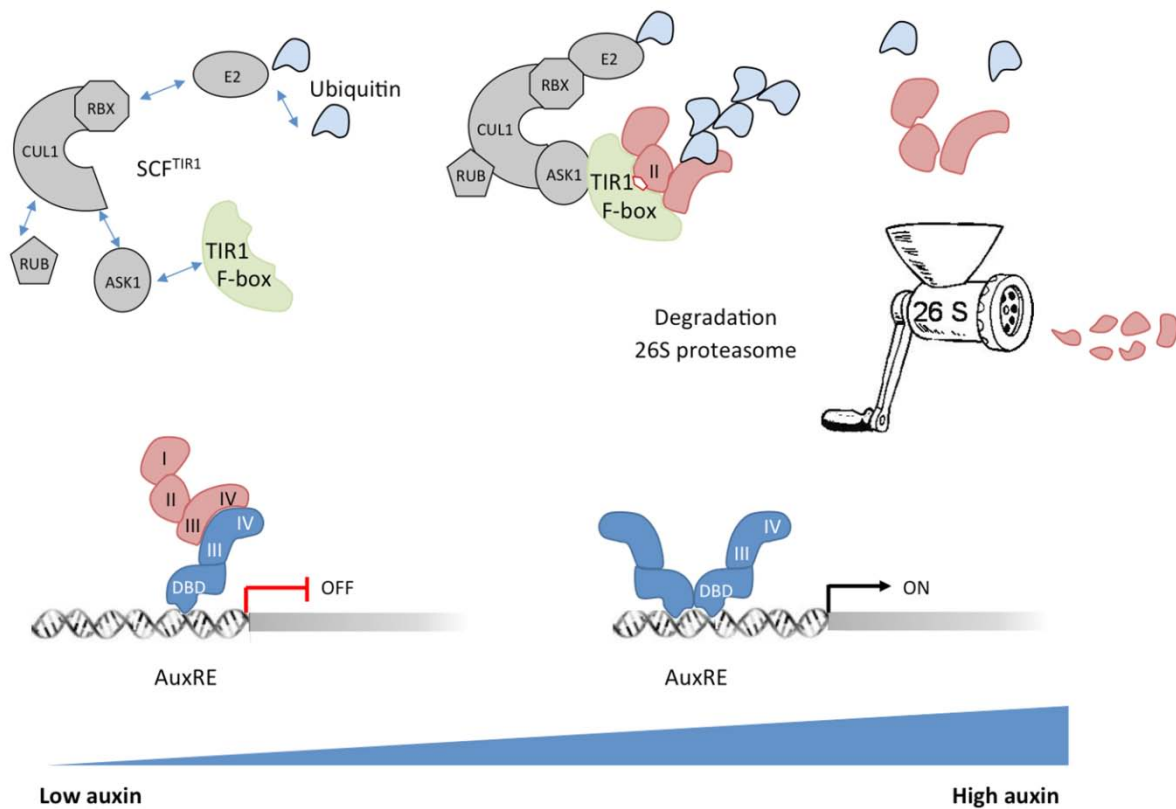


Figure A₁: Simplified overview of auxin signaling pathway. Auxin responsive genes contain AuxRE *cis-regulatory* elements in their promoters. Auxin Response Factor (ARF) binds to this *cis-regulatory* elements; at low auxin concentration transcriptional repressor Aux/IAA interact with ARFs through their domain III and IV (PB1) leading to the repression of ARF target genes. At higher concentration, auxin acts as a “molecular glue” triggering the interaction between TIR1/AFB F-BOX of the SCF^{TIR1/AFB} and Aux/IAA. This interaction leads to the polyubiquitination of Aux/IAA and subsequent addressing and degradation through 26S proteasome. ARF binding to AuxREs then triggers the transcription of auxin responsive genes.

Auxin sensing at the cellular level involves members of the TIR1/AFB F-box proteins. These genes encode F-Box proteins taking part in SCF^{TIR1/AFB} E3 ubiquitin ligase complexes (Dharmasiri et al., 2005; Parry et al., 2009). The interaction between auxin and the binding pocket of TIR1 has been shown to favor and stabilize the interaction with Aux/IAAs proteins that act as co-receptors but are also transcriptional repressors. This interaction between members of TIR/AFBs and Aux/IAAs leads to the poly-ubiquitination of Aux/IAAs and their subsequent degradation by the 26S proteasome (Gray et al., 2001; Dharmasiri et al., 2005; Kepinski and Leyser, 2005; Tan et al., 2007). Aux/IAAs degradation prevents their interaction with ARF transcription factor proteins thus allowing them to transcriptionally regulate the expression of their target genes through binding on specific *cis*-regulatory elements named Auxin Responsive Elements (AuxREs) (Ulmasov et al., 1995; Ulmasov et al., 1997, 1999; Liscum and Reed, 2002; Tiwari et al., 2004)(Figure A₁). At each level of this signaling pathway, additional levels of regulation occur. The following paragraphs will go back through each steps of the pathway and give some information on molecular structures of the actors and additional levels of regulation.

Structural organization of auxin signaling components:

Recent structural studies have provided partial information on the main structural organization of auxin signaling components. TIR/AFBs proteins (6 members in *Arabidopsis*) contain an F-BOX domain in the C-terminal region that is required for the interaction with the ARABIDOPSIS SKP1 HOMOLOGUE (ASK1) of the SCF complex. The N-terminal region comprises a domain formed of 18 Leucine Rich Repeat (LRR) motifs including the auxin binding pocket required to stabilize the interaction with Aux/IAA transcriptional repressors (Tan et al., 2007). AFB4 and 5 comprise other domains that might be responsible for their preferential affinity for other types of auxin (Calderon Villalobos et al., 2012). (Figure A₂ A).

Aux/IAAs proteins (28 members in *Arabidopsis*) are made of four highly conserved domains labelled I to IV that are all involved in protein-protein interactions. From the N-terminal to the C-terminal: domain I is a 1 or 2 ETHYLENE-

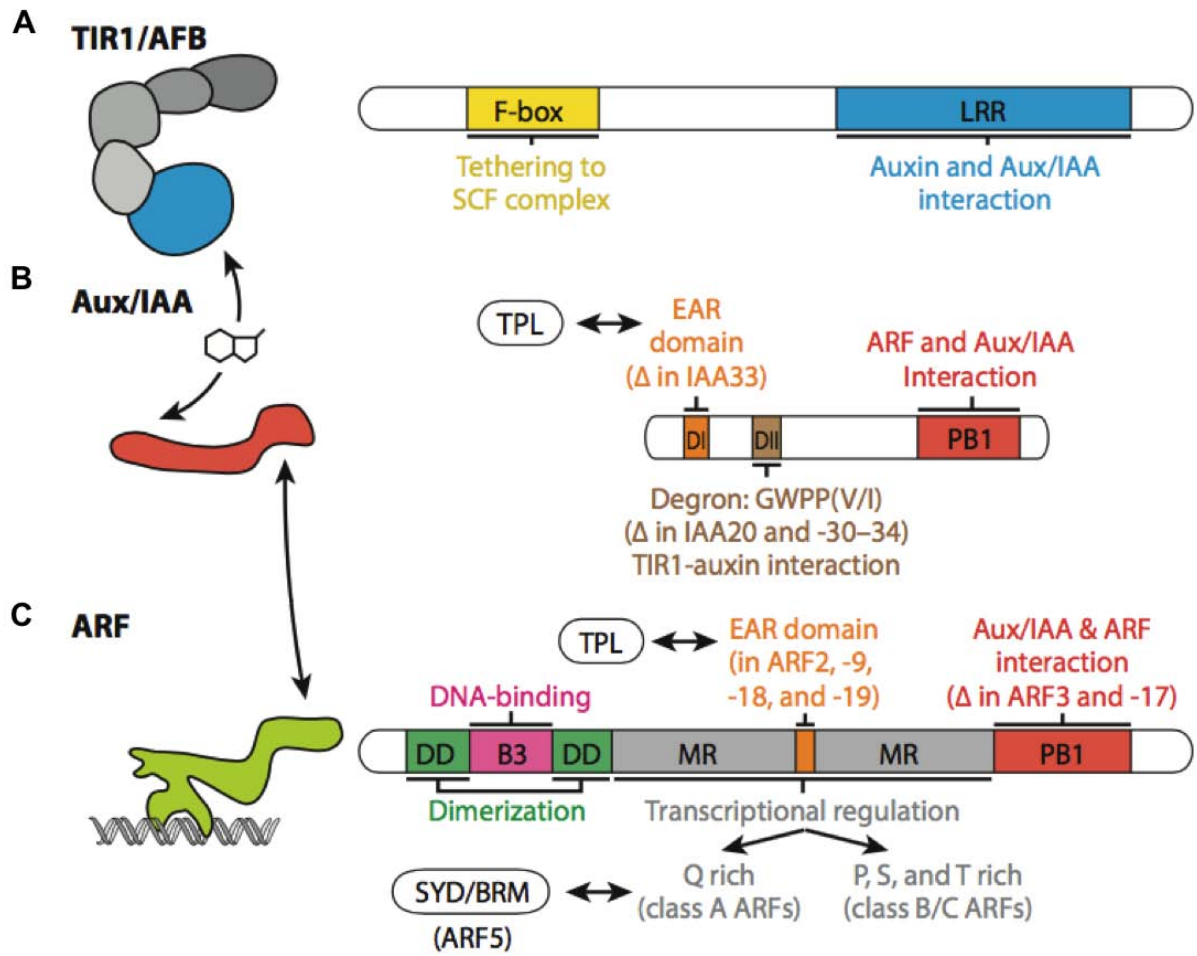


Figure A₂: Structural and functional organization of auxin signaling components. (A) TIR1/AFB auxin receptors. **(B)** Aux/IAA transcriptional repressors. **(C)** ARF transcription factors. This figure is from Weijers and Wagner 2016

RESPONSIVE ELEMENT BINDING FACTOR–ASSOCIATED REPRESSOR (EAR) or EAR-like repressor domains (Tiwari et al., 2004) that are hydrophobic motifs known to interact with the TOPLESS/TOPLESS-RELATED (TPL/TPR) family of co-repressors (Szemenyei et al., 2008) domain II (DII) contains the degron, a short sequence required for interaction with the F-box protein and the auxin-dependent regulation of Aux/IAA turn-over, and flanking regions modulating the strength of the interaction with the F-box in the presence of auxin (Calderon Villalobos et al., 2012) and domains III and IV now renamed a Phox and Bem 1 (PB1) domain for protein-protein interactions with other proteins containing a PB1 domain through electrostatic interactions (Dinesh et al., 2015). (Figure A₂ B)

ARFs (23 members in *Arabidopsis*) are also made of well-identified domains. At the N-terminus, a DNA Binding Domain (DBD) includes a B3 domain required for binding to AuxRE DNA motifs flanked by two Dimerization Domains (DD). The composition of a middle region (MR) was proposed to define the transcriptional activity of the ARFs. Some ARFs have an EAR domain within the MR (ARF2, 9, 18 and 19). The last domain is a PB1 domain as for Aux/IAAs (Korasick et al., 2014; Nanao et al., 2014) which is involved in the interaction with either ARFs or Aux/IAAs containing a PB1 domain (Figure A₂ C). ARF3, 13, 17 and 23 lack this PB1 domain indicating they cannot interact with Aux/IAA or other ARFs (Paponov et al., 2009). Initially ARFs were classified into Activators (ARFs A) or Repressors (ARFs R) according to the composition of their MR (glutamine-rich or proline, serine and threonine rich, respectively) and *trans*-activation assays in protoplasts (Ulmasov et al., 1999). More recent phylogenetic analysis including early land plants allowed their classification into 3 groups: the A class (the 5 ARFs A), the C class (ARFs R targeted by the microRNA mir160, see later in this introduction) and the B class (all the remaining ARFs) (Finet et al., 2013; Kato et al., 2015). The status of activator or repressor of ARFs is still a matter of debate as functional data are still missing for many of them and their effects might rely on specific conditions.

TIR/AFBs-AUX/IAAs interaction: affinity and specificity

The input of this signaling pathway is the sensing of auxin by the different couples of co-receptors resulting from the combination between TIR1/AFBs F-Box

and Aux/IAAs. Crystallography on such a complex has revealed that auxin binds the LRR domain of the F-Box (in the so called auxin binding pocket) allowing Aux/IAA to bind the upper part of the binding pocket through its DII (Tan et al., 2007; Calderon Villalobos et al., 2012). The resolution of the crystal structure of TIR1 also revealed the presence of a cofactor, the inositol (1,2,3,4,5,6) hexakisphosphate (InsP6), bound to the LRR domain. Some modification like S-Nitrosylation of a cysteine residue in the LRR domain of TIR1 was shown to stabilize the interaction with the Aux/IAAs (Terrile et al., 2012). In vitro auxin binding assays have revealed that distinct couples of TIR1/AFBs – Aux/IAA have distinct affinities for auxin, these affinities range for several orders of magnitude (Calderon Villalobos et al., 2012) Aux/IAA turnover can thus vary greatly between members of the family. In addition to the combinatorial TIR1/AFBs-Aux/IAAs co-receptor system, the response to auxin also depends on the relative amount of TIR1/AFBs and Aux/IAAs present in a cell at a given time. For a same auxin input concentration, the transcriptional output can vary greatly due to distinct affinities for auxin and resulting Aux/IAA turnover. The auxin co-receptor system is very versatile and allows differential sensing and responses. In terms of regulation, little is known on the transcriptional regulation of TIR1/AFB genes but TIR1, AFB2 and AFB3 are regulated at the post-transcriptional level as they are targeted by miRNA393 (Navarro et al., 2006; Parry et al., 2009).

AUX/IAAs inhibitory action on auxin transcriptional output

The PB1 domain of Aux/IAA exhibits two opposing electrostatic faces allowing the homodimerization of Aux/IAAs or heterodimerization with ARFs exhibiting also a PB1 domain. This interaction with ARF transcription factors brings Aux/IAAs and EAR domain interacting proteins, the TPL/TPR corepressors, close to regulatory sequences of ARF targets. TOPLESS recruits a HISTONE DEACETYLASE (HDAC) that mediates histone deacetylation leading to the closure of the chromatin structure. It has been shown that Aux/IAA oligomerization enhances their ability to repress transcriptional responses to auxin (Korasick et al., 2014). The charge composition at the interface of the PB1 domains was shown to determine the affinity and the homo- or hetero-oligomerization between Aux/IAA, between ARFs or Aux/IAA and ARFs. Based on structural and thermodynamic studies, the affinity of the interaction between ARF5 and IAA17 PB1 domains was found to be stronger than for ARF5-

ARF5 or IAA17-IAA17 by one to two orders of magnitude, respectively (Han et al., 2014). If this type of preferential interaction between Aux/IAAs and ARFs will be confirmed for other combinations of Aux/IAAs and ARFs, it will lead to a scenario in which the relative amount of Aux/IAAs and ARFs present in a cell at a given time will determinate the balance between homo- and hetero- oligomers and thus be crucial in the modulation of transcriptional responses to auxin.

In the context of flower organogenesis, it was shown that in response to auxin Aux/IAAs are degraded and ARF5 recruits BRAHMA (BRM) and SPLAYED (SYD), two subunits of SWI/SNF chromatin remodeling ATPase complexes. These proteins interact with the middle domain of ARF5, allowing re-opening of condensed chromatin and activation of ARF5 target genes (Wu et al., 2015). To what extent this mechanism is conserved for others ARFs A still remains to be investigated but it is likely that a mechanism allowing chromatin state switch is involved in auxin signaling.

Another level of complexity is added to the whole system since most Aux/IAA genes are transcriptionally upregulated in response to auxin thus providing an efficient negative feedback regulation. Some Aux/IAA genes are also regulated by other phytohormones, providing an entry point for hormone signaling cross talks. For instance cytokinin was reported to activate the expression of the SHY3/IAA3 gene via the involvement of ARABIDOPSIS RESPONSE REGULATOR 1 (ARR1) a B-type cytokinin response regulator. This activation reduces the expression of PIN and affects auxin redistribution, which in root affects the transition zone between elongation and differentiation. Reciprocally, auxin induces the degradation of SHY2/IAA3 sustaining PIN expression and maintaining cells within the root meristem (Dello Ioio et al., 2008).

ARFs oligomerization and organization of AuxREs drive the diversity of auxin responses

In addition to the formation of dimers or oligomers of ARFs via their C-terminal PB1 domain, ARFs are able to dimerize and to bind DNA motifs through their N-terminal DD and B3 domains respectively. DNA binding takes place on AuxREs. These *cis*-regulatory elements were first identified in the promoter of soybean *GRETCHEN HAGEN 3 (GH3)* auxin response gene as TGTCTC. This motif was not

found in the promoter of all auxin responsive genes suggesting that variants of this sequence could also act as AuxREs (Ulmasov et al., 1995). More recently, structural studies on the DBD of two rather divergent ARFs, ARF1 (class C) and ARF5 (class A), revealed that both of them preferentially bind to a TGTCGG motif however with some quantitative differences (Boer et al., 2014). In addition these two ARFs exhibited marked differences in their ability to bind complex motifs formed by two everted binding sites with various spacing. ARF5 dimer was shown to be efficient in the binding to such complex site for spacing ranging from 5 to 9 nucleotides whereas binding of ARF1 dimers was impaired for spacing lower or higher than 7 or 8 bases. . This property of ARFs to act as “molecular calipers”, as referred by the authors (Boer et al., 2014), to bind well-spaced binding sites for an ARF dimer represents a mechanism for generating variations between ARFs. According to the spacing and/or orientation between repeated AuxREs on gene promoters, distinct homodimers (or perhaps heterodimers) of ARFs can be preferentially recruited thus allowing to discriminate between auxin responsive genes (Boer et al., 2014).

Other levels of ARF regulations

Activity of ARFs can also be modulated via interaction with other transcription factors. For example, interaction of ARF7 with MYB77 was reported to result in a strong decrease in the number of lateral roots suggesting that transcriptional activity of ARF7 is impaired (Shin et al., 2007). During late development of petals, ARF8 interacts with the basic helix-loop-helix (bHLH) transcription factor BIGPETALp (BPEp) via their respective C-terminal domains resulting in a limitation of cell expansion, a role that was primarily attributed to BPEp (Szecsi et al., 2006; Brioudes et al., 2009). During early stages of petal development ARF8 acts as a negative regulator of petal growth by reducing cell proliferation (Varaud et al., 2011). Interestingly ARF8, together with its paralogue ARF6, were reported to promote jasmonic acid production and flower maturation (Nagpal et al., 2005) and BPEp originates from an alternative splicing of the BPE gene regulated by jasmonate signaling (Brioudes et al., 2009); which is another example of cross-talk.

On the basis of detailed mapping of the expression of the different ARF genes, in particular during embryogenesis, and also of genetic data, it has been shown that it is not only the activity of one ARF that is important but rather the combination of

several ARFs at a given time in a given cell to define downstream cellular responses (Rademacher et al., 2011; Rademacher et al., 2012). For example during early stages of embryo development distinct combinations of ARFs have been identified as being associated with cell division activities around and in the quiescent center or in cell elongation activities at the root apex, respectively. In most cell types, ARFs belonging to class A, B or C are co-expressed, each combination corresponding to a potentially distinct output (Rademacher et al., 2011).

The mode of action of ARFs R is not fully understood. Based on yeast two hybrid assays, they do not seem to interact with Aux/IAAs with few exceptions despite the presence of PB1 domains, thus questioning their mode of action (Vernoux et al., 2011; Piya et al., 2014). It has been proposed that they act through competitive occupancy of AuxREs on promoters of auxin response genes, impairing or preventing the binding of ARFs A. Those that include an EAR domain in their middle region might also recruit TOPLESS and promote chromatin remodeling via HDAC. ARF3/ETTIN, a non-canonical ARF, was shown to interact with INDEHISCENT bHLH TF in gynoecium morphogenesis to repress expression of target genes as PINOID (PID) a serine-threonine kinase regulating polar auxin transport, but auxin treatment somehow disrupts this interaction and suppresses the repression of PID (Simonini et al., 2016). This suggests that sensing of auxin acts to dissociate the interaction between ARF3/ETTIN and other TFs thus modifying transcriptional responses without the requirement of the TIR1/AFB - Aux/IAAs pathway. It is interesting to note, however, that expression of PID was demonstrated to be influenced directly by the long intergenic noncoding RNA (lincRNA) *APOLO* that is transcribed by RNA polymerases II and V in response to auxin regulating the formation of a chromatin loop encompassing the promoter of its neighboring gene PID and promoting its expression (Ariel et al., 2014) This example illustrates again the critical importance of the chromatin status in the auxin dependent regulation of gene expression.

Various *ARF* genes are also regulated at the post-transcriptional level. Relative abundance of their transcripts is regulated by microRNAs. *ARF6* and *ARF8*

are targeted by *miR167* (Wu et al., 2006) whereas *ARF10*, *ARF16*, and *ARF17* are targets of *miR160* (Mallory et al., 2005). In addition, another type of microARNs, *TAS3*, a transacting-small interfering RNAs (ta-siRNA), was reported to target *ARF2*, *ARF3* and *ARF4* in Arabidopsis (Williams et al., 2005). *TAS3* ta-siRNA requires miR390, which is induced in response to auxin, to be formed (Marin et al., 2010). Altogether, they constitute a complex auto-regulatory network that was shown to quantitatively regulate lateral root growth.

ARF2 is also regulated at the protein level by phosphorylation, for instance during photomorphogenesis. The BRASSINOSTEROID-INSENSITIVE2 (*BIN2*) kinase phosphorylates *ARF2* in a BR dependent manner resulting in a decrease of its ability to bind DNA and to exert transcriptional repression (Vert et al., 2008). In the context of lateral root organogenesis, *BIN2* was also reported to phosphorylate *ARF7* and *ARF19* (two closely related class A ARFs) in a BR independent manner suppressing their interaction with Aux/IAAs, potentiating their binding to AuxREs and enhancing transcriptional activity to their target genes (Cho et al., 2014). These two examples illustrate the importance of the developmental context, which influences the presence, relative abundance, or absence of key components of the signaling pathway in time and space. Cross talks with other signaling pathways represent additional levels of complexity. They occur through a direct effect on key components of the auxin signaling machinery but they operate also via modulation of hormone biosynthesis, metabolism or transport (Jones and Ljung, 2011; Schaller et al., 2015; Liu et al., 2017).

A recent study has reinvestigated the long time known inhibitory effect of auxin on root growth using real time imaging of growing roots coupled with microfluidics to follow the impact of changing auxin concentration on growth. It has revealed that auxin could inhibit root growth within seconds and that growth starts again few seconds after auxin removal. This effect was reported to rely on TIR/AFBs since this fast auxin growth inhibition was abolished in a *tir1afb2afb3* background, (Fendrych et al., 2018). It was interpreted as an involvement of TIR1/AFBs in fast non-genomic auxin responses. Such mutant is however likely to be affected in either qualitative or quantitative alterations of the highly complex molecular network involved in auxin

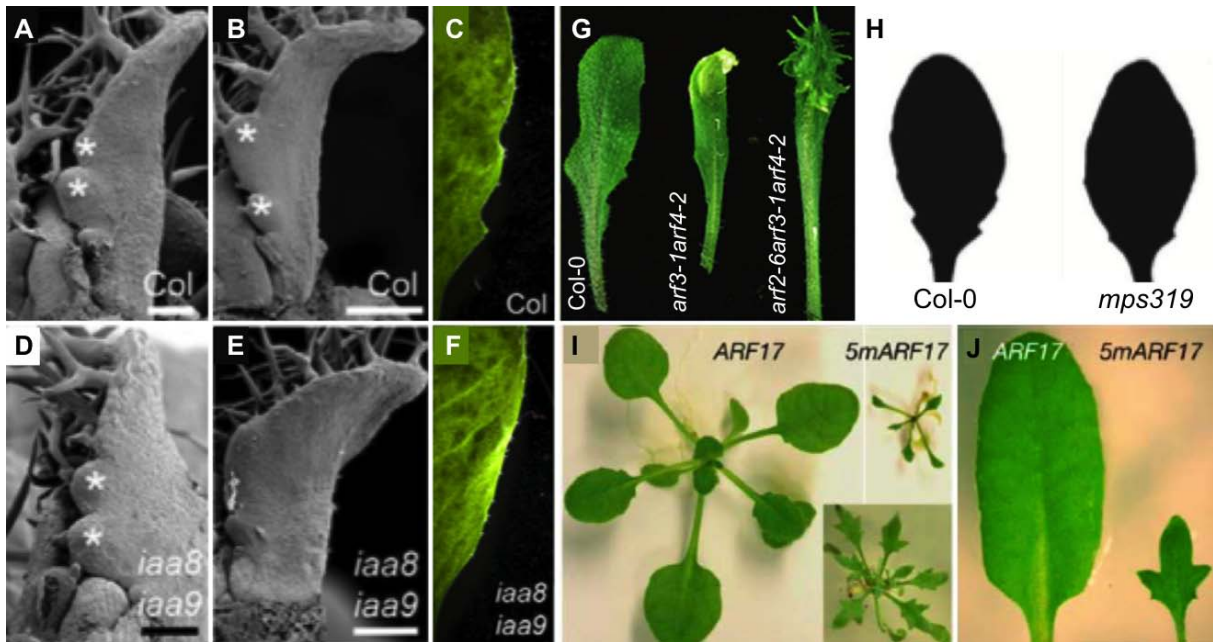


Figure A₃: Overview of leaf defects associated with impaired auxin signaling components. (A-B) Scanning electron micrographs of young Col-0 leaf. **(C)** Serrated margin of mature Col-0 leaf. **(D-E)** Scanning electron micrographs of young *iaa8iaa9* leaf. **(F)** Smoothed margin of *iaa8iaa9* mature leaf. **(G)** Col-0 leaf in comparison with *arf3-1arf4-2* and *arf2-6arf3-1arf4-2* mature leaves. **(H)** Leaf shapes of Col-0 and *mps319*, a weak allele for ARF5/MONOPTEROS. **(I-J)** Transgenic line expressing either wild-type ARF17 or a mutated version 5mARF17 resistant to mir160 degradation. **(A-F)** are from Koenig et al 2009, **(G)** is from Guan et al 2017, **(H)** is from Galbiati et al 2013 and **(I-J)** are from Mallory et al 2005

related responses. It remains us that even after 140 years of auxin studies we are still very far from a complete understanding of the multiples aspects of auxin actions.

Auxin signaling components involved in leaf serration

Soon after its initiation, leaf development involves a set of auxin responses. It has been proposed that soon after initiation, auxin depletion in the adaxial side of leaf takes part in the establishment of leaf polarity (Qi et al., 2014). Expression of ARF3 and 4 is restricted to the adaxial domain of leaf primordium by ASYMETRIC LEAVES 1/2 TFs (Iwasaki et al., 2013). ARF5 was shown to be involved in setting the identity of the middle domain of leaves (a domain at the junction of abaxial and adaxial domains of leaves) (Guan et al., 2017). ARF5 is also involved in the early steps of vascular strand patterning, just after auxin canalization mediated by PIN1, it is expressed and activates the transcription of ARABIDOPSIS THALIANA HOMEBOX 8 (ATHB8) gene that directs vascular differentiation (Scarpella et al., 2006). Finally the leaf margin of ARF5 weak allele *mpS319* was reported to be smoother than in wild type leaf (Galbiati et al., 2013), a phenotype that we however cannot observe in the lab suggesting that growth conditions might also influence this effect. Leaves of the Arabidopsis mARF17 line, that expresses a version of *ARF17* resistant to *miR160*, are far more serrated than wild type leaves (Mallory et al., 2005), indicating that over accumulation of ARF17 impairs the mechanisms involved in the control of leaf serrations. In tomato, overexpression of SIARF10/16/17 restricts lamina outgrowth and increases leaf complexity while overexpression of *miR160* increases lamina outgrowth and simplify leaf shape (Ben-Gera et al., 2016).

Although simple null mutants for IAA8 or IAA9 do not exhibit leaf phenotype, the double *iaa8iaa9* mutant initiates serrations but there are smoothed very early (Koenig et al., 2009). (figure A₃)

Apart these few studies, very little is known both on the dynamic of auxin response and auxin signaling components involved in leaf development in general and leaf serration in particular.

Results:

Pattern of auxin responses during leaf serration:

Auxin response is a general term which meaning can vary depending on the context. We took advantage of the availability of various types of auxin response reporters to investigate two levels of auxin responses: one reflects an auxin signaling input (i.e the ability of SCF^{TIR1/AFB} to interact with DII of Aux/IAA in presence of auxin) and the other is a transcriptional output of this signaling pathway (Figure A₄ and A₅).

Some data exhibiting DR5 pattern during early stages of serrations at the epidermis were already shown in chapter 1 (see figure 5 of the manuscript). Initial DR5 reporter consists in a minimal promoter containing 5 direct repeats of AuxREs (TGTCTC). More recently another version, pDR5v2, based on the AuxRE found to be preferentially bound by ARF1 and ARF5 (TGTCGG) (Boer et al., 2014) was generated and combined with a DR5 reporter within the same construct (Liao et al 2015). Here, we used a line expressing this double construct pDR5v2::ntdTomato-pDR5-n3GFPm (Liao et al., 2015). Maximal z-projections of fluorescent signals reflecting both DR5 and DR5v2 activities revealed an overall similar pattern of transcriptional responses with expression at the site of tooth initiation, at the tip of newly formed tooth, at the tip of the leaf and in the differentiating vascular network. Within young leaves, only slight differences were observed with a slightly more diffuse DR5v2 pattern around the vascular strands as it can be seen for example in figure A₅ D.

Auxin signaling input was followed using a DII-VENUS type of auxin response reporter where the DII domain of IAA 28 was fused to the yellow fluorescent protein VENUS (Brunoud et al., 2012). More recently a ratiometric version combining in a single construct DII-VENUS and a mutated version of DII altering the interaction with TIR1/AFB in the presence of auxin, mDII-tdTOMATO was made available, both of them under the control of the pRS5A promoter (R2D2,(Liao et al., 2015)) In order to get information on both early auxin signaling input and transcriptional output on the same material, a line carrying both R2D2 and DR5v2 was also generated (C3P0, unpublished D.Weijers lab, Wageningen). We used this C3P0 line (kindly provided by D. Weijers) to visualize the input response at the same time as the transcriptional

output (Figure A₅). The ratio between DII-Venus and mDII-Venus confirms a maximal response very early at the places of teeth initiation and at the tip of the teeth, including a distal tooth that can be seen at the right side of the leaf. However some differences are observed compared to DR5v2 expressed in the same leaf in particular DII-VENUS is observed at the tip of the leaf whereas DR5v2-CFP is still very strong highlighting the time frame difference between the two phases of the auxin signaling pathway. Another potential difference is that DII/mDII ratio does not allow visualizing the veins within the leaf as DR5v5 does but it is likely to result from the maximal z-projection that masks the response, i.e. decrease of DII, in the inner cells. Interestingly DII-mDII also allows to visualize a low auxin response at sinuses that is not seen with DR5v2 (figure A₅ C-E).

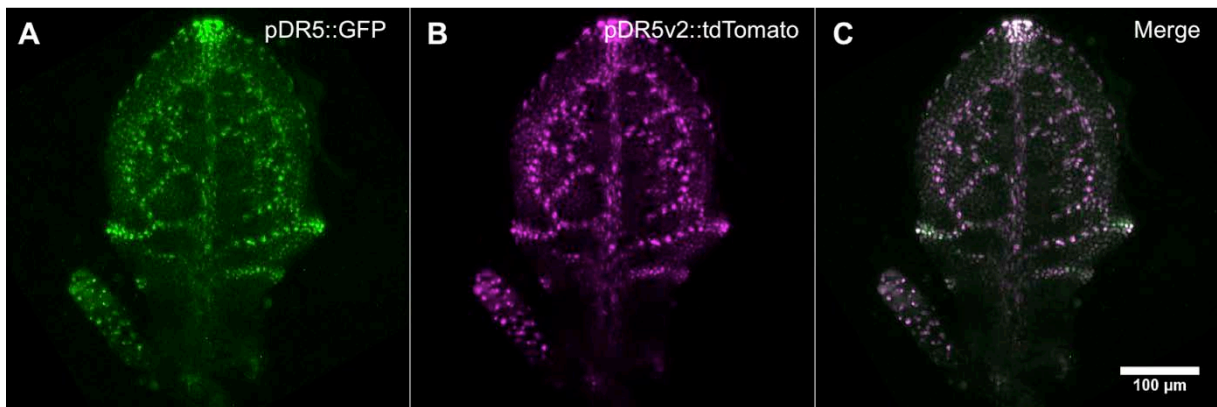


Figure A₄: Pattern of transcriptional auxin response in leaf. (A) Classical pDR5::GFP reporter **(B)** pDR5v2::tdTOMATO reporter **(C)** Merge of the two reporters. Images shown here are maximal z-projection of a 3D stack.

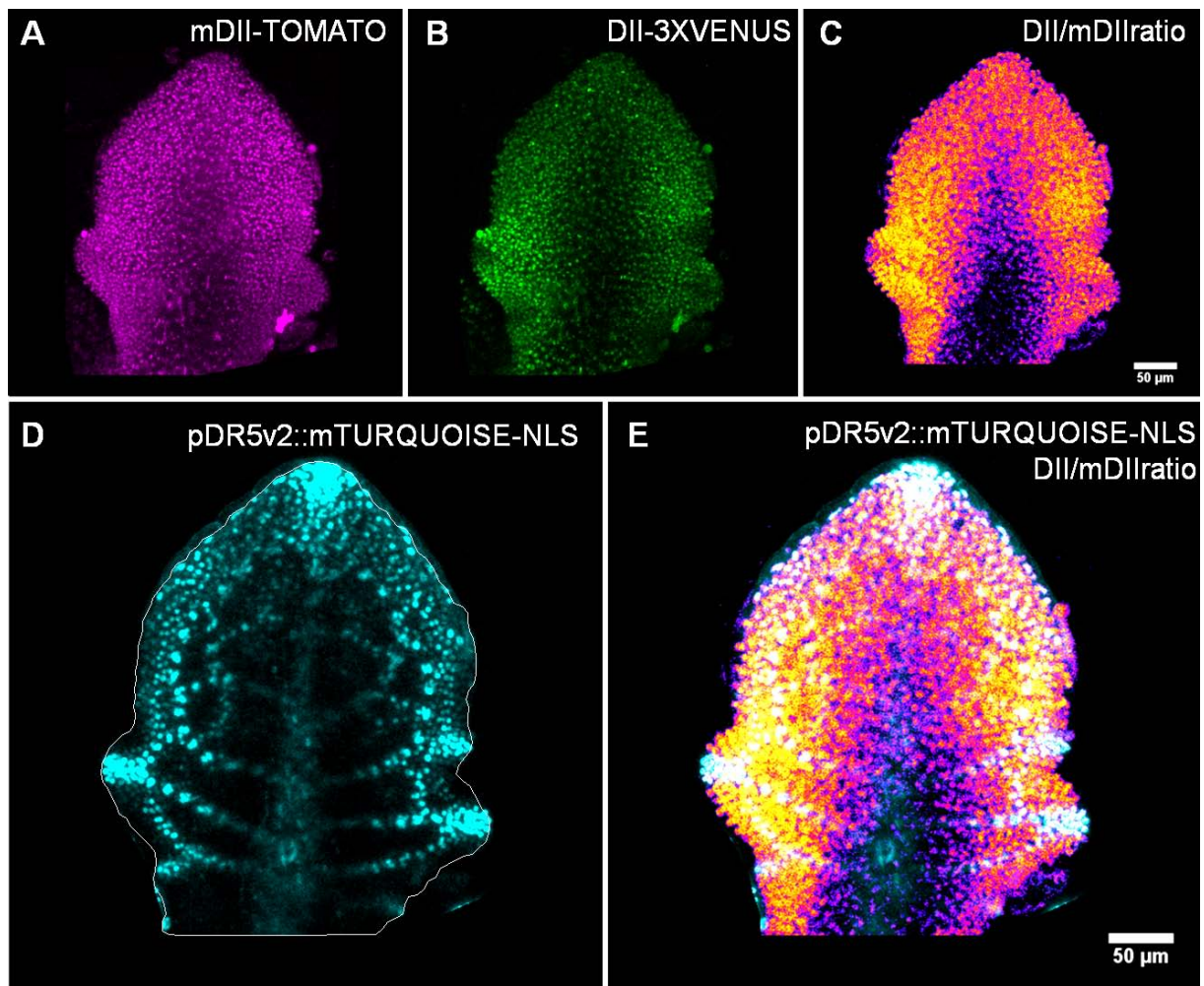


Figure A₅: Auxin signaling input and transcriptional response in leaf. (A-B) mDII-tdTOMATO and DII-3XVENUS channels. (C) representation of the ratio of DII-3XVENUS signal over the mDII-tdTOMATO signal colored according to FIRE look up table (High auxin response corresponding to low value of the ratio are in purple; low auxin response corresponding to high value of the ratio are in light yellow). (D) pDR5v2 transcriptional reporter. (E) Merge of pDR5v2 and DII/mDII ratio. All images are maximal z-projection from 3D stack.

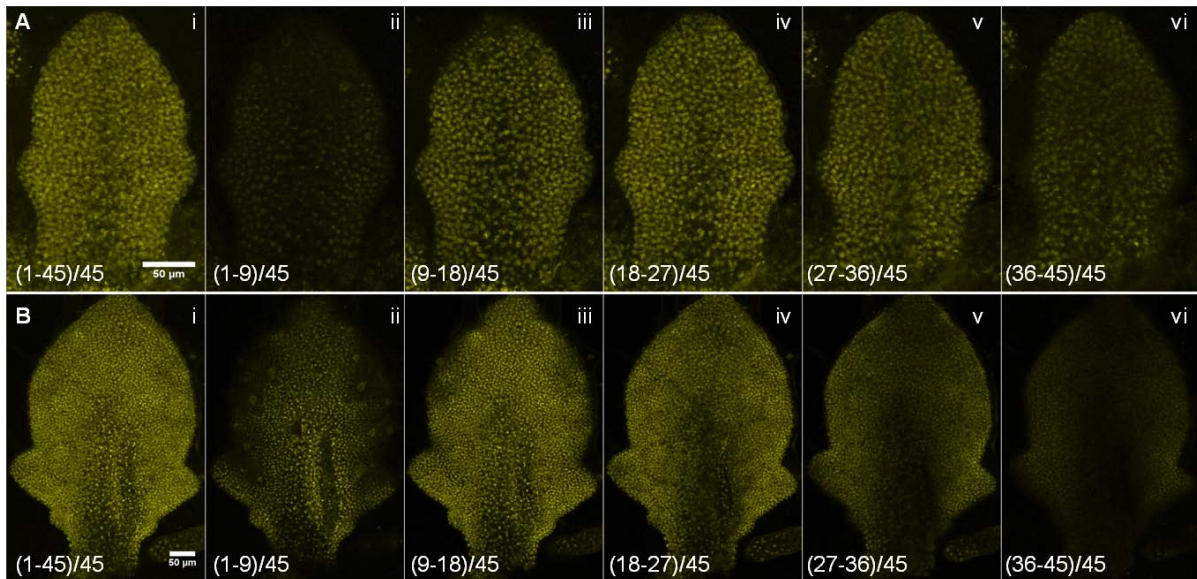


Figure A₆: TIR1 localization in leaf primordia based on *pTIR1::TIR1-VENUS* reporter line. **(A)** Pattern of TIR1 in leaf 11 when tooth pair 1 is initiated, maximal z-projection of the 3D stack is shown in (i), (ii) to (vi) show sequential grouped maximal z-projections across the stack from adaxial to the abaxial side of the leaf ((n-m)/x ; (n-m) range of images used for the maximal z projection; x number of images in the z-stack). **(B)** Pattern of TIR1 in leaf 11 at a later stage corresponding to initiation of teeth pair 2, (i) show the maximal z-projection of the 3D stack and (ii) to (vi) show sequential grouped maximal z-projections across the stack.

Pattern of TIR1, AFB2 and AFB3 during leaf serration:

In order to get insights on the patterns of TIR1/AFB during leaf serration, we took advantage of available translational reporter lines (Wang et al., 2016; Roychoudhry et al., 2017) . Instead of using dynamic imaging on growing leaves, we choose to perform static images on leaves at two distinct developmental stages: leaf primordia with one pair of initiated tooth and leaves with two pairs of initiated and formed serrations. Since the main purpose of our observation was to qualitatively describe the pattern of TIR1/AFB during leaf serration, we did not perform any quantification. However, in order to give a better appreciation of the observed pattern, we decided to present both a maximal z-projection of the 3D stack as well as a series of grouped maximal z-projection across the 3D stack from the adaxial to the abaxial faces of leaves.

At first sight, TIR1, AFB2 and AFB3 seem to be homogeneously distributed across the entire leaf, regardless of the developmental stage (Figures A₆, A₇, and A₈) but a closer examination shows slight heterogeneities in the patterns. TIR1 shows clearly lower intensities in vascular tissues which appear negative in relation to the whole leaf with a most visible effect in more developed leaves (Figure A₆ B v). For AFB2 and especially AFB3, such decrease of protein abundance in the vascular tissues is not seen with perhaps the exception of the mid vein (Figure A₈ B iv and v). The most divergent pattern is observed for AFB2 that is weakly accumulated or is absent at the tips serrations for the two developmental stages we looked at (Figure A₇). Although there are some differences in the pattern of TIR1, AFB2 and AFB3, their overall broad localization over leaf prompted us to suspect functional redundancy between these three closely related proteins, however we investigated leaf phenotypes of the related loss of function mutants.

Leaf phenotype of *tir1/afb* mutants:

Available genetic resources allowed us to investigate leaf phenotypes of simple, double, triple and quadruple mutants in the TIR1/AFB family. Although every simple mutant was investigated only the shape of *tir1-1*, *afb2-3* and *afb3-4* leaves are

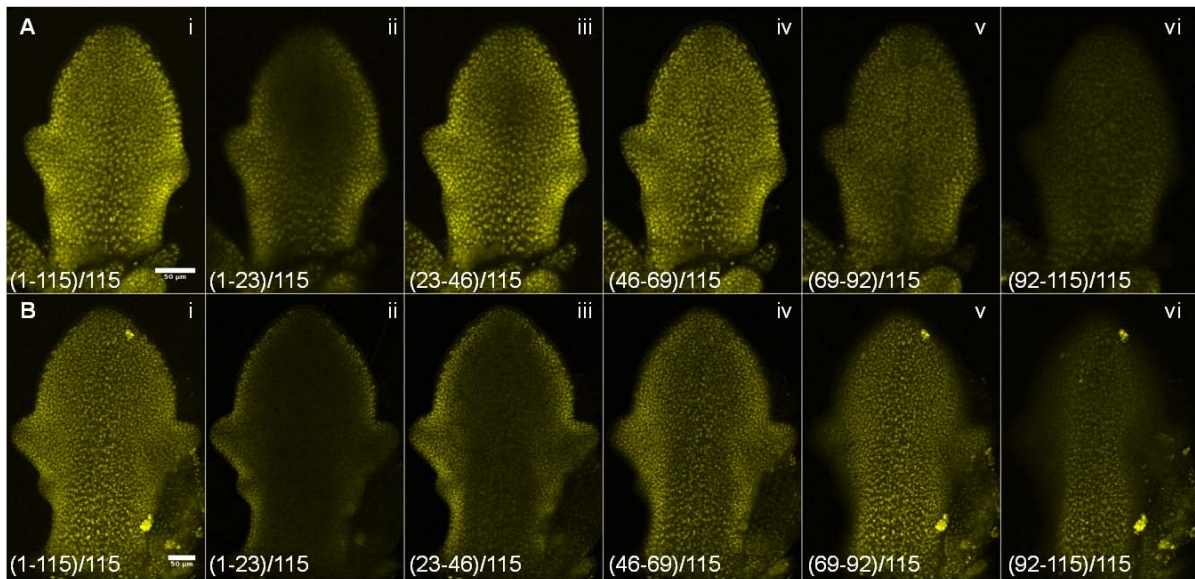


Figure A₇: AFB2 localization in leaf primordia based on *pAFB2::AFB2-VENUS* reporter line. (A) Pattern of AFB2 in leaf 11 when tooth pair 1 is initiated, maximal z-projection of the 3D stack is shown in (i), (ii) to (vi) show sequential grouped maximal z-projections across the stack from adaxial to the abaxial side of the leaf ((n-m)/x ; (n-m) range of images used for the maximal z projection; x number of images in the z-stack). **(B)** Pattern of AFB2 in leaf 11 at a later stage corresponding to initiation of teeth pair 2, (i) show the maximal z-projection of the 3D stack and (ii) to (vi) show sequential grouped maximal z-projections across the stack.

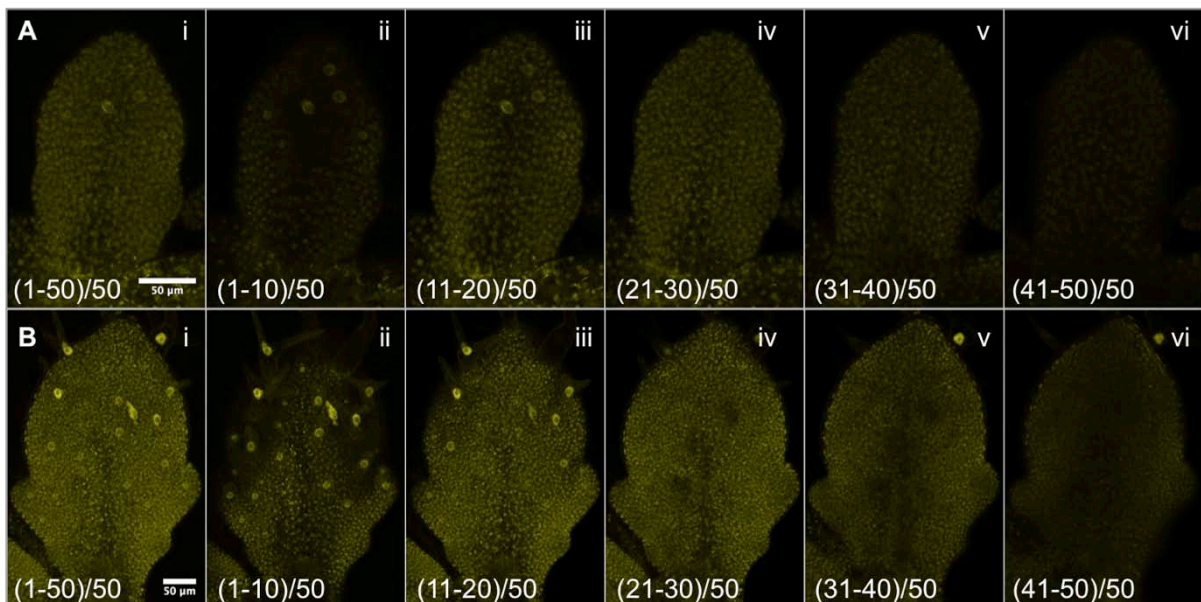


Figure A₈: AFB3 localization in leaf primordia based on *pAFB3::AFB3-VENUS* reporter line. (A) Pattern of AFB3 in leaf 11 when tooth pair 1 is initiated, maximal z-projection of the 3D stack is shown in (i), (ii) to (vi) show sequential grouped maximal z-projections across the stack from adaxial to the abaxial side of the leaf ((n-m)/x ; (n-m) range of images used for the maximal z projection; x number of images in the z-stack). **(B)** Pattern of AFB3 in leaf 11 at a later stage corresponding to initiation of teeth pair 2, (i) show the maximal z-projection of the 3D stack and (ii) to (vi) show sequential grouped maximal z-projections across the stack.

shown (Figure A₉) but none of them showed obvious defects whatever their developmental stage. Functional redundancy is very likely to explain the absence of phenotypes in simple mutants. To circumvent this drawback we next investigated phenotypes of various combinations of *tir1/afb* mutants (Dharmasiri et al., 2005) The quadruple mutant *tir1-1afb1-3afb2-3afb3-4* exhibits a range of strong phenotypes ranging into four classes and we had to select the seedlings that were able to grow enough to develop leaves even if they remain very small and curled. As we looked at a rather early stage of leaf morphogenesis, the difference of size was not as pronounced as later on. Dissection and flattening of the leaves revealed a surprising leaf shape: the leaves initiate serrations but they are located much more basal position than in the wild type and the medio-lateral growth of the leaf seems to be impaired (Figure A₉). This phenotype is not observed in triple mutants (Figure A₉) as well as in double mutants (not shown). Since the only marked leaf phenotype was seen in the quadruple mutant and therefore collection of a consequent pool of acquisition for quantitative morphometric analyses or cellular characterization was compromised (due to very low fertility of the class IV plants), we decided not to pursue this part of the project.



Figure A₉: Phenotypes of *tir1/afb* young leaves. Young leaf phenotypes of single or multiple *tir1/afb* mutants illustrated by a representative leaf 13 of 30 days-old plants cultivated in short photoperiod condition except for the quadruple mutant where leaf 11 is shown. Leaves presented here are all about 1 mm in length; *afb3-4* leaf has been symmetrized due to damages on the right side of the original leaf. Scale bar: 200µm

Discussion:

The contribution of auxin response pattern to leaf serration is known for several years (Bilsborough et al 2011). But apart from PIN1 local convergence points at the margin leading to local auxin accumulation and subsequent translation into transcriptional auxin responses (visualized with pDR5::GFP_{er}), the contribution of auxin to leaf serration is still scarcely described (to the exception of some studies presented at the end of the introduction to this chapter).

Our results confirm already known patterns of auxin signaling input, as well as transcriptional output (Kawamura et al., 2010; Bilsborough et al., 2011; Maugarny-Cales et al., 2019) (Figure A₅ and A₆). However, the comparison between the two versions of pDR5 reveals slight differences susceptible to reflect differences of reporter sensitivities (Liao et al., 2015). This statement remains to be clarified since transcriptional activation reported by various DR5 versions depend on the AuxRE motif used in artificial promoter as well as the configuration and relative spacing of AuxREs (Boer et al., 2014). In other words, the response depends on the distinct couples of ARFs that will be able to bind pDR5 promoter variants and activate the transcription. The terms auxin transcriptional output cover in fact a range of distinct responses that are highly dependent on the modulation of numerous entry points of the auxin signaling pathway. Anyhow DR5 reporters are to date the best tools we have to report on transcriptional responses to auxin. Concerning the relation between auxin signaling input, reported by DIIVENUS reporters, and transcriptional outputs, reported by pDR5v2 (Figure A₆), the apparent discrepancy observed between them relies on the difference of timing between these two events. It has recently been shown using time lapse imaging on SAM expressing DIIVENUS and DR5 reporters that DR5 signal is turned on several hours after the decrease in DII signal. DR5 driven reporter appears in cells where DIIVENUS is already detected indicating that transcriptional auxin response and auxin signaling input are not in phase (Galvan-Ampudia et al., 2019).

As it indicated earlier, this project was part of a bigger project aiming at providing an atlas of auxin signaling components in leaf serration. We (M.Boudin and I) provided a partial overview of the patterns for some TIR/AFBs, few *Aux/IAA* and number of ARFs expression patterns in leaf serrations. Reverse genetic approaches

was used in order to characterize the function of auxin signaling components in leaf serration. Due to functional redundancy, *tir1/afb* single mutants do not exhibit significant leaf phenotypes. The quadruple mutant is strongly affected in growth and developmental processes (Figure A₈) but for the plants that develop and form leaves, their shape is surprisingly not so severely altered and teeth are initiated. This indicates that the mechanisms involved in the control of differential growth at the margin are still efficient enough and allow tooth outgrowth. The fact that a proportion of quadruple mutants is able to develop is not so well understood. The current explanation is that other members of the family, AFB4 and AFB5, somehow compensate the loss of function of the other TIR1/AFBs even if their affinity for IAA is not as high as for the other proteins (Prigge et al., 2016). The basal positioning of the teeth might be due to the overall defect in leaf growth, it is however not a common feature of leaves from mutants with growth defects. It suggests that early tooth initiation along the margin is impaired when the entry into the auxin signaling pathway is disturbed. Another intriguing phenotype is that serrations are not smoothed as in wild type leaves. The basal serration observed for quadruple mutant could be explained by an overall decrease in auxin sensibility or the existence of an enhanced inhibitory field based on the leaf tip. It is also difficult to anticipate how the overall decrease in sensitivity of the quadruple *tir1afb* mutant will impact the other actors involved in leaf serration. Getting more information on the effect of a decreased auxin sensibility on CUCs patterns, auxin responses or cellular events would require the introgression of reporters into the quadruple mutant.

Material and methods:

Plant material and culture conditions:

All reporter lines used here have been described elsewhere except for C3P0 line which was kindly provided by D.Weijers. *pDR5v2::tdTOMATO/pDR5:GFP* was described in (Liao et al., 2015). *pTIR1::TIR1-VENUS* and *pAFB2::AFB2-VENUS* lines have been described in (Wang et al., 2016) and *pAFB3::AFB3-VENUS* in (Roychoudhry et al., 2017). ApopHusion reporter was described in (Gjetting et al., 2012). *tir1-1* has been described in (Ruegger et al., 1998), *afb1-3* and *afb2-3* in (Savaldi-Goldstein et al., 2008) *afb3-4* in (Parry et al., 2009) *afb4-8* and *afb5-5* in (Prigge et al., 2016).

All seeds were stratified in water at 4°C during 12 hours prior to be sown on soil and cultivated in short day photoperiod conditions for 21 to 30 days [1 h dawn (19°C, 65% hygrometry, 80 $\mu\text{mol}\cdot\text{m}^{-2}\cdot\text{s}^{-1}$ light), 6 h day (21°C, 65% hygrometry, 120 $\mu\text{mol}\cdot\text{m}^{-2}\cdot\text{s}^{-1}$ light), 1 h dusk (20°C, 65% hygrometry, 80 $\mu\text{mol}\cdot\text{m}^{-2}\cdot\text{s}^{-1}$ light), 16 h dark (18°C, 65% hygrometry, no light)].

Imaging and image processing:

Imaging of leaf expressing auxin response or TIR/AFB reporters were imaged on a Leica SP5 inverted or Leica TCS SP8X upright laser scanning confocal. VENUS signal was excited at 514 nm, tdTOMATO and mRFP at 560nm, GFP at 488nm, mTurquoise at 405 nm. VENUS signal were collected from 524 to 554 nm, tdTOMATO from 570 to 600nm, RFP from 570 to 650, GFP from 498 to 510nm and mTurquoise from 415 to 480nm. VENUS signal was collected on HyD detectors while the other fluorochromes were detected on PMT detectors.

For the leaf shape phenotypes, dissected leaf were imaged by collecting chlorophyll autofluorescence on a Carl Zeiss Axio Zoom V16 microscope equipped with Zeiss 63 HE filter set (excitation BP: 572/25, beam splitter 515, emission BP: 535/30)

Image binarization, maximal z-projections, grouped z-projection, channel merges and figure mounting were performed using ImageJ software (<https://imagej.nih.gov/ij/>).

Chapter IV: General discussion and perspectives

Growth control: multicellular levels and cell wall properties

One recurrent question in developmental biology is the scale at which growth is controlled. Our time lapse experiments presented in chapter 2 of this thesis revealed differential growth processes occurring at the clone level. Closer analyses at the resolution of the cells within the clones sustained by the analysis of cell surfaces on static acquisitions indicated that individual cells are smaller in the region of the sinuses than in the region of the tooth. However, bridging the gap between distinct levels is not straightforward. Indeed recent studies on sepal growth revealed that despite stereotypic growth patterns (in intensities and direction) observed at the tissue scale over a long time scale (several hours), growth of single clones is heterogeneous in direction and rate when looked at a lower time scale (hours) (Hong et al., 2016). It has been proposed that it is the spatio-temporal averaging of heterogeneous growth that gives rise to an overall homogeneous growth pattern (Hong et al., 2016). Moreover at the clone scale, it has been shown that each individual cell forming clones has distinct growth rate depending on their size at birth (Jones et al., 2017; Tsugawa et al., 2017). In our experiments, the temporal resolution was not high enough to assess the question of the relative contribution of single cells in overall growth of clones. However such heterogeneity in the contribution of single cells to the overall growth of clones is likely to take place in clones of the tooth. Indeed although the observed growth patterns in tooth are at the scale of several clones, individual cell surfaces are highly heterogeneous in this area at least for tooth larger than 100 μ m in width. On the contrary in sinus, cell size are much more homogeneous, which is likely to result from the repression of growth during the first phases of serrations and by a high level of mechanical stress in these cells and later on by a delayed differentiation. These assumptions remain however still speculative and only time lapse experiments with a higher temporal resolution would help to investigate the relation between individual cell growth and higher scales pattern of growth. Such experiment would necessarily induce additional

perturbations to the samples since repeated manipulations and laser exposure is not without consequence for plant physiology and development. Growth seems however to be controlled at the level of groups of cells/clones. Perhaps one potential way to control growth at the scale of groups of cells/clones is the dynamic control of cell wall properties.

Cell wall physico-chemical properties are known to be associated with its extensibility, partially through changes in pectin methyl esterification status and pH. Cell growth is indeed often associated with acidic apoplastic pH, this acidic pH could result from auxin mediated proton extrusion either through SAURs dependent activation of PM AHA (Ren et al., 2018) or K⁺ influx mediated by inward-rectifier K⁺ channels (Sottocornola et al., 2006) pectin de-methylation or a combination of both processes. Because we observed that auxin accumulates locally at the site of serration initiation and at the tip of the tooth, at some point during my Ph.D I explore whether local modifications of the pH can be observed. I performed primary microscopic acquisitions on leaves expressing a ratiometric reporter of apoplastic pH (ApopHusion (Gjetting et al., 2012)). ApopHusion reporter is made of two fluorescent proteins, a Red Fluorescent Protein (RFP) and a Green Fluorescent Protein (GFP) linked together and addressed to the apoplast by a chitinase signaling peptide. RFP is insensitive to pH variation and GFP is less photoactive at acidic pH. Imaging of both fluorochromes thus provides information on apoplastic pH. After calibration with a range of distinct pH buffers this reporter can be quantitatively analyzed to get numerical pH values. 3D representation from z-stack showing a merge of both RFP and GFP channels suggests that apoplastic acidic zones are present at the site of initiating serration as well as at the tip of already developed serrations. These regions are interspaced with zone of potentially less acidic pH. (Figure D₁). In addition I performed acquisitions on the same reporter in the shoot apical meristem, these acquisition revealed potential apoplastic acidification in the region of primordia initiation and in young flower primordia (Figure D₁). These data were somehow encouraging but this reporter has however some limitations impairing further use and reliable interpretation of the data: -GFP signal is found either in the apoplast and in the endoplasmic reticulum – the 35S promoter used to direct its expression is very unlikely to be ubiquitously expressed in plant shoots, thus giving rise to artefactual differences of signal intensities across shoot tissues – RFP and GFP are supposed to

be linked but they obviously exhibit distinct localizations suggesting a possible cleavage- settings required for the imaging of the RFP also trigger autofluorescence at the cell wall of differentiated cells interfering with the reporter. All these limitations made interpretation of the results quite uncertain. However, if the observed pattern of apopHusion is not an artefact, this pattern would correlate very well with the distribution of auxin transcriptional responses. The region thought to be less acidic would also correlate very well with zones where CUC3 is expressed. Even if a line expressing pCUC3::CFP in addition to apopHusion was generated it was decided not to use it because of the uncertainty in this reporter. Other tools reporting on apoplastic pH (like HPTS dye (Barbez et al., 2017)) might have been considered to explore further the relation between CUC3 effects and pH but they are likely to have other limitations and a choice had to be made to avoid dispersion in carrying the main thesis project. Our results showing that cell surfaces in *cuc3-105* sinus cells are much bigger than in the wild type and our preliminary results on lines overexpressing CUC3 showing an overall decrease in growth, very likely to be related to cell growth inhibition, give rise to some questions regarding the link between CUC3 and growth, including a possible inhibition of pH acidification.

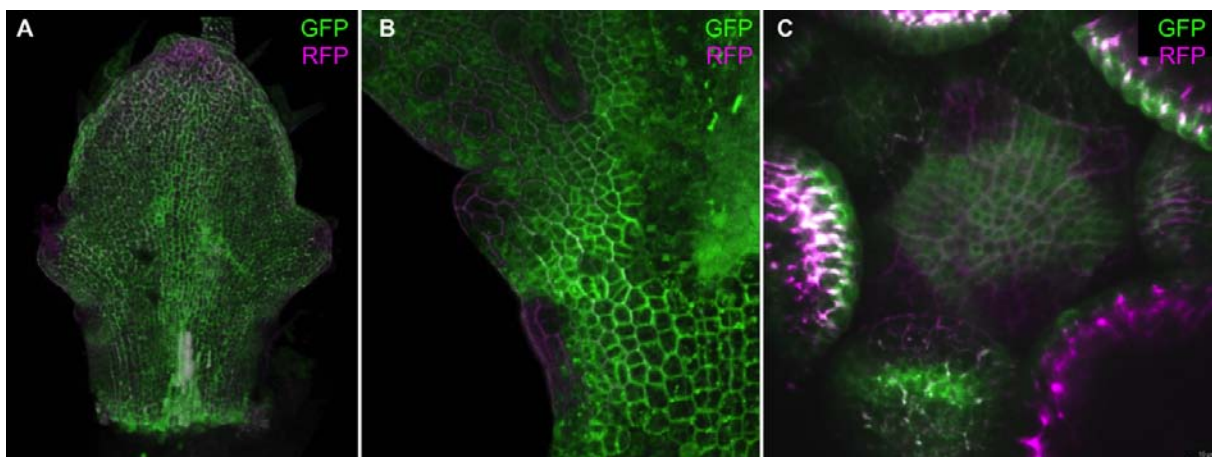


Figure D₁: Zones of suggested acidic apoplastic pH correlates with sites of auxin responses and growth. Image of a young leaf with a potential zone of acidic pH located at the tip of serrations and the tip of the leaf visualized by apopHusion (Gjetting et al 2012)(A). Zoom on serrations 2 and 3 of more developed leaf showing acidic zones at place of tooth initiation and tip of serrations (B). Shoot apical meristem, with acidic zone in organ primordia (C).

CUC3 is a transcription factor and its targets are not known but from our results we can postulate that it could negatively regulate numerous growth related genes and more particularly cell wall related genes. A recent publication published a

list of putative target genes for more than 250 Arabidopsis TFs, and CUC3 belongs to these TFs (O'Malley et al., 2016). Analyses of these putative target genes in comparison to growth related genes could be a primary work to investigate the mechanisms by which CUC3 represses growth. Comparative RNAseq transcriptomic analyses between DEX induced and non-induced *p35S::CUC3-GR* in a *cuc3-105* background could be an additional strategy, although the experimental setting would require to be well thought since this type of experiments have several levels of potential bias. To test the hypothesis that CUC3 locally modulates genes involved in regulation of pectin methyl esterification status, it would be possible to perform immunostaining of high and low methylated pectins using LM19 and JIM5 monoclonal antibodies which specifically bind to un-esterified and partially methoxy-esterified HG pectins, respectively (Clausen et al., 2003; Verhertbruggen et al., 2009) in transversal sections of fixed leaves of various genotypes. We could compare the pectin methylation status in sinuses and teeth of the wild type or compare sinus cells of *cuc3-105* mutant with sinus cells of the wild type or compare hypocotyls or leaves of DEX induced and non-induced *p35S::CUC3-GR* in a *cuc3-105* background. In addition, Atomic Force Microscopy could be used on the same lines to visualize the cell wall stiffness in cells with various levels of CUC3. Although we still do not know by which mechanisms CUC3 repress growth, we know that it does. This growth repressing activity coupled with the fact that CUC3 is induced by mechanical stress (Fal et al 2015) place it at the heart of an efficient regulatory loop between differential growth generating mechanical stress and growth repression. To date and to our knowledge no mechanism linking mechanical stress sensing to transcriptional activation of genes has been yet proposed in plants.

From mechanosensing to transcriptional activation of CUC3

Mechanical stress perception is known to influence plant development at various levels. Cell ablation in SAM was shown to induce a reorganization of CMT array in a circumferential pattern around the ablated cell, as well as triggering a reorientation of PIN1 polarity (Hamant et al., 2008). Organ scale mechanical stress pattern triggers MT transverse reorientation in the distal part of sepals, it was proposed that this MT reorientation participates in the organ growth arrest (Hervieux et al., 2016). More recently mechanical stress was shown to induce the expression of both STM and

CUC3 TFs (Fal et al., 2016). Even if some mechanisms involved in the perception of mechanical stress start to be reported, they are still scarcely described. In addition the signaling pathway linking mechanical stress perception to transcriptional output remains completely obscure. Here I will extrapolate on published data related to mechanical stress to propose several hypotheses to link these two events. There are two main places where mechanical stress can be sensed: the cell wall and the plasma membrane. Mechanical stress can cause damages in cell wall components, and induction of oligogalacturonids (OGs) release. These OGs have been proposed to be sensed by Wall Associated Kinases (WAKs), a group of Receptor Like Kinases (Decreux et al., 2006). This perception could lead to activation of a subsequent intracellular signaling cascade. Other RLKs with an extracellular domain could also mediate such a signaling cascade via rRLKs or members of the huge LRR-RLK family. It has also been proposed that calcium ion could be released from pectin egg-box upon stretching (Proseus and Boyer, 2007). Upon mechanical stress, the tension of the plasma membrane is affected and it has been shown that some ion channels could be opened upon stretch (Haswell et al 2011); mechanical stress would thus change ion flux and potentially trigger subsequent intracellular signaling pathway. Additionally, it has been shown that relative composition in Phospho-Inositol-Phosphate PI-(4)P and PI(4,5)P₂ could be changed when plasma membrane is under tension. Interestingly SAM boundary domains have been shown to be enriched in PI(4,5)P₂ (Stanislas et al., 2018) in a pattern very similar to CUC3. It has been shown that PIP participates in the electrostatic signature of the plasma membrane allowing the recruitment of some cytosolic protein kinases. For instance electronegative charge associated with PI(4)P enriched PM has been shown to recruit PINOID (PID) to the PM (Simon et al., 2016; Platre et al., 2018), others kinases or cytosolic proteins involved in signaling events might be recruited to the PM through similar mechanisms. Another potential actor involved in the early step of signaling event following mechanical stress sensing is DEK1. DEK1 is a transmembrane protein containing a cytosolic domain sharing some analogies with animal calpain which has been shown to be cleaved upon mechanical stress (Tran et al., 2017). This cleavage would activate the calpain domain. One could propose that this calpain domain can cleave a domain of a protein and thus participates in its translocation. Since some transcription factors have been shown to be transiently located in the cytosol and relocalized to the nucleus upon signaling, DEK1 calpain domain could be involved in

such TF translocation. One could test whether CUC3 is still able to be induced by mechanical stress in the weak allele *dek1-4* (Roeder et al., 2012). Although no mechanism allowing transduction of a signal from mechanoperception to transcriptional responses has been proposed here, each of the evoked actors can represent an entry point for further activation of a signaling cascade ending in transcriptional activation.

Differential auxin distribution and differential growth

PIN1 mediated polar auxin transport and local PIN1 convergence points are critical in the formation of local auxin maxima (Vernoux et al., 2000; Heisler et al., 2005). In the SAM, they have been associated with initiation and outgrowth of organ primordia. In leaf, they are associated with initiation of serrations (Bilborough et al., 2011). They have also been associated with the early steps of leaf vascular patterning (Scarpella et al., 2006; Marcos and Berleth, 2014; Verna et al., 2015). In this system, local PIN1 convergence points are formed at the leaf margin and then an auxin flux is directed from the margin toward the central vein. This auxin flux is further translated into transcriptional responses as visualized with pDR5 reporter prior leading to the expression of AtHB8 HD-zip involved in vascular differentiation (Scarpella et al., 2006). One particularity of these PIN1 convergence points is that they are not always associated with the initiation of a differential growth sustaining serration. Indeed the first local PIN1 convergence points formed at the margin are not associated with serration in the distal area of the leaf whereas at a more proximal position they are (approximately the third PIN1 convergence point in leaf 5 is associated to serration initiation). One hypothesis is that CUC2 is not expressed in the distal part of the leaf where this PIN1 convergence points occur and thus they are not able to reinforce PIN1 basal polarity and maintain it in time. This is one possible explanation but this is challenged by recent studies on a transgenic line exhibiting indeterminate growth of the leaf, i.e. the entire leaf is in proliferation. In such a leaf, every single PIN1 convergence point is translated into differential growth leading to the formation of a structure rather similar to serration (Alvarez et al., 2016). More surprisingly, small outgrowths still initiate in a *cuc2-1cuc3-105* background indicating that CUCs are not fundamentally required for local differential growth. These results

further indicate that differential auxin responses are able to trigger differential growth at the leaf margin if cells are in a proliferative state.

Although it has been proposed that CUC2 could trigger a local shift in PIN1 polarity from an apical polarity to a basal one no functional mechanism has been identified. This could result from downregulation of PINOID kinase that allows the apical polarization of PIN1 (Christensen et al., 2000; Friml et al., 2004; Huang et al., 2010). This could also result from upregulation of PP2A phosphatase involved in the basal reallocation of PIN1. An alternative hypothesis is that expression of CUCs induces local change in cell wall properties thus providing the basis for local mechanical heterogeneity. This local heterogeneity would impact PIN1 polarity and allow the formation of local auxin accumulation. To test this hypothesis, we could perform micro-application of fusicoccin containing lanoline paste (chemical known to induce apoplastic proton extrusion) at the smooth leaf margin of *cuc2-1* mutant since it is a place where PAT is still functional but where no PIN1 convergence point is associated with differential growth. Performing these experiments on *cuc2-1* line carrying a *pPIN1::PIN1-GFP* could contribute to see whether a local change in pH would be sufficient to induce initiation and maintenance of PIN1 convergence points. I initially planned to perform this fusicoccin experiment during my PhD but a prerequisite was to perform IAA lanoline application at the leaf margin at a very early stage to validate the experimental model. Unfortunately primary experiments did not give consistent and reproducible results.

Toward an integrative understanding of morphogenesis: interplay between developmental biology and computational science.

Laser scanning confocal microscopy on lines expressing fluorescent proteins (FP or protein fusion with FP) has been very useful to visualize various patterns (expression, proteins, auxin responses...). When it comes to obtaining a fine spatial and temporal dynamic atlas of various actors/processes, the natural variability inherent in any biological system can be a major drawback. In leaf for instance, even

if we focus our analyses on a specific rank, and we used leaves from plants of the same age cultivated in the same conditions, variability in both reporter patterns and shape of the leaves is far from being null. To circumvent this drawback, methods aiming at producing average maps based on individual acquisitions are being developed. For instance tools aiming at producing averaged leaf shape based on a set of individual real leaf shapes have been developed in the team, in collaboration with P. Andrey's team and A. Boudaoud (Morpholeaf, (Biot et al., 2016)). Similar approaches aiming at generating average maps of gene expression patterns based on individual acquisitions are currently being developed. To date these tools work on 2D objects (or approximated as being in 2D), but recently a study available on BioRxiv presents an image analysis pipeline able to reconstruct the fine spatio-temporal dynamic of the pattern of auxin response associated to primordia initiation on the PZ of SAM (Galvan-Ampudia et al., 2019). In this study 21 independent time lapse experiments on a line expressing a ratiometric version of DIIVENUS auxin reporter as well as a pCLV3::mCherry reporter were registered and interpolated to produce a fine mapping of auxin response dynamics on the L1 of the SAM. In this study the output dynamic map was in 2D (plus time) but no doubt that further developments of these tools will allow soon producing full 4D maps of developmental processes. The generation of such type of maps will be the basis for the integration of multiple informations (patterns of gene expression, protein localization, hormone responses, CMT array orientation, cell wall mechanical properties, etc...) on a common template.

In addition to producing a new generation of tools for quantitative image analyses, some teams working in the field of computational science applied to plant development are developing platforms of image analyses allowing to use real data as a template for modelling development. For instance 3D segmented epidermis pavement cells from 3D confocal z-stack have recently been used to model patterns of mechanical stress at the cellular level (Sapala et al., 2018). 3D or 4D maps of various actors with a cellular resolution could serve as a template for regulatory network modelling in both space and time. Such approaches are still challenging but will be very useful in a near future to provide a more comprehensive understanding of multiscale integrative processes occurring during plant morphogenesis.

References:

- Aida M, Ishida T, Fukaki H, Fujisawa H, Tasaka M** (1997) Genes involved in organ separation in Arabidopsis: an analysis of the cup-shaped cotyledon mutant. *Plant Cell* **9**: 841-857
- Aida M, Ishida T, Tasaka M** (1999) Shoot apical meristem and cotyledon formation during Arabidopsis embryogenesis: interaction among the CUP-SHAPED COTYLEDON and SHOOT MERISTEMLESS genes. *Development* **126**: 1563-1570
- Aida M, Tasaka M** (2006) Morphogenesis and patterning at the organ boundaries in the higher plant shoot apex. *Plant Mol Biol* **60**: 915-928
- Alvarez JP, Furumizu C, Efroni I, Eshed Y, Bowman JL** (2016) Active suppression of a leaf meristem orchestrates determinate leaf growth. *Elife* **5**
- Anastasiou E, Kenz S, Gerstung M, MacLean D, Timmer J, Fleck C, Lenhard M** (2007) Control of plant organ size by KLUH/CYP78A5-dependent intercellular signaling. *Dev Cell* **13**: 843-856
- Andriankaja M, Dhondt S, De Bodt S, Vanhaeren H, Coppens F, De Milde L, Muhlenbock P, Skirycz A, Gonzalez N, Beemster GT, Inze D** (2012) Exit from proliferation during leaf development in Arabidopsis thaliana: a not-so-gradual process. *Dev Cell* **22**: 64-78
- Ariel F, Jegu T, Latrasse D, Romero-Barrios N, Christ A, Benhamed M, Crespi M** (2014) Noncoding transcription by alternative RNA polymerases dynamically regulates an auxin-driven chromatin loop. *Mol Cell* **55**: 383-396
- Barbez E, Dunser K, Gaidora A, Lendl T, Busch W** (2017) Auxin steers root cell expansion via apoplastic pH regulation in Arabidopsis thaliana. *Proc Natl Acad Sci U S A* **114**: E4884-E4893
- Barbier de Reuille P, Routier-Kierzkowska AL, Kierzkowski D, Bassel GW, Schupbach T, Tauriello G, Bajpai N, Strauss S, Weber A, Kiss A, Burian A, Hofhuis H, Sapala A, Lipowczan M, Heimlicher MB, Robinson S, Bayer EM, Basler K, Koumoutsakos P, Roeder AH, Aegerter-Wilmsen T, Nakayama N, Tsiantis M, Hay A, Kwiatkowska D, Xenarios I, Kuhlemeier C, Smith RS** (2015) MorphoGraphX: A platform for quantifying morphogenesis in 4D. *Elife* **4**: 05864
- Bell EM, Lin WC, Husbands AY, Yu L, Jaganatha V, Jablonska B, Mangeon A, Neff MM, Girke T, Springer PS** (2012) Arabidopsis lateral organ boundaries negatively regulates brassinosteroid accumulation to limit growth in organ boundaries. *Proc Natl Acad Sci U S A* **109**: 21146-21151
- Ben-Gera H, Dafna A, Alvarez JP, Bar M, Mauerer M, Ori N** (2016) Auxin-mediated lamina growth in tomato leaves is restricted by two parallel mechanisms. *Plant J* **86**: 443-457
- Bennett T, van den Toorn A, Sanchez-Perez GF, Campilho A, Willemsen V, Snel B, Scheres B** (2010) SOMBRERO, BEARSKIN1, and BEARSKIN2 regulate root cap maturation in Arabidopsis. *Plant Cell* **22**: 640-654
- Besson S, Dumais J** (2011) Universal rule for the symmetric division of plant cells. *Proc Natl Acad Sci U S A* **108**: 6294-6299
- Bhatia N, Heisler MG** (2018) Self-organizing periodicity in development: organ positioning in plants. *Development* **145**

- Bilsborough GD, Runions A, Barkoulas M, Jenkins HW, Hasson A, Galinha C, Laufs P, Hay A, Prusinkiewicz P, Tsiantis M** (2011) Model for the regulation of *Arabidopsis thaliana* leaf margin development. *Proc Natl Acad Sci U S A* **108**: 3424-3429
- Biot E, Cortizo M, Burguet J, Kiss A, Oughou M, Maugarny-Cales A, Goncalves B, Adroher B, Andrey P, Boudaoud A, Laufs P** (2016) Multiscale quantification of morphodynamics: MorphoLeaf software for 2D shape analysis. *Development* **143**: 3417-3428
- Blein T, Pulido A, Vialette-Guiraud A, Nikovics K, Morin H, Hay A, Johansen IE, Tsiantis M, Laufs P** (2008) A conserved molecular framework for compound leaf development. *Science* **322**: 1835-1839
- Boer DR, Freire-Rios A, van den Berg WA, Saaki T, Manfield IW, Kepinski S, Lopez-Vidrieo I, Franco-Zorrilla JM, de Vries SC, Solano R, Weijers D, Coll M** (2014) Structural basis for DNA binding specificity by the auxin-dependent ARF transcription factors. *Cell* **156**: 577-589
- Breuil-Broyer S, Morel P, de Almeida-Engler J, Coustham V, Negrutiu I, Trehin C** (2004) High-resolution boundary analysis during *Arabidopsis thaliana* flower development. *Plant J* **38**: 182-192
- Brioudes F, Joly C, Szecsi J, Varaud E, Leroux J, Bellvert F, Bertrand C, Bendahmane M** (2009) Jasmonate controls late development stages of petal growth in *Arabidopsis thaliana*. *Plant J* **60**: 1070-1080
- Brunoud G, Wells DM, Oliva M, Larrieu A, Mirabet V, Burrow AH, Beeckman T, Kepinski S, Traas J, Bennett MJ, Vernoux T** (2012) A novel sensor to map auxin response and distribution at high spatio-temporal resolution. *Nature* **482**: 103-106
- Calderon Villalobos LI, Lee S, De Oliveira C, Ivetac A, Brandt W, Armitage L, Sheard LB, Tan X, Parry G, Mao H, Zheng N, Napier R, Kepinski S, Estelle M** (2012) A combinatorial TIR1/AFB-Aux/IAA co-receptor system for differential sensing of auxin. *Nat Chem Biol* **8**: 477-485
- Cho H, Ryu H, Rho S, Hill K, Smith S, Audenaert D, Park J, Han S, Beeckman T, Bennett MJ, Hwang D, De Smet I, Hwang I** (2014) A secreted peptide acts on BIN2-mediated phosphorylation of ARFs to potentiate auxin response during lateral root development. *Nat Cell Biol* **16**: 66-76
- Christensen SK, Dagenais N, Chory J, Weigel D** (2000) Regulation of auxin response by the protein kinase PINOID. *Cell* **100**: 469-478
- Clausen MH, Willats WG, Knox JP** (2003) Synthetic methyl hexagalacturonate hapten inhibitors of anti-homogalacturonan monoclonal antibodies LM7, JIM5 and JIM7. *Carbohydr Res* **338**: 1797-1800
- Cleland R** (1973) Auxin-induced hydrogen ion excretion from *Avena* coleoptiles. *Proc Natl Acad Sci U S A* **70**: 3092-3093
- Cosgrove DJ** (2005) Growth of the plant cell wall. *Nat Rev Mol Cell Biol* **6**: 850-861
- Cosgrove DJ** (2016) Plant cell wall extensibility: connecting plant cell growth with cell wall structure, mechanics, and the action of wall-modifying enzymes. *J Exp Bot* **67**: 463-476
- Das Gupta M, Nath U** (2015) Divergence in Patterns of Leaf Growth Polarity Is Associated with the Expression Divergence of miR396. *Plant Cell* **27**: 2785-2799
- Decreux A, Thomas A, Spies B, Bresseur R, Van Cutsem P, Messiaen J** (2006) In vitro characterization of the homogalacturonan-binding domain of the wall-

- associated kinase WAK1 using site-directed mutagenesis. *Phytochemistry* **67**: 1068-1079
- del Pozo JC, Diaz-Trivino S, Cisneros N, Gutierrez C** (2006) The balance between cell division and endoreplication depends on E2FC-DPB, transcription factors regulated by the ubiquitin-SCFSKP2A pathway in Arabidopsis. *Plant Cell* **18**: 2224-2235
- Dello Ioio R, Nakamura K, Moubayidin L, Perilli S, Taniguchi M, Morita MT, Aoyama T, Costantino P, Sabatini S** (2008) A genetic framework for the control of cell division and differentiation in the root meristem. *Science* **322**: 1380-1384
- Dharmasiri N, Dharmasiri S, Estelle M** (2005) The F-box protein TIR1 is an auxin receptor. *Nature* **435**: 441-445
- Dharmasiri N, Dharmasiri S, Weijers D, Lechner E, Yamada M, Hobbie L, Ehrismann JS, Jurgens G, Estelle M** (2005) Plant development is regulated by a family of auxin receptor F box proteins. *Dev Cell* **9**: 109-119
- Dinesh DC, Kovermann M, Gopalswamy M, Hellmuth A, Calderon Villalobos LI, Lilie H, Balbach J, Abel S** (2015) Solution structure of the PslAA4 oligomerization domain reveals interaction modes for transcription factors in early auxin response. *Proc Natl Acad Sci U S A* **112**: 6230-6235
- Donnelly PM, Bonetta D, Tsukaya H, Dengler RE, Dengler NG** (1999) Cell cycling and cell enlargement in developing leaves of Arabidopsis. *Dev Biol* **215**: 407-419
- Dumais J, Kwiatkowska D** (2002) Analysis of surface growth in shoot apices. *Plant J* **31**: 229-241
- Efroni I, Blum E, Goldshmidt A, Eshed Y** (2008) A protracted and dynamic maturation schedule underlies Arabidopsis leaf development. *Plant Cell* **20**: 2293-2306
- Efroni I, Han SK, Kim HJ, Wu MF, Steiner E, Birnbaum KD, Hong JC, Eshed Y, Wagner D** (2013) Regulation of leaf maturation by chromatin-mediated modulation of cytokinin responses. *Dev Cell* **24**: 438-445
- Eriksson S, Stransfeld L, Adamski NM, Breuninger H, Lenhard M** (2010) KLUH/CYP78A5-dependent growth signaling coordinates floral organ growth in Arabidopsis. *Curr Biol* **20**: 527-532
- Fal K, Landrein B, Hamant O** (2016) Interplay between miRNA regulation and mechanical stress for CUC gene expression at the shoot apical meristem. *Plant Signal Behav* **11**: e1127497
- Fendrych M, Akhmanova M, Merrin J, Glanc M, Hagihara S, Takahashi K, Uchida N, Torii KU, Friml J** (2018) Rapid and reversible root growth inhibition by TIR1 auxin signalling. *Nat Plants* **4**: 453-459
- Fendrych M, Leung J, Friml J** (2016) TIR1/AFB-Aux/IAA auxin perception mediates rapid cell wall acidification and growth of Arabidopsis hypocotyls. *Elife* **5**
- Finet C, Berne-Dedieu A, Scutt CP, Marletaz F** (2013) Evolution of the ARF gene family in land plants: old domains, new tricks. *Mol Biol Evol* **30**: 45-56
- Fox S, Southam P, Pantin F, Kennaway R, Robinson S, Castorina G, Sanchez-Corrales YE, Sablowski R, Chan J, Grieneisen V, Maree AFM, Bangham JA, Coen E** (2018) Spatiotemporal coordination of cell division and growth during organ morphogenesis. *PLoS Biol* **16**: e2005952
- Friml J, Yang X, Michniewicz M, Weijers D, Quint A, Tietz O, Benjamins R, Ouwwerkerk PB, Ljung K, Sandberg G, Hooykaas PJ, Palme K, Offringa R**

- (2004) A PINOID-dependent binary switch in apical-basal PIN polar targeting directs auxin efflux. *Science* **306**: 862-865
- Galbiati F, Sinha Roy D, Simonini S, Cucinotta M, Ceccato L, Cuesta C, Simaskova M, Benkova E, Kamiuchi Y, Aida M, Weijers D, Simon R, Masiero S, Colombo L** (2013) An integrative model of the control of ovule primordia formation. *Plant J* **76**: 446-455
- Galvan-Ampudia CS, Cerutti G, Legrand J, Azais R, Brunoud Gr, Moussu S, Wenzl C, Lohmann J, Godin C, Vernoux T** (2019) From spatio-temporal morphogenetic gradients to rhythmic patterning at the shoot apex. *bioRxiv*: 469718
- Gjetting KS, Ytting CK, Schulz A, Fuglsang AT** (2012) Live imaging of intra- and extracellular pH in plants using pHusion, a novel genetically encoded biosensor. *J Exp Bot* **63**: 3207-3218
- Goncalves B, Hasson A, Belcram K, Cortizo M, Morin H, Nikovics K, Vialette-Guiraud A, Takeda S, Aida M, Laufs P, Arnaud N** (2015) A conserved role for CUP-SHAPED COTYLEDON genes during ovule development. *Plant J* **83**: 732-742
- Gray WM, Kepinski S, Rouse D, Leyser O, Estelle M** (2001) Auxin regulates SCF(TIR1)-dependent degradation of AUX/IAA proteins. *Nature* **414**: 271-276
- Grbic V, Bleecker AB** (2000) Axillary meristem development in *Arabidopsis thaliana*. *Plant J* **21**: 215-223
- Greb T, Clarenz O, Schafer E, Muller D, Herrero R, Schmitz G, Theres K** (2003) Molecular analysis of the LATERAL SUPPRESSOR gene in *Arabidopsis* reveals a conserved control mechanism for axillary meristem formation. *Genes Dev* **17**: 1175-1187
- Guan C, Wu B, Yu T, Wang Q, Krogan NT, Liu X, Jiao Y** (2017) Spatial Auxin Signaling Controls Leaf Flattening in *Arabidopsis*. *Curr Biol* **27**: 2940-2950 e2944
- Hamant O** (2017) Mechano-devo. *Mech Dev* **145**: 2-9
- Hamant O, Heisler MG, Jonsson H, Krupinski P, Uyttewaal M, Bokov P, Corson F, Sahlin P, Boudaoud A, Meyerowitz EM, Couder Y, Traas J** (2008) Developmental patterning by mechanical signals in *Arabidopsis*. *Science* **322**: 1650-1655
- Han M, Park Y, Kim I, Kim EH, Yu TK, Rhee S, Suh JY** (2014) Structural basis for the auxin-induced transcriptional regulation by Aux/IAA17. *Proc Natl Acad Sci U S A* **111**: 18613-18618
- Han S, Hwang I** (2018) Integration of multiple signaling pathways shapes the auxin response. *J Exp Bot* **69**: 189-200
- Hasson A, Plessis A, Blein T, Adroher B, Grigg S, Tsiantis M, Boudaoud A, Damerval C, Laufs P** (2011) Evolution and diverse roles of the CUP-SHAPED COTYLEDON genes in *Arabidopsis* leaf development. *Plant Cell* **23**: 54-68
- Heisler MG, Hamant O, Krupinski P, Uyttewaal M, Ohno C, Jonsson H, Traas J, Meyerowitz EM** (2010) Alignment between PIN1 polarity and microtubule orientation in the shoot apical meristem reveals a tight coupling between morphogenesis and auxin transport. *PLoS Biol* **8**: e1000516
- Heisler MG, Ohno C, Das P, Sieber P, Reddy GV, Long JA, Meyerowitz EM** (2005) Patterns of auxin transport and gene expression during primordium development revealed by live imaging of the *Arabidopsis* inflorescence meristem. *Curr Biol* **15**: 1899-1911

- Herve C, Dabos P, Bardet C, Jauneau A, Auriac MC, Ramboer A, Lacout F, Tremousaygue D** (2009) In vivo interference with AtTCP20 function induces severe plant growth alterations and deregulates the expression of many genes important for development. *Plant Physiol* **149**: 1462-1477
- Hervieux N, Dumond M, Sapala A, Routier-Kierzkowska AL, Kierzkowski D, Roeder AH, Smith RS, Boudaoud A, Hamant O** (2016) A Mechanical Feedback Restricts Sepal Growth and Shape in Arabidopsis. *Curr Biol*
- Hibara K, Karim MR, Takada S, Taoka K, Furutani M, Aida M, Tasaka M** (2006) Arabidopsis CUP-SHAPED COTYLEDON3 regulates postembryonic shoot meristem and organ boundary formation. *Plant Cell* **18**: 2946-2957
- Hibara K, Takada S, Tasaka M** (2003) CUC1 gene activates the expression of SAM-related genes to induce adventitious shoot formation. *Plant J* **36**: 687-696
- Hisanaga T, Kawade K, Tsukaya H** (2015) Compensation: a key to clarifying the organ-level regulation of lateral organ size in plants. *J Exp Bot* **66**: 1055-1063
- Hofte H, Voxeur A** (2017) Plant cell walls. *Curr Biol* **27**: R865-R870
- Hong L, Dumond M, Tsugawa S, Sapala A, Routier-Kierzkowska AL, Zhou Y, Chen C, Kiss A, Zhu M, Hamant O, Smith RS, Komatsuzaki T, Li CB, Boudaoud A, Roeder AH** (2016) Variable Cell Growth Yields Reproducible OrganDevelopment through Spatiotemporal Averaging. *Dev Cell* **38**: 15-32
- Huang F, Zago MK, Abas L, van Marion A, Galvan-Ampudia CS, Offringa R** (2010) Phosphorylation of conserved PIN motifs directs Arabidopsis PIN1 polarity and auxin transport. *Plant Cell* **22**: 1129-1142
- Ishida T, Aida M, Takada S, Tasaka M** (2000) Involvement of CUP-SHAPED COTYLEDON genes in gynoecium and ovule development in Arabidopsis thaliana. *Plant Cell Physiol* **41**: 60-67
- Iwasaki M, Takahashi H, Iwakawa H, Nakagawa A, Ishikawa T, Tanaka H, Matsumura Y, Pekker I, Eshed Y, Vial-Pradel S, Ito T, Watanabe Y, Ueno Y, Fukazawa H, Kojima S, Machida Y, Machida C** (2013) Dual regulation of ETTIN (ARF3) gene expression by AS1-AS2, which maintains the DNA methylation level, is involved in stabilization of leaf adaxial-abaxial partitioning in Arabidopsis. *Development* **140**: 1958-1969
- Jackson MDB, Duran-Nebreda S, Kierzkowski D, Strauss S, Xu H, Landrein B, Hamant O, Smith RS, Johnston IG, Bassel GW** (2019) Global Topological Order Emerges through Local Mechanical Control of Cell Divisions in the Arabidopsis Shoot Apical Meristem. *Cell Syst* **8**: 53-65 e53
- Jones B, Ljung K** (2011) Auxin and cytokinin regulate each other's levels via a metabolic feedback loop. *Plant Signal Behav* **6**: 901-904
- Jones RA, Forero-Vargas M, Withers SP, Smith RS, Traas J, Dewitte W, Murray JAH** (2017) Cell-size dependent progression of the cell cycle creates homeostasis and flexibility of plant cell size. *Nat Commun* **8**: 15060
- Kalve S, De Vos D, Beemster GT** (2014) Leaf development: a cellular perspective. *Front Plant Sci* **5**: 362
- Kato H, Ishizaki K, Kouno M, Shirakawa M, Bowman JL, Nishihama R, Kohchi T** (2015) Auxin-Mediated Transcriptional System with a Minimal Set of Components Is Critical for Morphogenesis through the Life Cycle in *Marchantia polymorpha*. *PLoS Genet* **11**: e1005084
- Kawamura E, Horiguchi G, Tsukaya H** (2010) Mechanisms of leaf tooth formation in Arabidopsis. *Plant J* **62**: 429-441
- Kazama T, Ichihashi Y, Murata S, Tsukaya H** (2010) The mechanism of cell cycle arrest front progression explained by a KLUH/CYP78A5-dependent mobile

- growth factor in developing leaves of *Arabidopsis thaliana*. *Plant Cell Physiol* **51**: 1046-1054
- Kepinski S, Leyser O** (2005) The *Arabidopsis* F-box protein TIR1 is an auxin receptor. *Nature* **435**: 446-451
- Kieffer M, Master V, Waites R, Davies B** (2011) TCP14 and TCP15 affect internode length and leaf shape in *Arabidopsis*. *Plant J* **68**: 147-158
- Koenig D, Bayer E, Kang J, Kuhlemeier C, Sinha N** (2009) Auxin patterns *Solanum lycopersicum* leaf morphogenesis. *Development* **136**: 2997-3006
- Korasick DA, Westfall CS, Lee SG, Nanao MH, Dumas R, Hagen G, Guilfoyle TJ, Jez JM, Strader LC** (2014) Molecular basis for AUXIN RESPONSE FACTOR protein interaction and the control of auxin response repression. *Proc Natl Acad Sci U S A* **111**: 5427-5432
- Kwiatkowska D** (2004) Surface growth at the reproductive shoot apex of *Arabidopsis thaliana* pin-formed 1 and wild type. *J Exp Bot* **55**: 1021-1032
- Kwiatkowska D** (2008) Flowering and apical meristem growth dynamics. *J Exp Bot* **59**: 187-201
- Kwiatkowska D, Dumais J** (2003) Growth and morphogenesis at the vegetative shoot apex of *Anagallis arvensis* L. *J Exp Bot* **54**: 1585-1595
- Kwiatkowska D, Routier-Kierzkowska AL** (2009) Morphogenesis at the inflorescence shoot apex of *Anagallis arvensis*: surface geometry and growth in comparison with the vegetative shoot. *J Exp Bot* **60**: 3407-3418
- Landrein B, Kiss A, Sassi M, Chauvet A, Das P, Cortizo M, Laufs P, Takeda S, Aida M, Traas J, Vernoux T, Boudaoud A, Hamant O** (2015) Mechanical stress contributes to the expression of the STM homeobox gene in *Arabidopsis* shoot meristems. *Elife* **4**: e07811
- Laufs P, Peaucelle A, Morin H, Traas J** (2004) MicroRNA regulation of the CUC genes is required for boundary size control in *Arabidopsis* meristems. *Development* **131**: 4311-4322
- Liao CY, Smet W, Brunoud G, Yoshida S, Vernoux T, Weijers D** (2015) Reporters for sensitive and quantitative measurement of auxin response. *Nat Methods* **12**: 207-210, 202 p following 210
- Liscum E, Reed JW** (2002) Genetics of Aux/IAA and ARF action in plant growth and development. *Plant Mol Biol* **49**: 387-400
- Liu J, Moore S, Chen C, Lindsey K** (2017) Crosstalk Complexities between Auxin, Cytokinin, and Ethylene in *Arabidopsis* Root Development: From Experiments to Systems Modeling, and Back Again. *Mol Plant* **10**: 1480-1496
- Long J, Barton MK** (2000) Initiation of axillary and floral meristems in *Arabidopsis*. *Dev Biol* **218**: 341-353
- Louveaux M, Julien JD, Mirabet V, Boudaoud A, Hamant O** (2016) Cell division plane orientation based on tensile stress in *Arabidopsis thaliana*. *Proc Natl Acad Sci U S A* **113**: E4294-4303
- Luu DT, Martiniere A, Sorieul M, Runions J, Maurel C** (2012) Fluorescence recovery after photobleaching reveals high cycling dynamics of plasma membrane aquaporins in *Arabidopsis* roots under salt stress. *Plant J* **69**: 894-905
- Majda M, Robert S** (2018) The Role of Auxin in Cell Wall Expansion. *Int J Mol Sci* **19**
- Malivert A, Hamant O, Ingram G** (2018) The contribution of mechanosensing to epidermal cell fate specification. *Curr Opin Genet Dev* **51**: 52-58
- Mallory AC, Bartel DP, Bartel B** (2005) MicroRNA-directed regulation of *Arabidopsis* AUXIN RESPONSE FACTOR17 is essential for proper

- development and modulates expression of early auxin response genes. *Plant Cell* **17**: 1360-1375
- Marcos D, Berleth T** (2014) Dynamic auxin transport patterns preceding vein formation revealed by live-imaging of Arabidopsis leaf primordia. *Front Plant Sci* **5**: 235
- Marin E, Jouannet V, Herz A, Lokerse AS, Weijers D, Vaucheret H, Nussaume L, Crespi MD, Maizel A** (2010) miR390, Arabidopsis TAS3 tasiRNAs, and their AUXIN RESPONSE FACTOR targets define an autoregulatory network quantitatively regulating lateral root growth. *Plant Cell* **22**: 1104-1117
- Marty F** (1999) Plant vacuoles. *Plant Cell* **11**: 587-600
- Maugarny-Cales A, Cortizo M, Adroher B, Borrega N, Goncalves B, Brunoud G, Vernoux T, Arnaud N, Laufs P** (2019) Dissecting the pathways coordinating patterning and growth by plant boundary domains. *PLoS Genet* **15**: e1007913
- McKim SM, Stenvik GE, Butenko MA, Kristiansen W, Cho SK, Hepworth SR, Aalen RB, Haughn GW** (2008) The BLADE-ON-PETIOLE genes are essential for abscission zone formation in Arabidopsis. *Development* **135**: 1537-1546
- Miart F, Desprez T, Biot E, Morin H, Belcram K, Hofte H, Gonneau M, Vernhettes S** (2014) Spatio-temporal analysis of cellulose synthesis during cell plate formation in Arabidopsis. *Plant J* **77**: 71-84
- Nagpal P, Ellis CM, Weber H, Ploense SE, Barkawi LS, Guilfoyle TJ, Hagen G, Alonso JM, Cohen JD, Farmer EE, Ecker JR, Reed JW** (2005) Auxin response factors ARF6 and ARF8 promote jasmonic acid production and flower maturation. *Development* **132**: 4107-4118
- Nanao MH, Vinos-Poyo T, Brunoud G, Thevenon E, Mazzoleni M, Mast D, Laine S, Wang S, Hagen G, Li H, Guilfoyle TJ, Parcy F, Vernoux T, Dumas R** (2014) Structural basis for oligomerization of auxin transcriptional regulators. *Nat Commun* **5**: 3617
- Navarro L, Dunoyer P, Jay F, Arnold B, Dharmasiri N, Estelle M, Voinnet O, Jones JD** (2006) A plant miRNA contributes to antibacterial resistance by repressing auxin signaling. *Science* **312**: 436-439
- Nikovics K, Blein T, Peaucelle A, Ishida T, Morin H, Aida M, Laufs P** (2006) The balance between the MIR164A and CUC2 genes controls leaf margin serration in Arabidopsis. *Plant Cell* **18**: 2929-2945
- O'Malley RC, Huang SC, Song L, Lewsey MG, Bartlett A, Nery JR, Galli M, Gallavotti A, Ecker JR** (2016) Cistrome and Epicistrome Features Shape the Regulatory DNA Landscape. *Cell* **165**: 1280-1292
- Paponov IA, Teale W, Lang D, Paponov M, Reski R, Rensing SA, Palme K** (2009) The evolution of nuclear auxin signalling. *BMC Evol Biol* **9**: 126
- Parcy F, Vernoux T, Dumas R** (2016) A Glimpse beyond Structures in Auxin-Dependent Transcription. *Trends Plant Sci* **21**: 574-583
- Parry G, Calderon-Villalobos LI, Prigge M, Peret B, Dharmasiri S, Itoh H, Lechner E, Gray WM, Bennett M, Estelle M** (2009) Complex regulation of the TIR1/AFB family of auxin receptors. *Proc Natl Acad Sci U S A* **106**: 22540-22545
- Peaucelle A, Wightman R, Hofte H** (2015) The Control of Growth Symmetry Breaking in the Arabidopsis Hypocotyl. *Curr Biol* **25**: 1746-1752
- Perales M, Rodriguez K, Snipes S, Yadav RK, Diaz-Mendoza M, Reddy GV** (2016) Threshold-dependent transcriptional discrimination underlies stem cell homeostasis. *Proc Natl Acad Sci U S A* **113**: E6298-E6306

- Perrot-Rechenmann C** (2010) Cellular responses to auxin: division versus expansion. *Cold Spring Harb Perspect Biol* **2**: a001446
- Piya S, Shrestha SK, Binder B, Stewart CN, Jr., Hewezi T** (2014) Protein-protein interaction and gene co-expression maps of ARFs and Aux/IAAs in *Arabidopsis*. *Front Plant Sci* **5**: 744
- Platre MP, Noack LC, Doumane M, Bayle V, Simon MLA, Maneta-Peyret L, Fouillen L, Stanislas T, Armengot L, Pejchar P, Caillaud MC, Potocky M, Copic A, Moreau P, Jaillais Y** (2018) A Combinatorial Lipid Code Shapes the Electrostatic Landscape of Plant Endomembranes. *Dev Cell* **45**: 465-480 e411
- Prigge MJ, Greenham K, Zhang Y, Santner A, Castillejo C, Mutka AM, O'Malley RC, Ecker JR, Kunkel BN, Estelle M** (2016) The *Arabidopsis* Auxin Receptor F-Box Proteins AFB4 and AFB5 Are Required for Response to the Synthetic Auxin Picloram. *G3 (Bethesda)* **6**: 1383-1390
- Proseus TE, Boyer JS** (2007) Tension required for pectate chemistry to control growth in *Chara corallina*. *J Exp Bot* **58**: 4283-4292
- Qi J, Wang Y, Yu T, Cunha A, Wu B, Vernoux T, Meyerowitz E, Jiao Y** (2014) Auxin depletion from leaf primordia contributes to organ patterning. *Proc Natl Acad Sci U S A* **111**: 18769-18774
- Rademacher EH, Lokerse AS, Schlereth A, Llavata-Peris CI, Bayer M, Kientz M, Freire Rios A, Borst JW, Lukowitz W, Jurgens G, Weijers D** (2012) Different auxin response machineries control distinct cell fates in the early plant embryo. *Dev Cell* **22**: 211-222
- Rademacher EH, Moller B, Lokerse AS, Llavata-Peris CI, van den Berg W, Weijers D** (2011) A cellular expression map of the *Arabidopsis* AUXIN RESPONSE FACTOR gene family. *Plant J* **68**: 597-606
- Rast-Somssich MI, Broholm S, Jenkins H, Canales C, Vlad D, Kwantes M, Bilsborough G, Dello Iorio R, Ewing RM, Laufs P, Huijser P, Ohno C, Heisler MG, Hay A, Tsiantis M** (2015) Alternate wiring of a KNOXI genetic network underlies differences in leaf development of *A. thaliana* and *C. hirsuta*. *Genes Dev* **29**: 2391-2404
- Reinhardt B, Hanggi E, Muller S, Bauch M, Wyrzykowska J, Kerstetter R, Poethig S, Fleming AJ** (2007) Restoration of DWF4 expression to the leaf margin of a *dwf4* mutant is sufficient to restore leaf shape but not size: the role of the margin in leaf development. *Plant J* **52**: 1094-1104
- Reinhardt D, Mandel T, Kuhlemeier C** (2000) Auxin regulates the initiation and radial position of plant lateral organs. *Plant Cell* **12**: 507-518
- Reinhardt D, Pesce ER, Stieger P, Mandel T, Baltensperger K, Bennett M, Traas J, Friml J, Kuhlemeier C** (2003) Regulation of phyllotaxis by polar auxin transport. *Nature* **426**: 255-260
- Ren H, Park MY, Spartz AK, Wong JH, Gray WM** (2018) A subset of plasma membrane-localized PP2C.D phosphatases negatively regulate SAUR-mediated cell expansion in *Arabidopsis*. *PLoS Genet* **14**: e1007455
- Ribatti D** (2018) An historical note on the cell theory. *Exp Cell Res* **364**: 1-4
- Roeder AHK, Cunha A, Ohno CK, Meyerowitz EM** (2012) Cell cycle regulates cell type in the *Arabidopsis* sepal. *Development* **139**: 4416-4427
- Rossmann S, Kohlen W, Hasson A, Theres K** (2015) Lateral suppressor and Goblet act in hierarchical order to regulate ectopic meristem formation at the base of tomato leaflets. *Plant J* **81**: 837-848

- Roychoudhry S, Kieffer M, Del Bianco M, Liao CY, Weijers D, Kepinski S** (2017) The developmental and environmental regulation of gravitropic setpoint angle in Arabidopsis and bean. *Sci Rep* **7**: 42664
- Ruegger M, Dewey E, Gray WM, Hobbie L, Turner J, Estelle M** (1998) The TIR1 protein of Arabidopsis functions in auxin response and is related to human SKP2 and yeast grr1p. *Genes Dev* **12**: 198-207
- Rutschow HL, Baskin TI, Kramer EM** (2011) Regulation of solute flux through plasmodesmata in the root meristem. *Plant Physiol* **155**: 1817-1826
- Sablowski R** (2016) Coordination of plant cell growth and division: collective control or mutual agreement? *Curr Opin Plant Biol* **34**: 54-60
- Samuels AL, Giddings TH, Jr., Staehelin LA** (1995) Cytokinesis in tobacco BY-2 and root tip cells: a new model of cell plate formation in higher plants. *J Cell Biol* **130**: 1345-1357
- Sapala A, Runions A, Routier-Kierzkowska AL, Das Gupta M, Hong L, Hofhuis H, Verger S, Mosca G, Li CB, Hay A, Hamant O, Roeder AH, Tsiantis M, Prusinkiewicz P, Smith RS** (2018) Why plants make puzzle cells, and how their shape emerges. *Elife* **7**
- Savaldi-Goldstein S, Baiga TJ, Pojer F, Dabi T, Butterfield C, Parry G, Santner A, Dharmasiri N, Tao Y, Estelle M, Noel JP, Chory J** (2008) New auxin analogs with growth-promoting effects in intact plants reveal a chemical strategy to improve hormone delivery. *Proc Natl Acad Sci U S A* **105**: 15190-15195
- Scarpella E, Marcos D, Friml J, Berleth T** (2006) Control of leaf vascular patterning by polar auxin transport. *Genes Dev* **20**: 1015-1027
- Schaefer E, Belcram K, Uyttewaal M, Duroc Y, Goussot M, Legland D, Laruelle E, de Tauzia-Moreau ML, Pastuglia M, Bouchez D** (2017) The preprophase band of microtubules controls the robustness of division orientation in plants. *Science* **356**: 186-189
- Schaller GE, Bishopp A, Kieber JJ** (2015) The yin-yang of hormones: cytokinin and auxin interactions in plant development. *Plant Cell* **27**: 44-63
- Schwarz EM, Roeder AH** (2016) Transcriptomic Effects of the Cell Cycle Regulator LGO in Arabidopsis Sepals. *Front Plant Sci* **7**: 1744
- Segui-Simarro JM, Austin JR, 2nd, White EA, Staehelin LA** (2004) Electron tomographic analysis of somatic cell plate formation in meristematic cells of Arabidopsis preserved by high-pressure freezing. *Plant Cell* **16**: 836-856
- Shin R, Burch AY, Huppert KA, Tiwari SB, Murphy AS, Guilfoyle TJ, Schachtman DP** (2007) The Arabidopsis transcription factor MYB77 modulates auxin signal transduction. *Plant Cell* **19**: 2440-2453
- Sieber P, Wellmer F, Gheyselinck J, Riechmann JL, Meyerowitz EM** (2007) Redundancy and specialization among plant microRNAs: role of the MIR164 family in developmental robustness. *Development* **134**: 1051-1060
- Simon ML, Platre MP, Marques-Bueno MM, Armengot L, Stanislas T, Bayle V, Caillaud MC, Jaillais Y** (2016) A PtdIns(4)P-driven electrostatic field controls cell membrane identity and signalling in plants. *Nat Plants* **2**: 16089
- Simonini S, Deb J, Moubayidin L, Stephenson P, Valluru M, Freire-Rios A, Sorefan K, Weijers D, Friml J, Ostergaard L** (2016) A noncanonical auxin-sensing mechanism is required for organ morphogenesis in Arabidopsis. *Genes Dev* **30**: 2286-2296
- Sottocornola B, Visconti S, Orsi S, Gazzarrini S, Giacometti S, Olivari C, Camoni L, Aducci P, Marra M, Abenavoli A, Thiel G, Moroni A** (2006) The

- potassium channel KAT1 is activated by plant and animal 14-3-3 proteins. *J Biol Chem* **281**: 35735-35741
- Souer E, van Houwelingen A, Kloos D, Mol J, Koes R** (1996) The no apical meristem gene of *Petunia* is required for pattern formation in embryos and flowers and is expressed at meristem and primordia boundaries. *Cell* **85**: 159-170
- Stanislas T, Platre MP, Liu M, Rambaud-Lavigne LES, Jaillais Y, Hamant O** (2018) A phosphoinositide map at the shoot apical meristem in *Arabidopsis thaliana*. *BMC Biol* **16**: 20
- Szecszi J, Joly C, Bordji K, Varaud E, Cock JM, Dumas C, Bendahmane M** (2006) BIGPETALp, a bHLH transcription factor is involved in the control of *Arabidopsis* petal size. *EMBO J* **25**: 3912-3920
- Szemenyei H, Hannon M, Long JA** (2008) TOPLESS mediates auxin-dependent transcriptional repression during *Arabidopsis* embryogenesis. *Science* **319**: 1384-1386
- Takada S, Hibara K, Ishida T, Tasaka M** (2001) The CUP-SHAPED COTYLEDON1 gene of *Arabidopsis* regulates shoot apical meristem formation. *Development* **128**: 1127-1135
- Tan X, Calderon-Villalobos LI, Sharon M, Zheng C, Robinson CV, Estelle M, Zheng N** (2007) Mechanism of auxin perception by the TIR1 ubiquitin ligase. *Nature* **446**: 640-645
- Terrile MC, Paris R, Calderon-Villalobos LI, Iglesias MJ, Lamattina L, Estelle M, Casalongue CA** (2012) Nitric oxide influences auxin signaling through S-nitrosylation of the *Arabidopsis* TRANSPORT INHIBITOR RESPONSE 1 auxin receptor. *Plant J* **70**: 492-500
- Thompson D** (1917) On growth and form,
- Tiwari SB, Hagen G, Guilfoyle TJ** (2004) Aux/IAA proteins contain a potent transcriptional repression domain. *Plant Cell* **16**: 533-543
- Tran D, Galletti R, Neumann ED, Dubois A, Sharif-Naeini R, Geitmann A, Frachisse JM, Hamant O, Ingram GC** (2017) A mechanosensitive Ca(2+) channel activity is dependent on the developmental regulator DEK1. *Nat Commun* **8**: 1009
- Tsugawa S, Hervieux N, Kierzkowski D, Routier-Kierzkowska AL, Sapala A, Hamant O, Smith RS, Roeder AHK, Boudaoud A, Li CB** (2017) Clones of cells switch from reduction to enhancement of size variability in *Arabidopsis* sepals. *Development* **144**: 4398-4405
- Ulmasov T, Hagen G, Guilfoyle TJ** (1997) ARF1, a transcription factor that binds to auxin response elements. *Science* **276**: 1865-1868
- Ulmasov T, Hagen G, Guilfoyle TJ** (1999) Activation and repression of transcription by auxin-response factors. *Proc Natl Acad Sci U S A* **96**: 5844-5849
- Ulmasov T, Liu ZB, Hagen G, Guilfoyle TJ** (1995) Composite structure of auxin response elements. *Plant Cell* **7**: 1611-1623
- Varaud E, Brioude F, Szecszi J, Leroux J, Brown S, Perrot-Rechenmann C, Bendahmane M** (2011) AUXIN RESPONSE FACTOR8 regulates *Arabidopsis* petal growth by interacting with the bHLH transcription factor BIGPETALp. *Plant Cell* **23**: 973-983
- Verhertbruggen Y, Marcus SE, Haeger A, Ordaz-Ortiz JJ, Knox JP** (2009) An extended set of monoclonal antibodies to pectic homogalacturonan. *Carbohydr Res* **344**: 1858-1862

- Verna C, Sawchuk MG, Linh NM, Scarpella E** (2015) Control of vein network topology by auxin transport. *BMC Biol* **13**: 94
- Vernoux T, Brunoud G, Farcot E, Morin V, Van den Daele H, Legrand J, Oliva M, Das P, Larrieu A, Wells D, Guedon Y, Armitage L, Picard F, Guyomarc'h S, Cellier C, Parry G, Koumproglou R, Doonan JH, Estelle M, Godin C, Kepinski S, Bennett M, De Veylder L, Traas J** (2011) The auxin signalling network translates dynamic input into robust patterning at the shoot apex. *Mol Syst Biol* **7**: 508
- Vernoux T, Kronenberger J, Grandjean O, Laufs P, Traas J** (2000) PIN-FORMED 1 regulates cell fate at the periphery of the shoot apical meristem. *Development* **127**: 5157-5165
- Vert G, Walcher CL, Chory J, Nemhauser JL** (2008) Integration of auxin and brassinosteroid pathways by Auxin Response Factor 2. *Proc Natl Acad Sci U S A* **105**: 9829-9834
- Vlad D, Kierzkowski D, Rast MI, Vuolo F, Dello Iorio R, Galinha C, Gan X, Hajheidari M, Hay A, Smith RS, Huijser P, Bailey CD, Tsiantis M** (2014) Leaf shape evolution through duplication, regulatory diversification, and loss of a homeobox gene. *Science* **343**: 780-783
- Vroemen CW, Mordhorst AP, Albrecht C, Kwaaitaal MA, de Vries SC** (2003) The CUP-SHAPED COTYLEDON3 gene is required for boundary and shoot meristem formation in Arabidopsis. *Plant Cell* **15**: 1563-1577
- Wang R, Zhang Y, Kieffer M, Yu H, Kepinski S, Estelle M** (2016) HSP90 regulates temperature-dependent seedling growth in Arabidopsis by stabilizing the auxin co-receptor F-box protein TIR1. *Nat Commun* **7**: 10269
- Weijers D, Wagner D** (2016) Transcriptional Responses to the Auxin Hormone. *Annu Rev Plant Biol* **67**: 539-574
- Went FW** (1937) *Phytohormones*, By F.W. Went and Kenneth V. Thimann,
- Williams L, Carles CC, Osmont KS, Fletcher JC** (2005) A database analysis method identifies an endogenous trans-acting short-interfering RNA that targets the Arabidopsis ARF2, ARF3, and ARF4 genes. *Proc Natl Acad Sci U S A* **102**: 9703-9708
- Willis L, Refahi Y, Wightman R, Landrein B, Teles J, Huang KC, Meyerowitz EM, Jonsson H** (2016) Cell size and growth regulation in the Arabidopsis thaliana apical stem cell niche. *Proc Natl Acad Sci U S A* **113**: E8238-E8246
- Wu MF, Tian Q, Reed JW** (2006) Arabidopsis microRNA167 controls patterns of ARF6 and ARF8 expression, and regulates both female and male reproduction. *Development* **133**: 4211-4218
- Wu MF, Yamaguchi N, Xiao J, Bargmann B, Estelle M, Sang Y, Wagner D** (2015) Auxin-regulated chromatin switch directs acquisition of flower primordium founder fate. *Elife* **4**: e09269
- Yabuuchi T, Nakai T, Sonobe S, Yamauchi D, Mineyuki Y** (2015) Preprophase band formation and cortical division zone establishment: RanGAP behaves differently from microtubules during their band formation. *Plant Signal Behav* **10**: e1060385

Résumé de la thèse :

Tous les organismes vivants sont faits de cellules et pourtant les organes et les organismes présentent une palette de formes variées. Chez les plantes, puisqu'il n'y a pas de migration cellulaire et très peu de mort cellulaire, les cellules ne peuvent effectuer que deux types de processus : la prolifération cellulaire, qui combine la division cellulaire (la scission d'une cellule en deux cellules filles) et la croissance cellulaire (augmentation du volume cellulaire), et l'expansion cellulaire qui consiste en l'augmentation de la taille des cellules qui ne se divisent plus. Comment ces processus cellulaires sont coordonnés pour donner naissance à une forme est l'une des questions les plus fascinantes en biologie du développement. A l'échelle des tissus ou des organes, la croissance résulte de la combinaison de la prolifération et de l'expansion ; dans les parties aériennes de la plante, la régulation spatiale et temporelle de la croissance soutient la formation itérative de nouveaux axes de croissance (feuilles, branches latérales, fleurs), constituant la base de l'architecture aérienne des plantes. La morphogenèse foliaire est soutenue par l'initiation itérative de nouveaux axes de croissance associés à une découpe plus ou moins prononcée de la marge foliaire : marge séréée, formation de lobes ou de folioles selon les espèces. Les régions à forte croissance telles que les primordia dans la zone périphérique du méristème apical caulinaire et les excroissances marginales des feuilles sont séparées des régions environnantes par un domaine de croissance réduite : le domaine frontière. Des approches génétiques ont montré que la formation des domaines frontière nécessitait l'activité des facteurs de transcription CUP SHAPED COTYLEDON (CUCs). La perturbation des CUCs entraîne des défauts plus ou moins sévères dans la séparation des organes selon les organes ou les espèces. Chez la feuille simple d'*Arabidopsis thaliana*, outre CUC2, CUC3 est le seul autre CUCs à être exprimé, bien qu'avec un profil légèrement différent. CUC2 a une expression large au bord de la feuille avec un maximum dans la région des sinus alors que CUC3 est exprimé seulement dans quelques cellules au niveau des sinus. Tandis que le mutant *cuc2-1* présente une marge lisse lié à une absence d'initiation des dents, le mutant *cuc3-105* initie toujours des dents, mais elles ont tendance à être rapidement lissées pendant le développement des feuilles. Chez *Arabidopsis thaliana*, l'effet de CUC2 sur le maintien d'une excroissance marginale s'est avéré

partiellement dépendant de CUC3 puisque les feuilles très disséquées des lignées d'*Arabidopsis* présentant des niveaux plus élevés de CUC2 sont lissées dans un fond mutant *cuc3-105*. Dans l'ensemble, ces résultats suggèrent des rôles distincts pour CUC2 et CUC3, le module CUC2-PIN1-Auxin étant nécessaire pour initier séquentiellement la croissance au bord des feuilles et CUC3 nécessaire pour maintenir la croissance de ces nouveaux axes par un mécanisme encore inconnu.

Grâce aux nombreux progrès de l'imagerie en temps réel et du traitement des données quantitatives, nous entrons maintenant dans une ère où la compréhension intégrative multi-échelle du développement des plantes est accessible. À ce jour, nous pouvons avoir accès à diverses informations en même temps, y compris la dynamique de l'expression des gènes, le modèle des réponses hormonales ou les changements dans les propriétés physico-chimiques de la paroi cellulaire. Les objectifs de cette thèse étaient d'utiliser ces avancées techniques pour approfondir nos connaissances sur la morphogenèse des plantes, en particulier pour déterminer la base cellulaire de la croissance différentielle au bord des feuilles. Nous avons utilisé une combinaison d'imagerie en temps réel et d'imagerie statique du bord dentelé de la feuille d'*Arabidopsis thaliana* pour étudier la base cellulaire de la croissance différentielle au bord de la feuille d'*Arabidopsis*, de l'initiation à l'excroissance dentaire et plus tard au lissage dentaire. Le rôle du CUC3 dans ces réponses a été étudié à l'aide d'un rapporteur d'expression génique et d'outils génétiques et son influence sur les réponses de l'auxine a également été explorée. Après une brève introduction sur la morphogenèse des plantes (Chapitre I), les données et les analyses quantitatives portant sur les bases cellulaires de la formation des indentations à la marge foliaire d'*Arabidopsis thaliana* sont présentées sous la forme d'un manuscrit (Chapitre II). Un autre chapitre de résultats correspondant à l'exploration de l'implication des co-récepteurs de l'auxine (TIR1/AFBs) dans la morphogenèse foliaire est ensuite présenté (Chapitre III). Enfin, une discussion globale sur les résultats de ce travail de thèse et les perspectives est présentée à la fin du manuscrit (Chapitre IV).

Titre : Evénements cellulaires et régulations au cours de la morphogenèse foliaire chez *Arabidopsis thaliana*

Mots clés : Morphogenèse foliaire, Auxine, Croissance

Comprendre comment la coordination des cellules entre elles permet l'émergence d'une forme est une des questions les plus fascinantes en biologie du développement. Au cours de cette thèse, nous avons utilisé les premiers stades de développement des feuilles dentelées d'*Arabidopsis thaliana* comme modèle pour étudier la relation entre les événements cellulaires et la morphogenèse. Pendant le développement des feuilles d'*Arabidopsis thaliana*, le contrôle fin de la prolifération et de l'expansion cellulaire permet la croissance différentielle au niveau de la marge foliaire, nécessaire à la formation des indentations. Dans ce modèle, la croissance différentielle est le résultat de l'interaction entre la signalisation de l'auxine et l'activité des facteurs de transcription CUP

SHAPED COTYLEDONS impliqués dans le maintien de l'identité des domaines frontières. Pour affiner la compréhension des relations complexes entre les facteurs de transcriptions CUC, les réponses auxiniques et les événements cellulaires à l'origine des indentations foliaires, nous avons utilisé des expériences d'imagerie en temps réel sur des primordia foliaires de lignées exprimant des rapporteurs de développement et/ou de réponse auxinique. Nos résultats ont révélé un contrôle dynamique de la croissance différentielle à la marge des feuilles et l'implication critique de CUC3 dans la répression locale de la croissance cellulaire.

Title : Cellular events and regulations during leaf margin morphogenesis in *Arabidopsis thaliana*

Keywords : Leaf morphogenesis, Auxin, Growth

How a shape arises from the coordinated behavior of cells is one of the most fascinating questions in developmental biology. Here we used the early stages of development of serrated leaves in *Arabidopsis thaliana* as a model to study the tight relation between cellular behavior and morphogenesis. During *Arabidopsis thaliana* leaf development the fine control of cell proliferation and cell expansion sustains differential growth at the margin required for the formation of leaf outgrowth named teeth. In this model, differential growth is the result of interplay between auxin signaling and CUC transcription factors that are involved in the maintenance of boundary domain identity. To clarify the interconnected relations between patterns of CUC TFs and auxin responses as well as the cellular events behind serrations we used time

lapse experiments on vegetative primordia of lines expressing developmental and/or auxin response reporters. Our results revealed a tight and dynamic control of differential growth at the leaf margin and the critical involvement of CUC3 in the local repression of cell growth in combination with low auxin responses.

